Answer to referee #1:

We thank referee #1 for reviewing our manuscript. His/Her valuable comments and suggestions have significantly improved the quality of our manuscript.

Below, we include our detailed answers to all comments and questions.

Answers to general comments (GC):

General Comment #1:

Nissen and Vogt present a model study on the relative importance of the colonial form of Phaeocystis for ecosystem processes and biogeochemical fluxes; they evaluate their results with observations from different data sources. A comparable study (Nissen et al 2018) had been performed with a focus on coccolithophores instead of Phaeocystis with similar analyses. In that respect this work is not overly innovative nor are original ideas presented. More critical is, however, that there is no thread in this manuscript; a clear goal is missing. A number of topics (e.g. phenology, competition, carbon and DMS-fluxes) are touched but not thoroughly permeated. It is unclear whether the authors would like to study the success of Phaeocystis compared to other phytoplankton functional groups or the importance of Phaeocystis for carbon export fluxes. Either way, no comprehensible motivation for either of these broad themes is provided. Some aspects of the methodology also need to be revised with consequences for the model analyses. Last but not least, recent work on this topic has been ignored. Overall this manuscript is premature and the authors must clarify their focus before publication. To sharpen the focus maybe it helps to look at the unpublished, recent modelling work on Southern Ocean Phaeocystis and PFTs (Losa et al. 2019) that has been put up for discussion in Biogeosciences Discussion.

Answer to GC1:

We thank reviewer 1 for his/her constructive criticism on our work, regarding the focus, the motivation, the novelty, the methodology, and the presentation of our study. We address the concerns of the reviewer 1 with regard to these aspects in the revised manuscript through the following changes:

1) We have changed the title of the manuscript to "Factors controlling the competition between *Phaeocystis* and diatoms in the Southern Ocean and implications for carbon export fluxes" so that it better reflects the focus of the study, namely the links between the variability in phytoplankton community structure and downward carbon fluxes in the high-latitude Southern Ocean throughout the year.
2) We have entirely revised the introduction which now clarifies the focus and novelty of the study and includes additional recent literature.
3) We have restructured the result section and adjusted the relative weighting of the individual sections to have a more balanced representation of the different aspects of the study, especially regarding the drivers of the competition between *Phaeocystis* and diatoms and its biogeochemical implications.
4) Ultimately, within the discussion section of the revised version of the manuscript, we have adopted the same structure of subsections as in the result section, making it easier for the reader to follow. Furthermore, we have adjusted the lengths of the discussion of the individual aspects, in order to better represent the main focus of the study.

For the comment regarding the methodology (i.e., the temperature sensitivity of phytoplankton growth), we refer the reviewer to our detailed answer to SC4 and SC5 below.

In our study, we set out for a comprehensive assessment of the link between plankton biogeography and biogeochemical cycling in the Southern Ocean over the course of the year. Since we consider the comprehensiveness as a key strength and key aspect of novelty of the current paper as compared to previous work, the emphasis of our revision has been to (1) clarify the aims of the study in the revised version of the introduction, (2) highlight the current gaps in our understanding with regard to the

missing link between plankton biogeography and ecosystem function in terms of global biogeochemical cycling, and (3) improve upon the presentation of our study in the manuscript. Previous studies have often only presented snap shots of the factors controlling the relative importance of *Phaeocystis* and diatoms at high SO latitudes and its implications for downward carbon fluxes at a specific location and/or point in time (e.g. **Arrigo et al., 1998, Garcia et al., 2009, Wang et al., 2011**, but see the introduction of the manuscript for a comprehensive overview), meaning that the biogeochemical implications of the seasonally varying phytoplankton community remain under-explored, especially on larger spatial scales. We clarify these issues in the revised version of the manuscript, as detailed in the sections below.

In the following, we will address the individual concerns raised by the reviewer in more detail and summarize how we have addressed them in the revised version of the manuscript.

Focus/Novelty/Motivation

In this paper we set out to assess the link between the spatio-temporal variability in high-latitude Southern Ocean phytoplankton community structure and the variability in downward carbon fluxes. To that aim, we extended the work by **Nissen et al., 2018** to develop a model which would include all major biogeochemical actors of this region, a prerequisite to address this research question. Hence, with this tool, we were able to provide a first comprehensive assessment of the spatio-temporal variability of pathways leading to downward fluxes of carbon, which are inherently linked to the overlying phytoplankton community structure.

To clarify the focus of the study, we have changed the title of the manuscript to "Factors controlling the competition between *Phaeocystis* and diatoms in the Southern Ocean and implications for carbon export fluxes", so that it sets up the reader for the link between phytoplankton community structure and the implications for the carbon cycle.

Furthermore, we have substantially rewritten the introduction, to better highlight the focus, the novelty, and the motivation of our study. In this context, we apologize for the omission of certain recent papers in our initial submission. In response to the reviewer's comment, we have performed an additional extensive literature research and included the identified novel work in the revised version of our manuscript. We identified the following additional 7 papers that are of relevance for the current paper, and that were not included in the reference list of the initial submission:

Papers describing the succession from *Phaeocystis* to diatoms throughout the season in the Ross Sea (Ryan-Keogh et al., 2017) and off the Western Antarctic Peninsula (Arrigo et al. 2017):

Ryan-Keogh, T. J., DeLizo, L. M., Smith, W. O., Sedwick, P. N., McGillicuddy, D. J., Moore, C. M., & Bibby, T. S. (2017). Temporal progression of photosynthetic-strategy in phytoplankton in the Ross Sea, Antarctica. *Journal of Marine Systems*, *166*, 87–96. https://doi.org/10.1016/j.jmarsys.2016.08.014

Arrigo, K. R., van Dijken, G. L., Alderkamp, A., Erickson, Z. K., Lewis, K. M., Lowry, K. E., … van de Poll, W. (2017). Early Spring Phytoplankton Dynamics in the Western Antarctic Peninsula. *Journal of Geophysical Research: Oceans*, *122*(12), 9350–9369. https://doi.org/10.1002/2017JC013281

Paper describing the impact of Fe concentrations on colony formation by *Phaeocystis Antarctica*:

Bender, S. J., Moran, D. M., McIlvin, M. R., Zheng, H., McCrow, J. P., Badger, J., … Saito, M. A. (2018). Colony formation in Phaeocystis antarctica: connecting molecular mechanisms with iron biogeochemistry. *Biogeosciences*, *15*(16), 4923–4942. https://doi.org/10.5194/bg-15-4923-2018

Papers on recent modeling of *Phaeocystis Antarctica*, focusing either on interactions between light and temperature on growth rates (Moisan & Mitchel, 2018) or functional type modeling in the Southern Ocean (Losa et al., 2019):

Moisan, T. A., & Mitchell, B. G. (2018). Modeling Net Growth of Phaeocystis antarctica Based on Physiological and Optical Responses to Light and Temperature Co-limitation. *Frontiers in Marine Science*, *4*(February), 1–15. https://doi.org/10.3389/fmars.2017.00437

Losa, S. N., Dutkiewicz, S., Losch, M., Oelker, J., Soppa, M. A., Trimborn, S., Xi, H., and Bracher, A.: On modeling the Southern Ocean Phytoplankton Functional Types, Biogeosciences Discuss., https://doi.org/10.5194/bg-2019-289, 2019.

Papers discussing the role of aggregates (especially those from *Phaeoycstis Antarcitca*) as a vector for carbon transfer to depth in the Southern Ocean (relative to that of e.g. fecal pellets):

Asper, V. L., & Smith, W. O. (2019). Variations in the abundance and distribution of aggregates in the Ross Sea, Antarctica. *Elem Sci Anth*, *7*(1), 23. https://doi.org/10.1525/elementa.355

Ducklow, H. W., Wilson, S. E., Post, A. F., Stammerjohn, S. E., Erickson, M., Lee, S., … Yager, P. L. (2015). Particle flux on the continental shelf in the Amundsen Sea Polynya and Western Antarctic Peninsula. *Elementa: Science of the Anthropocene*, *3*, 000046. https://doi.org/10.12952/journal.elementa.000046

The analysis of this body of work reveals that these more recent findings are complementary to our results, and their inclusion into the introduction and discussion sections of our paper increases the quality of the discussion in the revised version of the manuscript.

In particular, we have included the references on the role of aggregates for POC export in the discussion section 4.2. of the revised manuscript (section on biogeochemical implications) and have added the study by **Losa et al. (2019)** in the discussion section 4.3 (Limitations & Caveats), discussing the complexity in marine ecosystem models:

"The transition from solitary to colonial cells is a function of the seed population and light and nutrient levels (Verity, 2000; Bender et al., 2018), and transition models have been applied in SO marine ecosystem models (e.g. Popova et al., 2007; Kaufman et al., 2017; Losa et al., 2019). For example, in their higher complexity, self-organizing ecosystem model (Follows et al., 2007), Losa et al. (2019) include both life stages of *Phaeocystis* and two types of diatoms to simulate phytoplankton competition at high SO latitudes. While our model results suggest that this is not required to reproduce the observed SO biogeography of *Phaeocystis* and diatoms in ROMS-BEC, it nevertheless highlights the need for further research on the impact of the chosen marine ecosystem complexity on the modeled biogeochemical fluxes (Ward et al., 2013)."

In the revised version of the manuscript, the introduction section now reads:

1 Introduction

Phytoplankton production in the Southern Ocean (SO) regulates not only the uptake of anthropogenic carbon in marine food-webs, but also controls global primary production via the lateral export of nutrients to lower latitudes (e.g. Sarmiento et al., 2004; Palter et al., 2010). The amount and stoichiometry of these laterally exported nutrients is determined by the combined action of multiple types of phytoplankton with differing ecological niches and nutrient requirements. Yet, despite their important role, the drivers of phytoplankton biogeography and competition and the relative contribution of different phytoplankton groups to SO carbon cycling are still poorly quantified. Today, the SO phytoplankton community is largely dominated by silicifying diatoms that efficiently fix and transport carbon from the surface ocean to depth (e.g. Swan et al., 2016) and have been suggested to be the major contributor to SO carbon export (Buesseler, 1998; Smetacek et al., 2012). However, calcifying coccolithophores and dimethylsulfide (DMS) producing *Phaeocystis* have been found to contribute in a significant way to total phytoplankton biomass at subantarctic (Balch et al., 2016; Nissen et al., 2018) and at high latitudes, respectively (Smith and Gordon, 1997; Arrigo et al., 1999; DiTullio et al., 2000; Poulton et al., 2007), thus suggesting that the succession and competition of different plankton groups governs biogeochemical cycles at the (sub)regional scale. As climate change is expected to differentially impact the competitive fitness of different phytoplankton groups and ultimately their contribution to total net primary production (NPP; IPCC, 2014; Constable et al., 2014; Deppeler and Davidson, 2017), with a likely increase in the relative importance of coccolithophores and *Phaeocystis* in a warming world at the expense of diatoms (Bopp et al., 2005; Winter et al., 2013; Rivero-Calle et al., 2015), the resulting change in SO phytoplankton community structure is likely to affect global nutrient and carbon distributions, ocean carbon uptake, and marine food web structure (Smetacek et al., 2004). While a number of recent studies have elucidated the importance of coccolithophores for subantarctic carbon cycling (e.g. Rosengard et al., 2015; Balch et al., 2016; Nissen et al., 2018; Rigual Hernández et al., 2020), few estimates quantify the role of present and future high-latitude SO phytoplankton community structure for ecosystem services such as NPP and carbon export.

Phaeocystis blooms in the SO have been regularly observed in early spring at high SO latitudes (especially in the Ross Sea, see e.g. Smith et al., 2011), thus preceding those of diatoms (Green and Sambrotto, 2006; Peloquin and Smith, 2007; Alvain et al., 2008; Arrigo et al., 2017; Ryan-Keogh et al., 2017), and *Phaeocystis* can dominate over diatoms in terms of carbon biomass at regional and sub-annual scales (e.g. Smith and Gordon, 1997; Alvain et al., 2008; Leblanc et al., 2012; Vogt et al., 2012; Ben Mustapha et al., 2014). Nevertheless, *Phaeocystis* is not routinely included as a phytoplankton functional type (PFT) in global biogeochemical models, possibly a result of the limited number of biomass validation data (Vogt et al., 2012) and its complex life cycle (Schoemann et al., 2005). In particular, *Phaeocystis* is difficult to model because traits linked to biogeochemistry-related ecosystem services, such as size and carbon content, vary due to its complex multi-stage life cycle. Its alternation between solitary cells of a few μm in diameter and gelatinous colonies of several mm to cm in diameter (e.g. Rousseau et al., 1994; Peperzak, 2000; Chen et al., 2002; Bender et al., 2018) directly impacts community biomass partitioning and the relative importance of aggregation, viral lysis, and grazing for *Phaeocystis* biomass losses, its susceptibility to zooplankton grazing relative to that of diatoms (Granéli et al., 1993; Smith et al., 2003), and ultimately the export of particulate organic carbon (POC; Schoemann et al., 2005). With *Phaeocystis* colonies typically dominating over solitary cells during the SO growing season (Smith et al., 2003), *Phaeocystis* biomass loss via aggregation possibly increases in relative importance at the expense of grazing as more colonies are formed and colony size increases (Tang et al., 2008). Altogether, this implies a complex seasonal variability in the magnitude and pathways of carbon transfer to depth as the phytoplankton community changes throughout the year, which is difficult to comprehensively assess through in situ studies and therefore calls for marine ecosystem models.

Across those marine ecosystem models including a *Phaeocystis* PFT, the representation of its life cycle differs in terms of complexity (Pasquer et al., 2005; Tagliabue and Arrigo, 2005; Wang and Moore, 2011; Le Quéré et al., 2016; Kaufman et al., 2017; Losa et al., 2019). While some models include rather sophisticated parametrizations to describe life cycle transitions (accounting for nutrient concentrations, light levels, and a seed population, see e.g. Pasquer et al., 2005; Kaufman et al., 2017), the majority includes rather simple transition functions (accounting for iron concentrations only, see Losa et al., 2019) or only the colonial life stage of *Phaeocystis* (Tagliabue and Arrigo, 2005; Wang and Moore, 2011; Le Quéré et al., 2016). Despite these differences, all of the models see improvements in the simulated SO phytoplankton biogeography as compared to observations upon the implementation of a *Phaeocystis* PFT. In particular, Wang and Moore (2011) find that *Phaeocystis*

contributes substantially to SO integrated annual NPP and POC export (23% and 30% south of 60° S, respectively; Wang and Moore, 2011), implying that models not accounting for *Phaeocystis* possibly overestimate the role of diatoms for high-latitude phytoplankton biomass, NPP, and POC export (Laufkötter et al., 2016). Overall, the link between ecosystem composition, ecosystem function, and global biogeochemical cycling in general (e.g. Siegel et al., 2014; Guidi et al., 2016; Henson et al., 2019) and the contribution of *Phaeocystis* to SO export of POC in particular are still under debate. While some have found blooms of *Phaeocystis* to be important vectors of carbon transfer to depth through the formation of aggregates (Asper and Smith, 1999; DiTullio et al., 2000; Ducklow et al., 2015; Asper and Smith, 2019), others suggest their biomass losses to be efficiently degraded in the upper water column through bacterial and zooplankton activity, making *Phaeocystis* a minor contributor to SO POC export (Gowing et al., 2001; Accornero et al., 2003; Reigstad and Wassmann, 2007). This demonstrates the major existing uncertainty in how the high-latitude phytoplankton community structure impacts carbon export fluxes.

In general, the relative importance of different phytoplankton types for total phytoplankton biomass is controlled by a combination of top-down factors, i.e. processes impacting phytoplankton biomass loss such as grazing by zooplankton, aggregation of cells and subsequent sinking, or viral lysis, and bottom-up factors, i.e. physical and biogeochemical variables impacting phytoplankton growth (Le Quéré et al., 2016). The observed spatio-temporal differences in the relative importance of *Phaeocystis* and diatoms in the SO are thought to be largely controlled by differences in light and iron levels, but the relative importance of the different bottom-up factors appears to vary depending on the time and location of the sampling (Arrigo et al., 1998, 1999; Goffart et al., 2000; Sedwick et al., 2000; Garcia et al., 2009; Tang et al., 2009; Mills et al., 2010; Feng et al., 2010; Smith et al., 2011, 2014). Concurrently, while available models agree with the observations on the general importance of light and iron levels, differences in the dominant bottom-up factors controlling the distribution of *Phaeocystis* at high SO latitudes across models are possibly a result of differences in how this phytoplankton type is parametrized (Tagliabue and Arrigo, 2005; Pasquer et al., 2005; Wang and Moore, 2011; Le Quéré et al., 2016; Kaufman et al., 2017; Losa et al., 2019). Besides bottom-up factors, some observational studies suggest that top-down factors are important in controlling the relative importance of *Phaeocystis* and diatoms as well. For instance, van Hilst and Smith (2002) suggest grazing by zooplankton to be an important factor explaining the observed distributions of these two phytoplankton types in the SO, likely resulting from the generally lower grazing pressure on *Phaeocystis* colonies than on diatoms (Granéli et al., 1993; Smith et al., 2003). Yet, further evidence suggests a role for other biomass loss processes such as aggregation and subsequent sinking (Asper and Smith, 1999; Ducklow et al., 2015; Asper and Smith, 2019). Altogether, this calls for a comprehensive quantitative analysis of the relative importance of bottom-up and top-down factors in controlling the competition between *Phaeocystis* and diatoms over the course of the SO growing season and its ramifications for carbon transfer to depth.

In this study, we investigate the competition between *Phaeocystis* and diatoms and its implications for carbon cycling using a regional coupled physical-biogeochemical-ecological model configured at eddy-permitting resolution for the SO (ROMS-BEC, Nissen et al., 2018). To address the missing link between SO phytoplankton biogeography and the global carbon cycle, we have added *Phaeocystis* colonies as an additional PFT to the model, so that it includes all major identified biogeochemically relevant phytoplankton types of the SO. We then assess the relative importance of bottom-up and top-down factors in controlling the relative importance of *Phaeocystis* colonies and diatoms over a complete annual cycle in the high-latitude SO. We show that a correct representation of SO phytoplankton biogeography leaves a distinct imprint on upper ocean carbon cycling and POC export across the SO.

Structure

In response to the reviewer's comments, we have revised the results and the discussion section of the manuscript to make the order and relative weighting of individual sections clearer to the reader, and to better align the presentation of results with the core questions this paper aims to address.
In particular, we have merged the result sections 3.3 & 3.4 of the original version of the manuscript into a single section in the revised manuscript, which is entitled "Drivers of SO phytoplankton biogeography, phenology, and succession patterns". This section was shortened in the merging process, with the aim to make it more readable and to better balance the amount of text spent on the description of a) simulated patterns of biogeography, phenology, and succession, b) the drivers of the competition, and c) its biogeochemical implications. Please see our answer to SC8 for the new result section 3.3.

Furthermore, in order to make it easier for the reader to follow, we have adjusted the order of subsections within the discussion section to reflect their order in the result section, i.e., swapped discussion section 4.1 & 4.2 of the original manuscript. In the revised manuscript, the discussion of the

drivers of the competition of *Phaeocystis* and diatoms (section 4.1) is now followed by the discussion of its biogeochemical implications (section 4.2). In addition, in the latter, we have modified the paragraph on the implications of Southern Ocean *Phaeocystis* biogeography for DMS fluxes. In particular, we have shortened the paragraph on DMS from the method section 2.3.1 and moved it to section 4.2 in the revised manuscript, so that the manuscript is more clearly focused on carbon fluxes up until this point. Please see our answer to SC14 for the new paragraph on DMS.

Answers to specific comments (SC):

SC1: *title: the title only partly reflects the content of this study*

We thank the reviewer for this important comment, as it made us aware of imbalances in terms of content in the original version of the manuscript. As the analysis regarding the implications of the variability in phytoplankton community structure on high-latitude carbon fluxes is an important, novel aspect of the study, which has been highlighted even more in the revised version of the manuscript (see also answer to GC 1 above), the revised version of the manuscript will be entitled "Factors controlling the competition between *Phaeocystis* and diatoms in the Southern Ocean and implications for carbon export fluxes". Thereby, the content of the manuscript is better reflected by its title, helping the reader to follow.

SC2: *abstract and entire manuscript: it is unclear which research gap the authors want to fill. What is currently unclear - which open question in this research field are attempted to be answered with ROMS-BEC?*

In response to the reviewer's comments, we have substantially reworked the manuscript, in order to more clearly highlight the knowledge gap filled with this study. After having added *Phaeocystis* as a functional type to ROMS-BEC, we were able to provide a first comprehensive assessment of the spatio-temporal variability of pathways leading to downward fluxes of carbon at high Southern Ocean latitudes, which are inherently linked to the overlying phytoplankton community structure, especially the competition between *Phaeocystis* and diatoms. We kindly refer the reviewer to our response to GC1 above for more details.

SC3: *the manuscript should stand alone. Currently important parts of the model description are missing. The prognostic equation for Phaeocystis with all source and sink terms as well as all functional dependencies of rates to environmental drivers need to be provided.*

We fully agree with the reviewer on this point and apologize for not having included a full description of growth and loss terms for phytoplankton biomass in the original version of the manuscript. In the revised version, we have included a full description of the relevant model equations of BEC in Appendix B and added corresponding references to this section in the method section 2.1 and throughout the text:

Appendix B: BEC equations: Phytoplankton growth & loss

Any change in phytoplankton biomass P [mmol C m^{-3}] of phytoplankton i ($i \in \{PA, D, C, SP, N\}$) over time is determined by the balance of growth and loss terms:

$$\frac{\mathrm{dP^i}}{\mathrm{dt}} = \mathrm{Growth} - \mathrm{Loss} \tag{B1}$$

$$= \mu^{\mathrm{i}} \cdot \mathrm{P^i} - \gamma^{\mathrm{i}}(\mathrm{P^i}) \cdot \mathrm{P^i} \tag{B2}$$

$$= \mu^{\mathrm{i}} \cdot \mathrm{P^i} - \gamma^{\mathrm{i}}_{\mathrm{g}}(\mathrm{P^i}) \cdot \mathrm{P^i} - \gamma^{\mathrm{i}}_{\mathrm{m}} \cdot \mathrm{P^i} - \gamma^{\mathrm{i}}_{\mathrm{a}}(\mathrm{P^i}) \cdot \mathrm{P^i} \tag{B3}$$

In the above equation, γ_{g} denotes the loss by zooplankton grazing, γ_{m} the loss by non-grazing mortality, and γ_{a} the loss by aggregation.

B1 Phytoplankton growth

The specific growth rate μ^{i} [day^{-1}] of phytoplankton i ($i \in \{D, C, SP, N\}$, i.e., all but *Phaeocystis*) is determined by the maximum growth rate $\mu^{\mathrm{i}}_{\mathrm{max}}$ (Table 1) and modifications due to temperature (T), nutrients (N) and irradiance (I), following:

$$\mu^{\mathrm{i}} = \mu^{\mathrm{i}}_{\mathrm{max}} \cdot \mathrm{f^i(T)} \cdot \mathrm{g^i(N)} \cdot \mathrm{h^i(I)} \tag{B4}$$

The temperature function $f(T)$ is an exponential function, which is modified by the constant $\mathrm{Q_{10}}$ specific to every phytoplankton i (Table 1):

$$\mathrm{f^i(T)} = \mathrm{Q^i_{10}} \cdot \exp\left(\frac{\mathrm{T} - \mathrm{T_{ref}}}{10°\mathrm{C}}\right) \tag{B5}$$

Note that for *Phaeocystis* in ROMS-BEC, an optimum temperature function is used (Eq. 1), as this PFT is parametrized to only represent *Phaeocystis Antarctica* in the SO application of this study (see section 2.1).

First, the limitation of growth of phytoplankton i ($i \in \{PA, D, C, SP, N\}$) by the surrounding nutrient $L^{\mathrm{i}}(N)$ is calculated individually for each nutrient (nitrogen, phosphorus, iron for all phytoplankton, silicate for diatoms only) following a Michaelis-Menten function (see Table 1 for half-saturation constants $\mathrm{k^i_N}$). Accordingly, the limitation factor is calculated as follows for iron (Fe) and silicate (SiO3):

$$\mathrm{L^i(N)} = \frac{\mathrm{N}}{\mathrm{N} + \mathrm{k^i_N}} \tag{B6}$$

For nitrogen and phosphorus, the combined limitation by nutrient N and M (nitrate (NO3) and ammonium (NH4) for nitrogen, phosphate (PO4) and dissolved organic phosphorus (DOP) for phosphorus) is accounted for following:

$$\mathrm{L^i(N,M)} = \frac{\mathrm{N}}{\mathrm{k^i_N} + \mathrm{N} + \mathrm{M} \cdot (\mathrm{k^i_N}/\mathrm{k^i_M})} + \frac{\mathrm{M}}{\mathrm{k^i_M} + \mathrm{M} + \mathrm{N} \cdot (\mathrm{k^i_M}/\mathrm{k^i_N})} \tag{B7}$$

In the model, the phytoplankton growth rate is then only limited by the most limiting nutrient:

$$\mathrm{g^i(N)} = \min(\mathrm{L^i(NO3,NH4)}, \mathrm{L^i(PO4,DOP)}, \mathrm{L^i(Fe)}, \mathrm{L^i(SiO3)}) \tag{B8}$$

The light limitation function $h^{\mathrm{i}}(I)$ includes the effects of photoacclimation by including the chlorophyll-to-carbon ratio θ^{i} and the growth of the respective phytoplankton i ($i \in \{PA, D, C, SP, N\}$) limited by nutrients and temperature:

$$\mathrm{h^i(I)} = 1 - \exp\left(-1 \cdot \frac{\alpha^{\mathrm{i}}_{\mathrm{PI}} \cdot \theta^{\mathrm{i}} \cdot \mathrm{I}}{\mu^{\mathrm{i}}_{\mathrm{max}} \cdot \mathrm{g^i(N)} \cdot \mathrm{f^i(T)}}\right) \tag{B9}$$

Here, same as in Nissen et al. (2018), growth by coccolithophores is set to zero at PAR levels <1 W m^{-2} (Zondervan, 2007) and is linearly reduced at temperatures $<6°$C following:

$$\mu^{\mathrm{C}} = \mu^{\mathrm{C}} \cdot \frac{\max(\mathrm{T} + 2°\mathrm{C}), 0)}{8°\mathrm{C}} \tag{B10}$$

Coccolithophore calcification amounts to 20% of their photosynthetic growth at any location and point in time in ROMS-BEC.

Diazotroph growth is zero at temperatures $<14°$C.

B2 Phytoplankton loss

In ROMS-BEC, the corrected phytoplankton biomass P'^i is used to compute loss rates of phytoplankton biomass, to prevent phytoplankton biomass loss at very low biomass levels:

$$P'^i = \max(P^i - c^i_{loss}, 0) \quad \text{(B11)}$$

In this equation, c^i_{loss} is the threshold of phytoplankton biomass P^i below which no losses occur (c^N_{loss}=0.022 mmol C m^{-3} and $c^{PA,D,C,SP}_{loss}$=0.04 mmol C m^{-3}).

The single zooplankton grazer Z [mmol C m^{-3}] feeds on the respective phytoplankton P'^i [mmol C m^{-3}] at a grazing rate γ^i_g [mmol C m^{-3} day^{-1}] that is given by:

$$\gamma^i_g = \gamma^i_{max} \cdot f^Z(T) \cdot Z \cdot \frac{P'^i}{z^i_{grz} + P'^i} \quad \text{(B12)}$$

with

$$f^Z(T) = 1.5 \cdot \exp\left(\frac{T - T_{ref}}{10°C}\right) \quad \text{(B13)}$$

The non-grazing mortality rate γ^i_m [mmol C m^{-3} day^{-1}] of phytoplankton i [mmol C m^{-3}] is the product of a maximum mortality rate m^i_0 [day^{-1}] scaled by the temperature function $f^i(T)$ with the modified phytoplankton biomass P'^i:

$$\gamma^i_m = m^i_0 \cdot f^i(T) \cdot P'^i \quad \text{(B14)}$$

with m^i_0 being 0.15 day^{-1} for diazotrophs and 0.12 day^{-1} for all other phytoplankton.

Phytoplankton P'^i [mmol C m^{-3}] aggregate at an aggregation rate γ^i_a [mmol C m^{-3} day^{-1}] which is computed with the quadratic mortality rate constants $\gamma^i_{a,0}$ ([m^3 (mmol C)$^{-1}$ d^{-1}], Table 1) and :

$$\gamma^i_a = \min(\gamma^i_{a,max} \cdot P'^i, \gamma^i_{a,0} \cdot P'^i \cdot P'^i) \quad \text{(B15)}$$

$$\gamma^i_a = \max(\gamma^i_{a,min} \cdot P'^i, \gamma^i_a) \quad \text{(B16)}$$

In ROMS-BEC, $\gamma^i_{a,min}$ is 0.01 day^{-1} for small phytoplankton and coccolithophores and 0.02 day^{-1} for *Phaeocystis* and diatoms, and with $\gamma^i_{a,max}$ being 0.9 day^{-1} for *Phaeocystis*, diatoms, coccolithophores, and small phytoplankton. Note that phytoplankton immediately stop photosynthesizing upon aggregation and that aggregation losses do not occur for diazotrophs in ROMS-BEC.

SC4: *the newly introduced formulation of the temperature dependent growth for the PFT Phaeocystis is fundamentally different from the description of the PFTs of the original BEC model. The former is a "Gauss-like" temperature dependent growth function with a temperature optimum. Any deviation from the optimum is a limitation, varying between 0...1. In contrast, the Q10-approach with different Q10 values that is applied to the other PFTs denotes the "sensitivity" in the exponential growth towards temperature - in these cases the higher the temperature, the higher the growth. Even if a relatively high reference temperature of 30 degrees Celsius is given (which is likely not reached in the Southern Ocean), there is no such thing as an optimum in the Q10 approach. Thus, the "limitation" values used in the analyses cannot easily be compared.*
[Generally the question arises whether the Q10 approach should be applied to PFTs at all. Introduced by Eppley it is valid and a good description for bulk phytoplankton but as soon as the bulk is divided into groups, "Gauss-like functions" with a clear optimum seem to be more adequate.]

We thank the reviewer for raising this important point. First of all, we completely agree with the reviewer in that the two approaches ("optimum" vs "Q10") to model the temperature-limited growth rates of phytoplankton are fundamentally different. However, we think that a comparison of the temperature-limited growth rates of *Phaeocystis* ("optimum") to that of diatoms (Q10) is still valid in our model, for reasons outlined in the following.

In lab experiments, individual phytoplankton species typically show an optimum temperature for growth, above and below which its growth is slowed down (see Fig. 1 below). Yet, in models, the Q10-approach describes the temperature-limited growth as an exponential function without a temperature optimum (see black lines in Fig. 2 below or Fig. A1 in our manuscript). Since models typically represent the whole phytoplankton community by a set of plankton functional types (PFTs,

Le Quéré et al., 2005), thereby combining multiple species into a single PFT, this Q10-function can hence be interpreted as the overlap of numerous optimum curves of numerous individual species.

In the 5-PFT setup of ROMS-BEC presented here, the PFT "*Phaeocystis*" only represents the single species of *Phaeocystis* present in the SO, namely *Phaeocystis antarctica* (**Schoemann et al., 2005**). This species has been shown to stop growing above temperatures of ~8°C (**Buma et al., 1991**), thus an optimum curve applies. At the same time, within the model PFT "diatoms", we do not model a specific species of diatoms, but the whole diatom community (typical PFT approach; **Le Quéré et al., 2005**). This means that with increasing temperatures towards lower latitudes, diatom growth will be less and less temperature-limited (relative to the prescribed maximum growth rate at 30°C), as we assume that there is always a species that can cope with these higher temperatures (see also blue dots in Fig. 2 below). Yet, this is not the case for *Phaeocystis antarctica*, which is not observed northwards of approximately 60°S (**Schoemann et al., 2005**). At latitudes north of 60°S, other bloom-forming species of *Phaeocystis* are typically found (**Schoemann et al., 2005** and Fig. 3 below). While these are *not* included in our study, there is no reason not to include these other species in global models, thus suggesting that the applicability of a temperature optimum curve to describe the growth of *Phaeocystis* in global models may be limited (see also black line in the lower panel of Fig. 2 below). Yet, the literature review of available growth rates of all *Phaeocystis* species presented in **Schoemann et al. (2005)** is best fit by using a temperature optimum curve despite multiple species being included in the analysis (see Fig. 3 below; compare to the fit Fig. 2), suggesting that the Q10 approach may be unsuitable – at least for the bloom-forming species of this phytoplankton type.

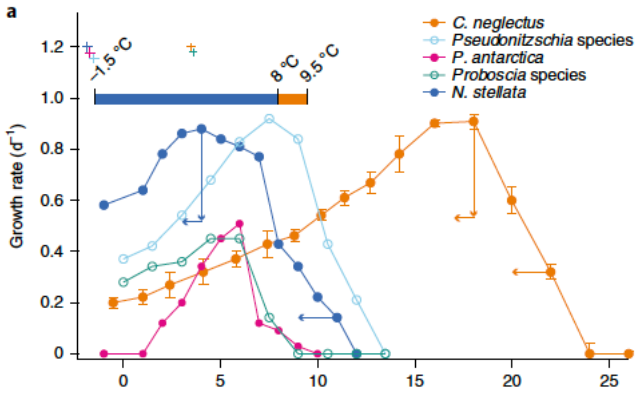

Fig. 1: Growth rates as a function of temperature for example high-latitude SO species of diatoms and *Phaeocystis* (**Boyd 2019**).

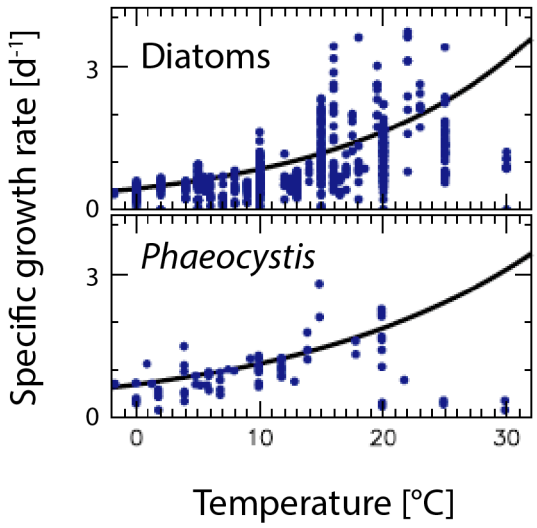

Fig. 2: Global compilation of diatom (top) and *Phaeocystis* (bottom) growth rates as a function of temperature by **Le Quéré et al. (2016)**. Black lines are Q10-functions fit to the data with Q10=1.93 and Q10=1.66 for diatoms and *Phaeoycstis*, respectively., as used in the PlankTOM10 model.

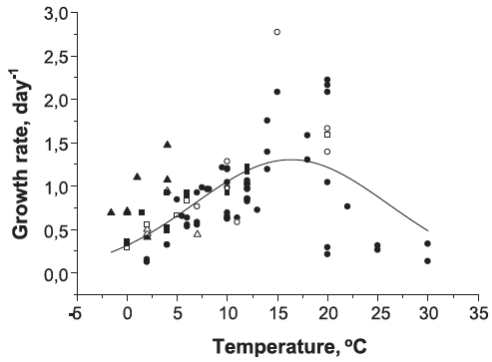

Fig. 3: Global compilation of *Phaeocystis* growth rates as a function of temperature by **Schoemann et al. (2005)**. Triangles represent *Phaeocystis Antarctica*, filled triangles its colonial stage.

To account for the different formulations to describe the temperature-limited growth rates of *Phaeocystis* and diatoms in ROMS-BEC in our analysis of their competition over time (section 3.4 of the manuscript), we directly compare the temperature-limited growth rates (in d^{-1}) rather than the growth limitation by temperature of these two phytoplankton types (see Eq. 2 of the manuscript).

SC5: *temperature-dependent growth functions of any organism group usually have a negatively skewed thermal reaction norm. This is also true for Phaeocystis antarctica. Since there already exists a mathematical description for the temperature-& light-dependent growth function of Phaeocystis antarctica (Moisan and Mitchell 2018), I wonder why the authors have not used it. In fact there are more recent observation-based publications on Phaeocystis antarctica that may be of interest for this study.*

We thank the reviewer for pointing us to the manuscript by **Moisan and Mitchell (2018)**, which we had not been aware of. In comparison to the formulation used in ROMS-BEC (**Geider et al., 1998**), the equations presented in **Moisan & Mitchell (2018)** include the possibility for photoinhibition at high light intensities (expressed by beta; **Platt et al. 1980**) and a temperature dependent initial slope of the photosynthesis-irradiance-curve (alpha), but do not explicitly account for all effects of photoacclimation in their equations that are included in ROMS-BEC (e.g., the local chlorophyll:carbon ratio of phytoplankton and the nutrient limitation of its growth, see Eq. 3a-3d in

Moisan & Mitchell, 2018 and Eq. B9 of the revised manuscript for ROMS-BEC). As a result, the set of equations provided by **Moisan & Mitchell (2018)** and the ones currently used in ROMS-BEC predict different temperature-light-limited net growth rates of *Phaeocystis antarctica* for any given temperature and PAR level (see Fig. 4 below). Furthermore, the ratio of the growth rate predicted by ROMS-BEC and that obtained with **Moisan & Mitchell (2018)** varies substantially across temperatures and light levels (see Fig. 4d).

Overall, as a result of the differences between the formulation in **Moisan & Mitchell (2018)** and that in **Geider et al. (1998)**, the light limitation of growth by *Phaeocystis* is generally lower in ROMS-BEC than that predicted with the equations by **Moisan & Mitchell (2018)**, leading to substantially higher net growth rates in the current model than would be predicted if we were to apply the parameterization in **Moisan & Mitchell (2018)** to describe temperature and light-limited growth of *Phaeocystis* in ROMS-BEC (especially at low PAR levels, see Fig. 4d below). Due to the impact of nutrient limitation and chlorophyll:carbon ratios on the simulated net growth rates in ROMS-BEC, implementing the formulation by **Moisan & Mitchell 2018** would lead to substantially lower *Phaeocystis* biomass south of 60°S and would require a major retuning in the model to facilitate any substantial biomass accumulation of *Phaeocystis antarctica* colonies relative to diatoms in the high-latitudes, where these two phytoplankton types have been shown to locally and temporarily reach equally high biomass concentrations (**Vogt et al., 2012; Leblanc et al., 2012**).

A further issue with the parameterization that we encounter is its applicability within the temperature regime that constitutes the ecological niche of *Phaeocystis* in ROMS-BEC. We note that the parametrization by **Moisan & Mitchell (2018)**, being derived from laboratory experiments conducted at temperatures between -1.5-4°C, is currently only defined for temperatures below 6.8°C, above which the predicted growth rate becomes ecologically meaningless due to a negative alpha value (whereas this value should be >0, as it describes the sensitivity of photosynthetic rates of phytoplankton to increases of irradiance levels at low light). Altogether, given that the equations by **Moisan & Mitchel (2018)** do not account for all effects of photoacclimation which are accounted for in ROMS-BEC for all phytoplankton types and given that the alphaPI currently used in ROMS-BEC is backed up by the literature review in **Schoemann et al. (2005)**, we refrain from implementing the formulation by **Moisan & Mitchell (2018)** at this stage.

Nevertheless, taken together, this highlights the uncertainty still associated with model formulations describing the growth of phytoplankton functional types in general and *Phaeocystis* in particular. In response to the reviewer, we have modified section 4.3 (Limitations & Caveats) and added the following statement in the revised version of the manuscript:

"Furthermore, other functional relationships than those used in ROMS-BEC exist to describe the light and temperature dependent growth of *Phaeocystis* (e.g. Moisan and Mitchell, 2018). In comparison to the equations used in ROMS-BEC (see appendix B), the ones suggested by Moisan and Mitchell (2018; based on laboratory cultures of *Phaeocystis antarctica* grown under continuous blue light and at 4 different temperatures between -1.5°C and 4°C) lead to generally lower *Phaeocystis* growth rates, especially at PAR<50 W m^{-2}, suggesting that our biomass estimates at high latitudes and early/late in the season are associated with substantial uncertainty."

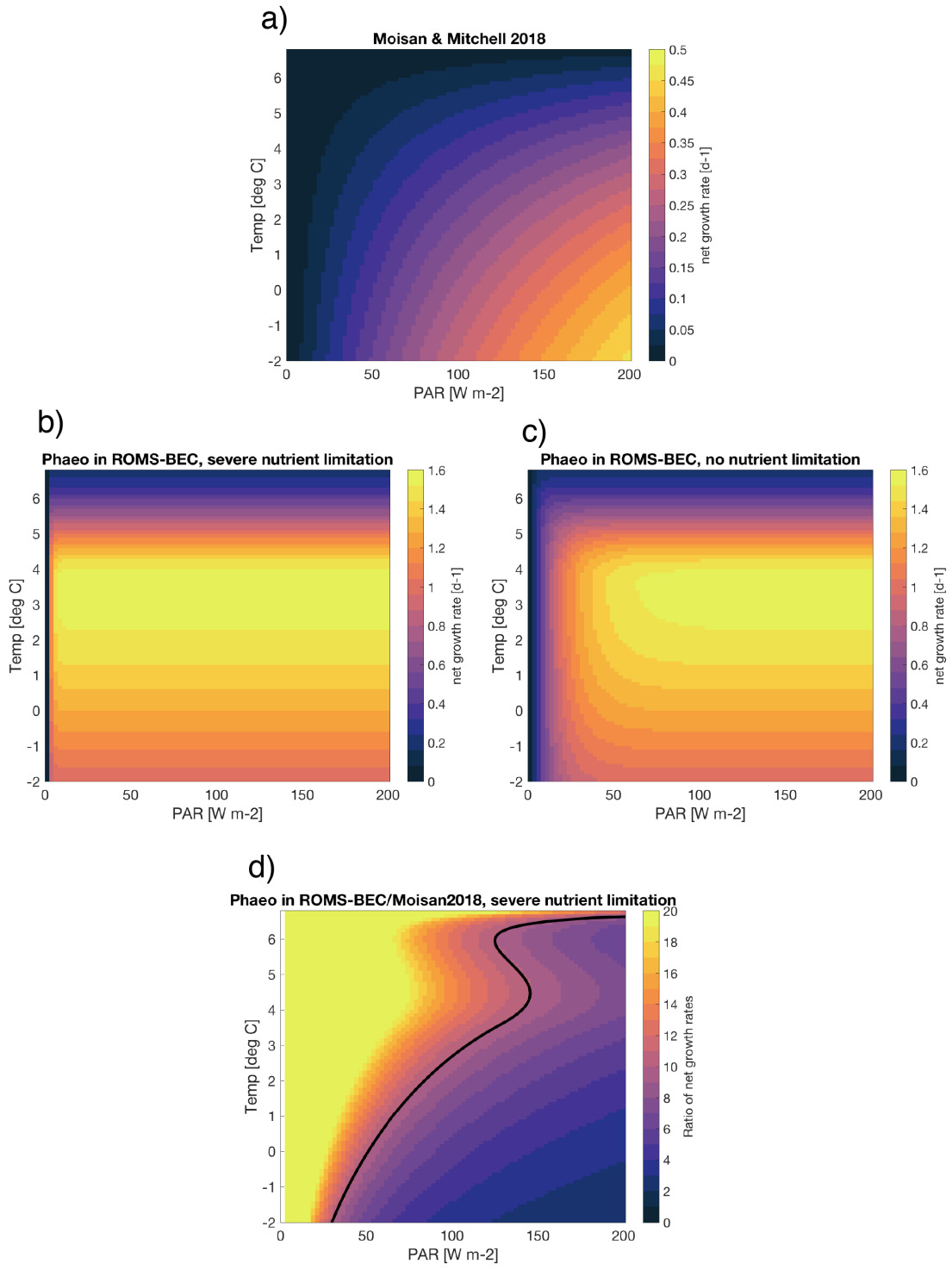

Fig. 4: a) Net growth rate of *Phaeocystis antarctica* as a function of temperature and light levels based on the equations in **Moisan & Mitchell (2018)**, assuming no photoinhibition (same as in ROMS-BEC), i.e., beta=0. b) & c) Same plot as a) obtained with the equations used in ROMS-BEC (see appendix B of revised manuscript and answer to SC3 above). Panel b) and c) show the resulting net growth rates for different nutrient conditions, with "severe nutrient limitation" in panel b) using g(N)=0.1 in Eq. B9 of the revised manuscript and "no nutrient limitation" in panel c) using g(N)=1. For both cases, we have here taken the surface annual average chlorophyll:carbon ratio of *Phaeocystis* in the *Baseline* simulation of the model (0.1434 mg chl / mmol C). Note that the formulation by **Moisan & Mitchell (2018)** does not account for the nutrient conditions or the chlorophyll:carbon ratio. Panel d) shows the ratio of panel a) and b), with the black contour denoting a 10-times higher growth rate in panel a) as compared to panel b).

SC6: *please specify which atmospheric forcing fields have been used.*
We refer the reviewer to L. 185/186 of the original version of the manuscript, where we state "At the ocean surface, the model is forced with a 2003-normal year forcing for momentum, heat, and freshwater fluxes (**Dee et al., 2011**)."

SC7: *model results: there is a mixture of model results, model evaluation, model comparison with results from previous experiments which makes it difficult to read and to follow the arguments; the entire results section needs to be revised.*

We thank the reviewer for this helpful comment, which made us reassess the chosen structure in the result section of the original version of manuscript, leading to changes in the revised version as outlined in the following. As we consider the addition of a new phytoplankton functional type a major change in the complexity of ROMS-BEC, we have decided to first present a thorough model evaluation of this new model setup by comparing to available observational data sets (sections 3.1 & 3.2). For the purpose of this study, a realistic representation of the high-latitude phytoplankton community structure in both space and time is essential to address the competition of *Phaeocystis* and diatoms throughout the year on the one hand and the implications for downward carbon fluxes on the other. This part of the result section therefore also had the purpose to highlight model improvements compared to the earlier version of the model without *Phaeocystis*, in order to stress why the 5-PFT setup was essential for the questions at hand. Thereafter, we first present a detailed analysis on the drivers of the competition between *Phaeocystis* and diatoms (sections 3.3 & 3.4 of the original manuscript) and secondly on the implications for downward carbon fluxes (section 3.5 of the original manuscript).

To increase the clarity of the result section and to overall better reflect the focus of the manuscript, sections 3.3 & 3.4 of the original manuscript are merged into a single section called "Drivers of SO phytoplankton biogeography, phenology, and succession patterns" in the revised version of the manuscript. This new section 3.3 was shortened in the merging process (see also SC8 & SC10), in order to better balance the two aspects of the study, namely the drivers of the competition between *Phaeocystis* and diatoms and the implications for high-latitude carbon cycling. Furthermore, the title of section 3.2 was changed in the revision process (now: "Patterns of phytoplankton phenology and seasonal succession"), so that the reader is more clearly guided throughout the result section, starting with a description of the simulated biogeography (section 3.1) and succession patterns (section 3.2) and ending with a description of the drivers of these spatial and temporal patterns (section 3.3) and their implications for carbon cycling (section 3.4). Please see also our answer to SC8-SC10 for more details.

SC8: *the sections about the ecological niches, bottom-up and top-down effects are tedious to read and questionable with respect to temperature (see my comments above).*

In the revised version of the manuscript, we tried to improve upon the readability of sections 3.3 and 3.4. In particular, we have moved the part on coccolithophores from section 3.3 of the original manuscript to the supplement, in order to focus more clearly on the main topic of this study, namely the competition between *Phaeocystis* and diatoms (see also our response to the reviewer's comment SC10). Furthermore, we have merged the sections 3.3 & 3.4 of the original manuscript into a single section in the revised version of the manuscript and revised its content in the process, in order to improve the readability (see also SC7). The revised section 3.3 of the manuscript reads:

3.3 Drivers of SO phytoplankton biogeography, phenology, and succession patterns

Relating the observed or simulated PFT biomass concentrations to the concurrent environmental conditions allows for an assessment of the ecological niche of the PFT in question. In ROMS-BEC, *Phaeocystis* and diatoms occupy distinct ecological niches in the *Baseline* simulation, in agreement with their distinct geographic distributions in summer (Fig. 1c-d). Between 40-90° S, the niche center of DJFM average *Phaeocystis* biomass is simulated at a nitrate concentration of 18.8 mmol m^{-3} (inter quartile range (IQR) 16.6-20.5 mmol m^{-3}), a temperature of 1.1° C (IQR -0.2-2.6° C), and MLPAR of 27.8 W m^{-2} (IQR 24.3-32 W m^{-2}, Fig. 4a & c). Since the diatom PFT in ROMS-BEC represents multiple species (in contrast to the *Phaeocystis* PFT), diatoms occupy a wider niche in temperature (IQR 0.8-8.5° C, niche center at 5° C) and nitrate (IQR 11-19.5 mmol m^{-3}, niche center at 15.5 mmol m^{-3}) in the model, which is in agreement with the ecological niches of important SO diatom and *Phaeocystis* species derived by Brun et al. (2015) based on presence/absence observations and species distribution models (Fig. 4a & b). In ROMS-BEC, the niche center is only at marginally higher MLPAR for diatoms than for *Phaeocystis* (28.9 W m^{-2} compared to 27.8 W m^{-2}, respectively, Fig. 4c & d) and is at higher MLPAR for both PFTs than available observations for important SO species suggest ($\sim$10 W m^{-2} and $\sim$20 W m^{-2} for *Phaeocystis* and diatoms, respectively, see Fig. 4c & d). While this bias in the MLPAR niche is consistent with the mixed layer depth bias in ROMS-BEC ($\sim$10 m; Nissen et al., 2018), the small difference in the MLPAR niche center between *Phaeocystis* and diatoms implies a minor role for MLPAR in controlling the differences in DJFM average biomass concentrations of these two PFTs (Fig. 1c-d). With regard to iron, the two PFTs do not occupy distinct ecological niches in ROMS-BEC (niche centers at 0.32 μmol m^{-3} for both PFTs, see Fig. S9). Yet, as all simulated phytoplankton growth is limited by iron availability in the high-latitude SO (Fig. S1), this suggests that the spatio-temporal averaging applied for the niche analysis here potentially precludes the assessment of the role of iron in the competition between *Phaeocystis* and diatoms, especially on a sub-seasonal scale. We conclude that the simulated ecological niches of *Phaeocystis* and diatoms are largely in agreement with available observations, but acknowledge the difficulties in comparing the ecological niche of a model PFT to those of individual phytoplankton species or groups, a sampling bias towards temperate and tropical species/strains and the overall low data coverage in the high-latitude SO in Brun et al. (2015), and the limitation of this niche analysis to inform about the role of top-down factors and sub-seasonal environmental variability in controlling the simulated biogeography of phytoplankton types.

The temporal evolution of the relative growth ratio, i.e., the ratio of the specific growth rates of diatoms and *Phaeocystis*, informs about the competitive advantage of one PFT over the other throughout the year due to bottom-up factors and can be broken down into the different environmental contributors for each phytoplankton type at any point in time (Eq. 2). In the 5-PFT *Baseline* simulation of ROMS-BEC, the relative growth ratio is only positive ($\mu^{D} > \mu^{PA}$) between early December and early February between 60-90° S (μ^{D} is on average 5% larger than μ^{PA} in summer, but 5-6% smaller in the other seasons, Fig. 5a & c) and only between mid-December and mid-January in the Ross Sea (μ^{PA} is up to 38% larger than μ^{D} in spring, Fig. 5b & d). Hence, bottom-up factors promote the accumulation of *Phaeocystis* relative to diatom biomass over much of the year, particularly in the Ross Sea. In both areas, as expected from the chosen half-saturation constants ($k_{Fe}^{PA} > k_{Fe}^{D}$; Table 1), the iron limitation of *Phaeocystis* growth is stronger than that of diatoms in the model, and iron availability is an advantage for diatoms at all times ($\beta_{Fe} > 0$; up to 14% stronger iron limitation of *Phaeocystis* in both areas in summer, blue areas in Fig. 5a-d). Yet, the two subareas differ in the simulated temperature and light limitation of growth of *Phaeocystis* and diatoms. Overall, temperature is limiting diatom growth more than *Phaeocystis* growth in both subareas throughout the year ($\beta_{T} < 0$), but this difference is rather small in summer between 60-90° S (5%, but up to 19% stronger growth limitation in the Ross Sea, red areas in Fig. 5a-d, see also Fig. A1). Similarly, the difference in light limitation between diatoms and *Phaeocystis* is rather small between 60-90° S (3-4% throughout the year, yellow areas in Fig. 5a & c), implying that their differences in α_{PI} (43% higher for *Phaeocystis*, see Table 1) are balanced by differences in photoacclimation in ROMS-BEC in this area (see Eq. B9 and Geider et al., 1998). In contrast, in the Ross Sea, differences in light limitation between diatoms and *Phaeocystis* are large, especially in spring (the growth of diatoms is 32% more light limited; Fig. 5b & d). Therefore, the difference in light limitation predominantly controls the seasonality of the relative growth ratio (Fig. 5b) and promotes the dominance of *Phaeocystis* over diatoms early in the growing season in this area in our model (Fig. 5j), which is not simulated when averaging over 60-90° S (Fig. 5i). Nevertheless, acknowledging the sensitivity of the simulated *Phaeocystis* and diatom biomass levels to all chosen model parameters describing the growth of the respective PFT (the annual mean biomass changes by >17% and >14% for *Phaeocystis* and diatoms, respectively, in the experiments TEMPERATURE, $ALPHA_{PI}$, and IRON, Fig. A2 & Fig. S11), the sensitivity simulations support the importance of light in controlling the annual mean high-latitude phytoplankton community structure for both subareas, as the elimination of the differences in α_{PI} between the PFTs results in the largest biomass changes both between 60-90° S (-76% and +52% for *Phaeocystis* and diatoms, respectively) and in the Ross Sea (-87% and +86%, Fig. A2). Altogether, in ROMS-BEC, differences in growth between diatoms and *Phaeocystis* are mostly controlled by seasonal differences in iron/temperature (60-90° S) and iron/light conditions (Ross Sea), respectively. Still, given the simulated growth

advantage of *Phaeocystis* throughout much of the growing season in both subareas, bottom-up factors alone cannot explain why *Phaeocystis* only dominates over diatoms temporarily (Fig. 5i & j), implying that top-down factors need to be considered to explain their biomass evolution in our model.

In both subareas, the simulated relative total loss ratio is positive throughout spring and summer, implying that the specific total loss rate of *Phaeocystis* is higher than that of diatoms ($\gamma^{PA}_{total} > \gamma^{D}_{total}$, see Eq. 6), which favors the accumulation of diatom biomass relative to that of *Phaeocystis* (Fig. 5e-h). In fact, the total loss rate of *Phaeocystis* is on average 17%/38% (60-90° S) and 18%/40% (Ross Sea) higher than that of diatoms in spring/summer (Fig. 5g & h), despite the higher prescribed maximum grazing rate on *Phaeocystis* in ROMS-BEC (Table 1). In the model, the relative total loss ratio is only negative in early fall in both subareas ($\gamma^{D}_{total} > \gamma^{PA}_{total}$, Fig. 5e & f), but the difference between diatoms and *Phaeocystis* in their specific total loss rates is rather small in this season (9% and 3% between 60-90° S and in the Ross Sea, respectively, Fig. 5g & h). In all top-down sensitivity experiments, the simulated change in *Phaeocystis* biomass levels is larger than for the bottom-up experiments (>20% for experiments GRAZING, AGGREGATION, and MORTALITY, see Fig. A2), and the dominance of *Phaeocystis* over diatoms increases in magnitude and duration both between 60-90° S and in the Ross Sea if disadvantages of *Phaeocystis* in the loss processes are eliminated (Fig. S11). The simulated seasonality of the total loss ratio is the result of the interplay between losses through grazing, aggregation, and non-grazing mortality of each phytoplankton type in ROMS-BEC (Eq. 6, colors in Fig. 5e-h). Of all three loss pathways, differences in aggregation losses in the *Baseline* simulation are largest between *Phaeocystis* and diatoms both between 60-90° S (up to 200% higher aggregation losses for *Phaeocystis* in summer, yellow in Fig. 5e & g) and in the Ross Sea (up to 250% higher in summer, Fig. 5f & h). In comparison, differences between *Phaeocystis* and diatoms in grazing (up to 16% and 14% between 60-90° S and in the Ross Sea, respectively) and mortality losses (50% everywhere) are considerably smaller (see blue and red areas in Fig. 5e-h, respectively), suggesting that aggregation losses predominantly contribute to the simulated differences in the total loss rates between *Phaeocystis* and diatoms.

In summary, between 60-90° S, the simulated growth advantage of *Phaeocystis* early in the season (facilitated by advantages in the temperature limitation of their growth) are not large enough to outweigh the disadvantages in iron limitation of their growth and in the biomass losses they experience. As a result, in spring and summer, *Phaeocystis* do not accumulate substantial biomass relative to (or even dominate over) diatoms in this subarea in ROMS-BEC. In the Ross Sea, however, the simulated growth advantages of *Phaeocystis* (resulting from advantages in the light and temperature limitation of their growth) are large enough to outweigh the disadvantages in iron limitation and specific biomass loss rates, allowing them to dominate over diatoms early in the growing season in our model and explaining the simulated succession from *Phaeocystis* to diatoms close to the Antarctic continent (see also section 3.2). Ultimately, this simulated spatio-temporal variability in the relative importance of *Phaeocystis* and diatoms has implications for SO carbon cycling, which we will assess in the following.

Regarding the importance of temperature, the reviewer is kindly referred to our answer to SC4.

SC9: *the section about carbon cycling arises out of sudden.*

We thank the reviewer for this important comment. We fully agree with the reviewer in that the parts on the cycling of carbon were not motivated thoroughly enough in the original version of the manuscript. In response, we have added this aspect to the title of the revised manuscript, so that it now better reflects the content of the study (see also SC1). Further, we have substantially rewritten the introduction, so that it now better reflects and motivates the aspects covered in the result section and discussed thereafter, in particular the implications of variability in phytoplankton community structure for downward fluxes of carbon at high SO latitudes. The reviewer is referred to our answer to GC1 for more details.

SC10: *figures: some of the selected figures are not convincing. Why focus sometimes on Phaeocystis and diatoms, sometimes on Phaeocystis, diatoms and coccolithophores and sometimes on all PFTs?*

In general, we decided to show all PFTs in the model validation (Fig. 1 & 2). Furthermore, we chose to show the whole phytoplankton community whenever showing averages/integrals over 30-90°S (Fig. 6 & 7), where coccolithophores and small phytoplankton are non-negligible members of the community. In the manuscript, Fig. 3 & 5 directly concern the competition of diatoms and *Phaeocystis* at high latitudes. In these areas, these two phytoplankton types contribute >90% of the simulated NPP, which is why no other PFT is included in these figures (see Table 3 and Fig. 2 of the manuscript).

The only exception to the above reasoning in the original manuscript is Figure 4, where we had decided to show coccolithophores in addition to diatoms and *Phaeocystis*, but not the small phytoplankton PFT. The choice "pro coccolithophores" and "contra small phytoplankton" was motivated by the fact that coccolithophores do occupy a niche that is distinct from that of diatoms and *Phaeocystis*, whereas small phytoplankton do less so and are therefore not shown. Yet, we thank the reviewer for pointing out that this choice might be confusing for the reader. In order to make the focus of the paper clearer, we changed Fig. 4 so that the new version of this figure shows diatoms & *Phaeocystis only* in the revised version of the manuscript, thus moving the niche plots for coccolithophores to the supplement (new Fig. S8, see Figure below). This way, Fig. 3-5 of the revised manuscript include only diatoms and *Phaeocystis*. Together with the substantial revisions of result sections 3.3 & 3.4 of the original manuscript (see SC7 & SC8), the result section of the revised version of the manuscript is thereby now more clearly divided into a descriptive part of the simulated patterns in space and time (partly including coccolithophores and small phytoplankton, sections 3.1 & 3.2), a section describing the drivers of the competition of *Phaeocystis* and diatoms at high latitudes (section 3.3) and its implications for carbon cycling (section 3.4).

In the method section 2.3.1 of the revised manuscript, we have added the following statement: "In section 3.3 of this manuscript, only the results for *Phaeocystis* and diatoms will be shown, the corresponding figures for coccolithophores can be found in the supplementary material (Fig. S8 & S9)."

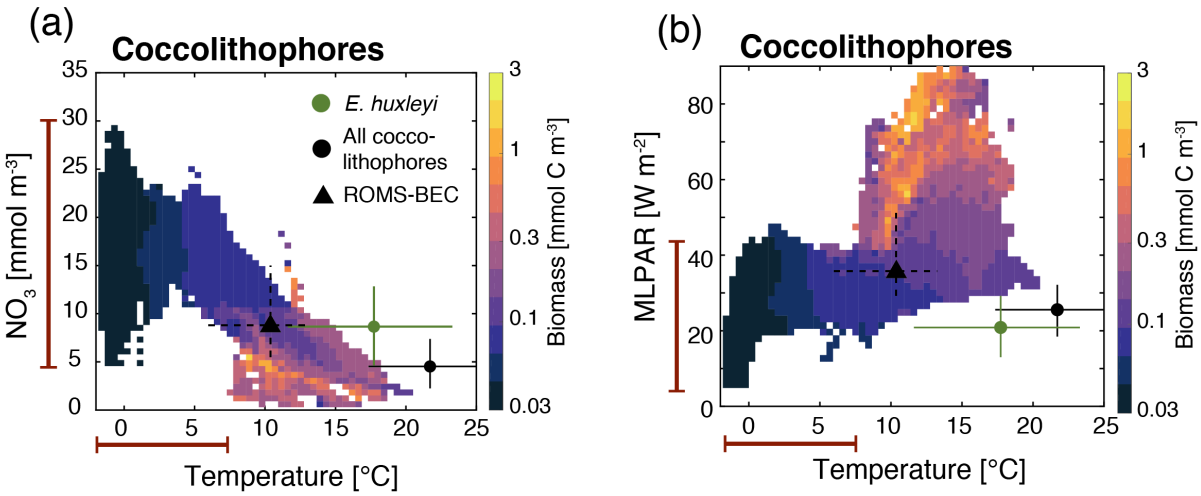

Fig. 5: Fig. S8 in the revised version of the manuscript

SC11: *Fig. 2 presents a rather artificial classification of the phytoplankton community. Why is the 25% used for Phaeocystis and coccolithophores but 75% for diatoms (Fig 2a)? Is "Mixed" (Fig. 2a) the same as "Others" (Fig. 2b-d)?*

Admittedly, the chosen thresholds are rather arbitrary and were chosen with the sole goal to indicate broad patterns of phytoplankton biogeography across the SO. The different thresholds for diatoms on the one hand and *Phaeocystis* and coccolithophores on the other hand were motivated by their different relative importance in their main region of occurrence. E.g., coccolithophores never dominate over diatoms, but still, we can define a clear SO coccolithophore biogeography – simply based on where they contribute most to NPP across the SO. If the 75% threshold was used for all PFTs, it would only be "diatoms" or "mixed". In this context, "mixed" denotes areas where diatoms do not contribute >75%, but neither coccolithophores nor *Phaeocystis* contribute >25%, e.g. if diatoms contribute 60% and coccolithophores and *Phaeocystis* 20%, respectively.

Consequently, "mixed" in panel a is not the same as "other" in panels b-d. As indicated in the method section 2.3.1 (L 224-226 of the original manuscript): *"The CHEMTAX analysis splits the*

phytoplankton community into diatoms, nitrogen fixers (such as Trichodesmium), pico-phytoplankton (such as Synechococcus and Prochlorococcus), dinoflagellates, cryptophytes, chlorophytes (all three combined into the single group "Others" here), and haptophytes (such as coccolithophores and Phaeocystis).”

In order to clarify this, areas, that were labeled “mixed” in the original version of Fig. 2a, are now labeled “co-existence” and we changed the figure caption accordingly. Furthermore, we added a statement in the figure caption in the revised version of the manuscript defining “others” in the panels including CHEMTAX information: “[…] “others” in the CHEMTAX fractions corresponds to dinoflagellates, cryptophytes, and chlorophytes […]”

SC12: *how does the annual or climatological “relative contribution of the five PFTs” looks like (and not the seasonal contribution as in Fig. 2b-c)? If such a figure were shown the statements in the paragraph l. 348–354 might be more comprehensible.*

We decided to only give the annual mean/integral numbers for NPP (see Table 3) and focus on the seasonal evolution for chlorophyll in Figure 2, which we can directly compare to HPLC-based estimates. The annual mean contribution to mixed layer chlorophyll levels of *Phaeocystis*/diatoms/coccolithophores amounts to 12.2/64.5/9.8 (30-90°S) and 31.1/54.8/2.4 (60-90°S) in our model, in rather close agreement with the estimates for NPP (15.3/53/14.6 between 30-90°S and 45.8/49.1/0.7 between 60-90°S, see Table 3).
Furthermore, we want to highlight the data scarcity in general and especially in all seasons besides summer in this context (see numbers printed below upper pie charts in Fig. 2), preventing a meaningful comparison of *annual mean* community structure in the model with the CHEMTAX data, which is why no annual mean figure is shown for the CHEMTAX data.

SC13: *Fig. 4 - why is silicate not chosen as an important factor for diatoms? At least in the northern part of the SO (south of ~40°S) diatoms are limited by silicate.*

As shown in Fig. S1, the reviewer is correct in pointing to a growth limitation of diatoms by silicic acid close to 40°S. Yet, as the focus of this paper is the competition between diatoms and *Phaeocystis*, which mainly takes place south of 60°S in ROMS-BEC, we chose not to show silicic acid as one of the environmental variables here, as the availability of silicic acid does not limit diatom growth in the focus area of this study. In fact, across Si levels, diatom biomass varies substantially south of 40°S (see Figure below), indicating that it is not a major control on diatom biomass levels in the area.
For completeness, we add the figure below to the supplementary material (Fig. S8 in original manuscript, S9 in revised version) in the revised version of the manuscript.

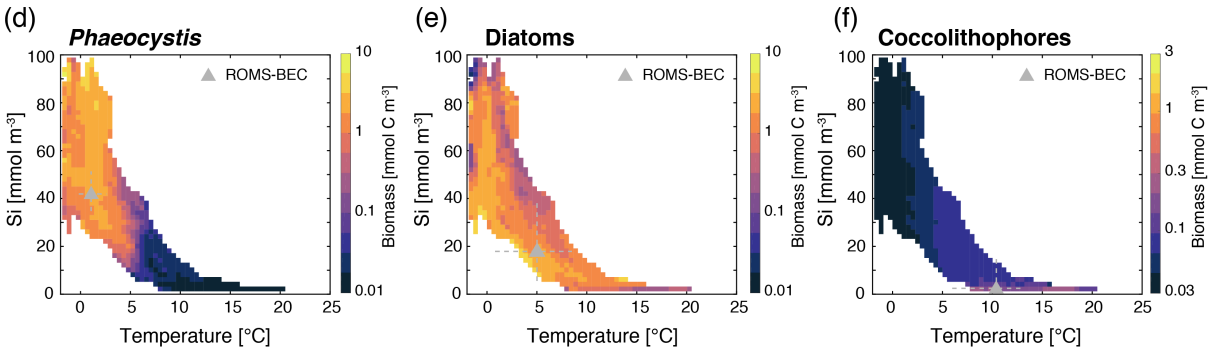

Fig. 6: Same as the ecological niche plots in Fig. 4 of the manuscript, but showing phytoplankton biomass as a function of silicic acid concentrations [mmol m^{-3}]. This figure will be added as Fig. S9 to the revised manuscript.

SC14: *the discussion and conclusion sections suffer from what I commented above. The authors must make clear what the paper is about in the first place. I am confident that also the discussion and conclusion section will then be easier to write.*

We thank the reviewer for this comment, in direct response to which we have made several modifications to the manuscript. Besides small modifications to the text of all discussion sections and the conclusion section to improve upon the clarity of the text and to better reflect the focus of the study, we have changed the order of discussion sections 4.1 & 4.2 in the revised version of the manuscript, so that it reflects the order in which these aspects are described in the result sections (first drivers, then biogeochemical implications).
Furthermore, we have moved the part about DMS from the method section 2.3.1 in the original version of the manuscript to the new discussion section 4.2, to more clearly focus the method section on aspects regarding carbon cycling, which is the main focus of the paper.

The part about DMS was shortened in the process, and the new paragraph reads:

Besides its impact on the carbon cycle, *Phaeocystis* is the major contributor to the marine sulphur cycle in the SO through its production of DMSP (Keller et al., 1989; Liss et al., 1994; Stefels et al., 2007). Though not explicitly including the biogeochemical cycling of sulphur, we can nevertheless use model output from ROMS-BEC to obtain an estimate of DMS production by *Phaeocystis* through a simple back-of-the-envelope calculation. Integrating the modeled *Phaeocystis* biomass loss rates via zooplankton grazing and non-grazing mortality over the top 10 m, assuming a molar DMSP:C ratio for *Phaeocystis* of 0.011 (Stefels et al., 2007), and a DMSP-to-DMS conversion efficiency between 0.2-0.7 (the DMS yield depends on the local sulphur demand of bacteria, Stefels et al., 2007; Wang et al., 2015), our estimated annual DMS production by *Phaeocystis* in ROMS-BEC amounts to 3.3-11.5 Tg S and 1.8-6.4 Tg S south of 30° S and 60° S, respectively. Consequently, assuming that all of this DMS production quickly escapes to the atmosphere, our estimates correspond to 11.6-40.1% (30-90° S) and 6.5-22.7% (60-90° S) of the global flux of DMS to the atmosphere previously estimated by Lana et al. (2011, 28.1 Tg S yr^{-1}). Our estimate is an upper bound, however, as not all DMS produced in seawater is readily released to the atmosphere. In fact, a fraction is likely broken down by bacteria, by photolysis, or is mixed down in the water column (see e.g. Simó and Pedrós-Alló, 1999; Stefels et al., 2007). Still, given that other phytoplankton types also produce DMS(P) (Keller et al., 1989; Stefels et al., 2007), the ROMS-BEC-based contribution of SO *Phaeocystis* alone (3.3-11.5 Tg S yr^{-1}) to the global flux of DMS to the atmosphere is in agreement with the flux suggested in Lana et al. (2011, 8.1 Tg S yr^{-1} south of 30° S, i.e., 29% of their global estimate), and the substantial contribution of SO *Phaeocystis* underpins its major role for the global cycling of sulphur.

Cited literature

Arrigo, K. R., Schnell, A., & Lizotte, M. P. (1998). Primary production in Southern Ocean waters. *Journal of Geophysical Research*, *103*(C8), 15587–15600. https://doi.org/10.1029/98JC00930

Boyd, P. W. (2019). Physiology and iron modulate diverse responses of diatoms to a warming Southern Ocean (supplement). *Nature Climate Change*, *9*(2), 148–152. https://doi.org/10.1038/s41558-018-0389-1

Brun, P., Vogt, M., Payne, M. R., Gruber, N., O'Brien, C. J., Buitenhuis, E. T., … Luo, Y.-W. (2015). Ecological niches of open ocean phytoplankton taxa. *Limnology and Oceanography*, *60*(3), 1020–1038. https://doi.org/10.1002/lno.10074

Buma, A. G. J., Bano, N., Veldhuis, M. J. W., & Kraay, G. W. (1991). Comparison of the pigmentation of two strains of the prymnesiophyte Phaeocystis sp. *Netherlands Journal of Sea Research*, *27*(2), 173–182. https://doi.org/10.1016/0077-7579(91)90010-X

Dee, D. P., Uppala, S. M., Simmons, A. J., Berrisford, P., Poli, P., Kobayashi, S., … Vitart, F. (2011). The ERA-Interim reanalysis: configuration and performance of the data assimilation system.

Quarterly Journal of the Royal Meteorological Society, *137*(656), 553–597. https://doi.org/10.1002/qj.828

Garcia, N., Sedwick, P., & DiTullio, G. (2009). Influence of irradiance and iron on the growth of colonial Phaeocystis antarctica: implications for seasonal bloom dynamics in the Ross Sea, Antarctica. *Aquatic Microbial Ecology*, *57*(2), 203–220. https://doi.org/10.3354/ame01334

Geider, R. J., MacIntyre, H. L., & Kana, T. M. (1998). A dynamic regulatory model of phytoplanktonic acclimation to light, nutrients, and temperature. *Limnology and Oceanography*, *43*(4), 679–694. https://doi.org/10.4319/lo.1998.43.4.0679

Leblanc, K., Arístegui, J., Armand, L., Assmy, P., Beker, B., Bode, A., … Yallop, M. (2012). A global diatom database – abundance, biovolume and biomass in the world ocean. *Earth System Science Data*, *4*(1), 149–165. https://doi.org/10.5194/essd-4-149-2012

Le Quéré, C., Harrison, S. P., Colin Prentice, I., Buitenhuis, E. T., Aumont, O., Bopp, L., … Wolf-Gladrow, D. (2005). Ecosystem dynamics based on plankton functional types for global ocean biogeochemistry models. *Global Change Biology*, *11*, 2016–2040. https://doi.org/10.1111/j.1365-2486.2005.1004.x

Le Quéré, C., Buitenhuis, E. T., Moriarty, R., Alvain, S., Aumont, O., Bopp, L., … Vallina, S. M. (2016). Role of zooplankton dynamics for Southern Ocean phytoplankton biomass and global biogeochemical cycles. *Biogeosciences*, *13*(14), 4111–4133. https://doi.org/10.5194/bg-13-4111-2016

Nissen, C., Vogt, M., Münnich, M., Gruber, N., & Haumann, F. A. (2018). Factors controlling coccolithophore biogeography in the Southern Ocean. *Biogeosciences*, *15*(22), 6997–7024. https://doi.org/10.5194/bg-15-6997-2018

Platt, T., Gallegos, C. L., & Harrison, W. G. (1980). Photoinhibition of Photosynthesis in Natural Assemblages of Marine Phytoplankton. *Journal of Marine Research*.

Schoemann, V., Becquevort, S., Stefels, J., Rousseau, V., & Lancelot, C. (2005). Phaeocystis blooms in the global ocean and their controlling mechanisms: a review. *Journal of Sea Research*, *53*(1–2), 43–66. https://doi.org/10.1016/j.seares.2004.01.008

Vogt, M., O'Brien, C., Peloquin, J., Schoemann, V., Breton, E., Estrada, M., … Peperzak, L. (2012). Global marine plankton functional type biomass distributions: *Phaeocystis* spp. *Earth System Science Data*, *4*(1), 107–120. https://doi.org/10.5194/essd-4-107-2012

Wang, S., & Moore, J. K. (2011). Incorporating Phaeocystis into a Southern Ocean ecosystem model. *Journal of Geophysical Research*, *116*(C1), C01019. https://doi.org/10.1029/2009JC005817

Answer to referee #2:

We thank referee #2 for taking the time to provide valuable comments and suggestions that have helped to improve our manuscript.

Below, we include our detailed answers to all comments and questions.

Answers to general comments (GC):

" […] a few additional sentences might help that discuss

***GC1**: The choice of food preferences and feeding parameterization of zooplankton. What I could find in preceding papers of the BEC model is that zooplankton is parameterized via fixed feeding preferences. However, other biogeochemical models have applied zooplankton grazing formulations that saturate with the total amount of food, or even employ a switching behaviour of zooplankton (see, e.g., Appendix A of the classic paper by Fasham et al., 1990, J. Mar. Res., 591-639). A few notes on that could complement the discussion; also, given that this process seems to be of importance, it might be helpful for the reader to have a brief explanation of the grazing formulation (and the preferences) in the methods description (so that the reader does not have to look up earlier papers).*

We thank the reviewer for raising this point. The reviewer is correct in that BEC currently assumes fixed feeding preferences, which are set by differences in the maximum grazing rate $\gamma_{g,max}$ across the PFTs. Here, based on size assumptions, we assume a preferential feeding of the single zooplankton grazer in ROMS-BEC on smaller phytoplankton (higher $\gamma_{g,max}$ for small phytoplankton and coccolithophores than larger ones like diatoms and *Phaeocystis*, see table 1 in manuscript). Similarly, we assume preferential feeding on diatoms relative to *Phaeocystis* colonies (see section 2.1 of the original version of the manuscript).

Admittedly, by only including a single grazer that includes characteristics of both micro- and macrozooplankton (see **Moore et al., 2002**, but especially **Sailley et al., 2013**), the grazing formulation in ROMS-BEC is likely overly simplistic (e.g. **Le Quéré et al. 2016**). Furthermore, not accounting for adaptive feeding preferences or for total biomass to saturate zooplankton feeding at high total biomass levels are major shortcomings of the current parametrization (**Vallina et al. 2014**; **Vallina and Le Quéré, 2011**). These can be expected to significantly alter the interactions of the zooplankton with each PFT over the course of the growing season by e.g. temporarily alleviating the grazing pressure on all or single phytoplankton PFTs. The inclusion of multiple zooplankton functional types in ROMS-BEC is planned in current and ongoing work in our lab, but goes beyond the scope of this paper. Rather, the action of the zooplankton FT upon its prey should be viewed as a closure term, with phyto- and zooplankton biomass tightly coupled in space and time.

To clarify for the reader what parametrizations are currently used in ROMS-BEC, we have included a full description of the model equations describing growth and loss rates of phytoplankton biomass, including the equation for grazing, in the appendix of the revised version of the manuscript (see also our answer to reviewer #1):

The single zooplankton grazer Z [mmol C m^{-3}] feeds on the respective phytoplankton $P^{\prime i}$ [mmol C m^{-3}] at a grazing rate γ_g^i [mmol C m^{-3} day^{-1}] that is given by:

$$\gamma_g^i = \gamma_{max}^i \cdot f^Z(T) \cdot Z \cdot \frac{P^{\prime i}}{z_{grz}^i + P^{\prime i}} \quad \text{(B12)}$$

with

$$f^Z(T) = 1.5 \cdot \exp\left(\frac{T - T_{ref}}{10°C}\right) \quad \text{(B13)}$$

In the discussion section 4.1, we have modified the text to mention the shortcomings of the grazing parametrization in ROMS-BEC more explicitly:

"Additionally, as discussed in Nissen et al. (2018), the lack of multiple zooplankton groups in the SO model (Le Quéré et al. 2016), and the parametrization of the single zooplankton grazer using fixed prey preferences and separate grazing on each prey using a Holling Type II function (Holling et al., 1959), which thus precluding a saturation of feeding at high total phytoplankton biomass, are major limitations of ROMS-BEC."

***GC2**: Aggregation: To my opinion, this term is somehow loosely defined in the present paper. Sometimes it is referred to as "mortality" (Table 1), sometimes as aggregation. Do phytoplankton become detritus after aggregation? But why? Theoretically, this process only describes that the cells or colonies collide and stick together - will they instantaneously stop being "green", i.e. cease photosynthesis and growth and become detritus? I assume that this is the case in the model, possibly with the argument that in this case they sink out of the euphotic quickly. However, given that in many cases aggregates ("marine snow") sink rather slowly, or not at all, this does not have to be the case. As for (a), given the large importance of this loss term for the simulated biogeochemistry, I would recommend some more in depth model description and discussion of this assumption"*

We thank the reviewer for this point and apologize for any confusion. Yes, phytoplankton biomass in ROMS-BEC immediately becomes detritus after aggregation, thus immediately stops being "green". We agree with the reviewer in that this is likely not what happens for small aggregates in the real ocean, which do not sink out of the euphotic zone rapidly, suggesting that current model formulations in ROMS-BEC and other models are overly simplistic (see e.g. **Laufkötter et al., 2016**). Assuming that aggregation is less effective in quickly removing the smaller phytoplankton cells from the upper ocean, aggregation is formulated to be more effective for larger phytoplankton in ROMS-BEC (in our case diatoms and *Phaeocystis* colonies). Still, once formed, no differentiation is made in the model in how quickly the particles are transferred to depth between POC originating from aggregated small phytoplankton cells and those from larger phytoplankton types. We note, however, that this differentiation is prevented by the currently used single POC class in the model (see also section 4.3 in the originally submitted manuscript, L. 657ff). Furthermore, ideally, aggregation losses of each PFT should be calculated based on total biomass rather than based on the biomass of each PFT separately and should additionally consider larger detritus particles (POC) of different size classes. Since the ROMS-BEC set-up we use currently uses an implicit sinking formulation in which POC is directly redistributed and remineralized across the water column upon its formation, this precludes a tracking of aggregates and their fate in space and time (**Lima et al., 2014**).

Overall, we fully agree with the reviewer that our model (and other models, see discussion in **Laufkötter et al., 2016**) would benefit from an increased complexity regarding the fate of biomass losses and the resulting particles, and quantitative relationships should be established as more observations become available to guide model parametrizations (see e.g. **Guidi et al., 2015**).

In direct response to the reviewer's comment, we have revised the text in the manuscript to make a clearer distinction between non-grazing mortality and aggregation. In particular, we have revised the respective part of method section 2.1, which now reads:

"Furthermore, based on the assumption that for a given biomass concentration, larger cells are more likely than smaller cells to form aggregates and to subsequently stop photosynthesizing and sink as POC, we use a higher quadratic loss rate for *Phaeocystis* (0.005 d^{-1}) than for diatoms (0.001 d^{-1}) in the model (see $\gamma_{a,0}$ in Table 1)."

In Table 1 of the revised manuscript, we refer to the constant $\gamma_{a,0}$ as "quadratic loss rate in aggregation" in the revised manuscript:

Table 1. BEC parameters controlling phytoplankton growth and loss for the five phytoplankton PFTs diatoms (D), *Phaeocystis* (PA), coccolithophores (C), small phytoplankton (SP), and diazotrophs (N). Z=zooplankton, P=phytoplankton, PI=photosynthesis-irradiance. If not given in section 2.1, the model equations describing phytoplankton growth and loss rates are given in Nissen et al. (2018).

Parameter	Unit	Description	D	PA	C	SP	N†
μ_{max}	d^{-1}	max. growth rate at 30° C	4.6	‡	3.8	3.6	0.9
Q_{10}		temperature sensitivity	1.55	‡	1.45	1.5	1.5
k_{NO3}	mmol m^{-3}	half-saturation constant for NO_3	0.5	0.5	0.3	0.1	1.0
k_{NH4}	mmol m^{-3}	half-saturation constant for NH_4	0.05	0.05	0.03	0.01	0.15
k_{PO4}	mmol m^{-3}	half-saturation constant for PO_4	0.05	0.05	0.03	0.01	0.02
k_{DOP}	mmol m^{-3}	half-saturation constant for DOP	0.9	0.9	0.3	0.26	0.09
k_{Fe}	μmol m^{-3}	half-saturation constant for Fe	0.15	0.2	0.125	0.1	0.5
k_{SiO3}	mmol m^{-3}	half-saturation constant for SiO_3	1.0	-	-	-	-
α_{PI}	$\frac{mmol\ C\ m^2}{mg\ Chl\ W\ s}$	initial slope of PI-curve	0.44	0.63	0.4	0.44	0.38
$\gamma_{g,max}$	d^{-1}	max. growth rate of Z grazing on P	3.8	3.6	4.4	4.4	3.0
z_{grz}	mmol m^{-3}	half-saturation constant for ingestion	1.0	1.0	1.05	1.05	1.2
$\gamma_{m,0}$	d^{-1}	linear non-grazing mortality	0.12	0.18	0.12	0.12	0.15
$\gamma_{a,0}$	$\frac{m^3}{mmol\ C\ d}$	quadratic loss rate in aggregation	0.001	0.005	0.001	0.001	-
r_g	-	fraction of grazing routed to POC	0.3	0.42	0.2	0.05	0.05

† Compared to Nissen et al. (2018), the k_{Fe} of diazotrophs in ROMS-BEC is higher than for all other PFTs, consistent with literature reporting high Fe requirements of *Trichodesmium* (Berman-Frank et al., 2001). Furthermore, the maximum grazing rate on diazotrophs is lowest in the model (Capone, 1997). Still, diazotrophs continue to be a minor player in the SO phytoplankton community, contributing <1% to domain-integrated NPP in ROMS-BEC.

‡ The temperature-limited growth rate of *Phaeocystis* is calculated based on an optimum function according to Eq. 1 (see also Fig. A1a).

Furthermore, in order to make the differences between all the loss terms in the model more apparent, we have added a full description of the model equations as an appendix in the revised version of the manuscript (see also our response to reviewer #1). There, we have also included a sentence stating that phytoplankton in the model stop photosynthesizing upon aggregation:

Phytoplankton P'^i [mmol C m^{-3}] aggregate at an aggregation rate γ_a^i [mmol C m^{-3} day^{-1}] which is computed with the quadratic mortality rate constants $\gamma_{a,0}^i$ ([m^3 (mmol C)$^{-1}$ d^{-1}], Table 1) and :

$$\gamma_a^i = \min(\gamma_{a,max}^i \cdot P'^i, \gamma_{a,0}^i \cdot P'^i \cdot P'^i) \quad \text{(B15)}$$

$$\gamma_a^i = \max(\gamma_{a,min}^i \cdot P'^i, \gamma_a^i) \quad \text{(B16)}$$

In ROMS-BEC, $\gamma_{a,min}^i$ is 0.01 day^{-1} for small phytoplankton and coccolithophores and 0.02 day^{-1} for *Phaeocystis* and diatoms, and with $\gamma_{a,max}^i$ being 0.9 day^{-1} for *Phaeocystis*, diatoms, coccolithophores, and small phytoplankton. Note that phytoplankton immediately stop photosynthesizing upon aggregation and that aggregation losses do not occur for diazotrophs in ROMS-BEC.

As an important caveat of this study, we have added the following sentences regarding the current formulation of aggregation in ROMS-BEC in section 4.1 of the revised manuscript:

«Here, our findings suggest an important role for biomass loss processes in controlling the relative importance of *Phaeocystis* and diatoms in ROMS-BEC, but very little quantitative information exists to constrain model parameters (see section 2.1) or to validate the simulated non-grazing mortality, grazing, or aggregation loss rates of *Phaeocystis* and diatoms over time. **Certainly, the simulated aggregation rates in the model and their impact on spatio-temporal distributions of PFT biomass concentrations and rates of NPP are associated with substantial uncertainty due to the immediate conversion of biomass to sinking detritus in the model, the equal treatment of POC originating from all PFTs, the neglect of disaggregation, and due to the calculation of aggregation rates based on the biomass concentrations of individual PFTs rather than all PFTs or even particles combined (see e.g. Turner, 2015).**»

Answers to specific comments (SC):

SC1: *Table 1 and line 175: The unit of quadratic mortality (aggregation) is given as 1/d. Shouldn't it be 1/((mmol N/m3)*d), given that it will be multiplied with the squared concentration?*
We thank the reviewer for this comment. The unit of the constant $\gamma_{a,0}$ given in Table 1 should indeed be 1/(mmol C m-3 d-1) and we have corrected this in the revised version of the manuscript (see also the revised Table 1 on the previous page). Furthermore, in response to a comment by reviewer #1, we have provided a full description of the model equations describing phytoplankton growth and loss in the appendix of the revised version of the manuscript.

SC2: *Line 184: "we use monthly climatological fields for all tracers" - For all nutrients? Dissolved inorganic tracers? Please specify.*
Yes, we use monthly climatological fields for all nutrient tracers. We used climatological data from World Ocean Atlas 2013 for all macronutrients (**Garcia et al., 2013**), data from GLODAP for DIC and alkalinity (**Lauveset et al., 2016**), and climatological output fields from a global simulation with CESM-BEC for ammonium, dissolved inorganic Fe, and all dissolved organic phases of the nutrients (DOC, DOP, DOPr, DON, DONr, DOFe, **Yang et al., 2017**).

SC3: *Lines 197-214, spin up procedure of the coupled model: here a simple diagram of the spinup procedure could help a lot! E.g. (if I understood correctly), ...30y physics.....10yBEC...10yBaseline (5 yr analysis)..10ySensitivity (5 yr analysis)*
Indeed, the reviewer has understood our procedure of the model simulations correctly. Given that the results presented in this study are not qualitatively dependent on the exact years analyzed (due to the climatological forcing applied in the simulations) and in light of the length of the manuscript, we refrain from adding another figure after careful consideration of the issue. However, we have slightly modified the description of the setup of the sensitivity experiments to make things even clearer:

"All sensitivity experiments use the same physical and biogeochemical spin-up as the *Baseline* simulation and start from the end of year 10 of the coupled ROMS-BEC spin-up."

SC4: *Line 275: "phytoplankton biomass ... is the balance" - I suggest to rephrase this as "phytoplankton biomass ... is determined by the balance"*
We have rephrased as suggested.

SC5: *Line 320 and elsewhere: "In ROMS-BEC" - I assume what is referred to here is the baseline experiment? If so, I'd suggest to use "Baseline", to not confuse this simulation with the earlier non-Phaeocystis model and simulation.*

We have modified the indicated sentence to start by "In the 5-PFT *Baseline* simulation of ROMS-BEC, […]". Furthermore, for the revised version of the manuscript, we have double-checked the whole text and clarified wherever we thought confusion was possible.

SC6: *Figure 4: The upper and lower panels would be easier to compare if in the lower panels the x- and y-axis were swapped (i.e., to have always temperature on the x-axis.*

We thank the reviewer for this excellent suggestion regarding Fig. 4. We have adopted this in the revised version of the manuscript (see Figure below). Furthermore, in response to a comment by reviewer #1, we have additionally moved the panels showing the ecological niches of coccolithophores to the supplementary material, in order to focus the manuscript earlier on the competition between *Phaeocystis* and diatoms.

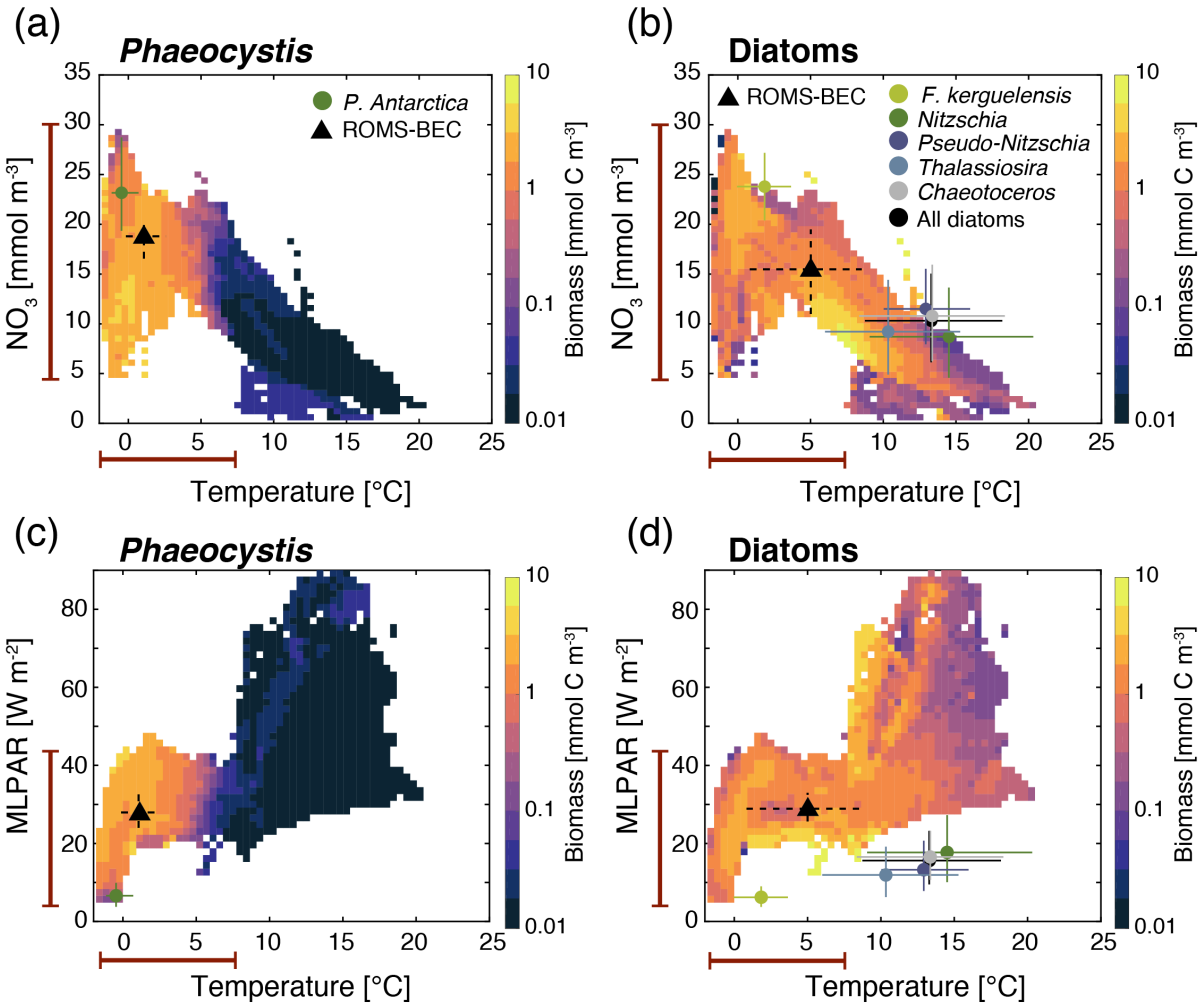

Fig. 1: Revised version of Fig. 4 in the manuscript.

SC7: *Figure 5: The caption could also note over what depth these terms were calculated.*

We have modified the figure caption to state that Fig. 5 only shows the quantities at the surface:

"For all metrics, the left panels are surface averages over 60-90° S and those on the right for the Ross Sea."

We note that this choice is mainly motivated by the higher available temporal frequency in the necessary output variables. Overall, the dynamics of the seasonal competition between diatoms and *Phaeocystis* also broadly hold (at least qualitatively) for averages over the mixed layer over the growing season (not shown).

SC8: *Figure 6: If I add up the different contributions to POC formation in the right panel (60- 90S) I end up with (6+17+4(bluearrow)+0.2+0.1+13+9=49.3% but the p-ratio is given as 45%. Does the blue arrow not contribute to the total flux? If so, then in the left panel the p-ratio should be 3+19+0.8+3+5+2=32.8% (and not 37%). Please clarify.*

We thank the reviewer for spotting this inconsistency of the numbers, as there was indeed a mistake in the figure in the submitted manuscript regarding the individual pathways leading to POC production (i.e., the indicated p ratio was correct). As a result of correcting the respective factor applied in the post-processing of the model output, the fraction of grazing on *Phaeocystis* leading to POC production

are now corrected down to 3.4% (5% before) and 9.2% (13% before) for 30-90°S and 60-90°S, respectively (see corrected Fig. 6 below).

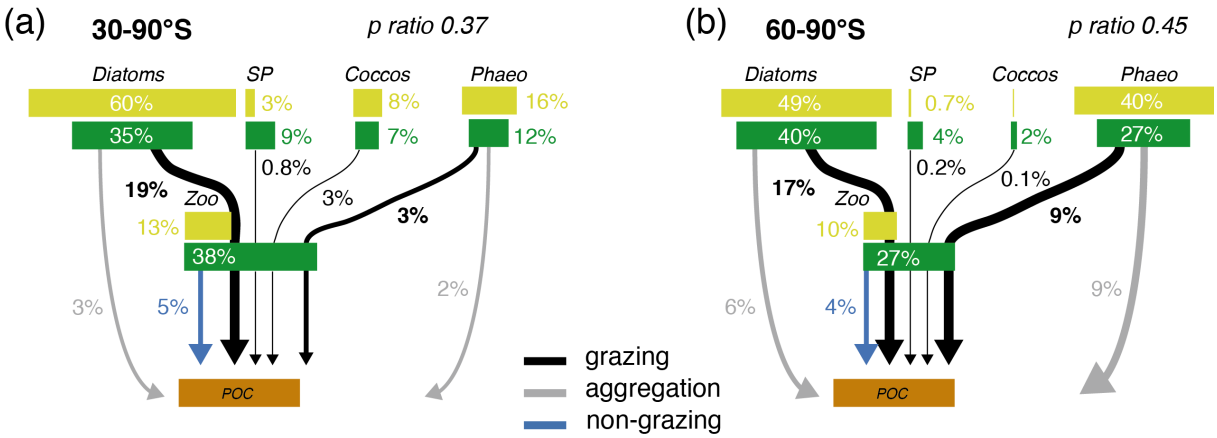

Fig. 2: revised Fig. 6 of the manuscript.

While this does not affect the general conclusion from this analysis, we note that this affects the discussion in the text (see below). While grazing remains the main POC production pathway for *Phaeocystis*, the difference to aggregation is now minor at high latitudes (9.2% for grazing, 8.9% for aggregation).

Accordingly, we reformulate the corresponding part of the manuscript, which now reads:

"For both diatoms and *Phaeocystis*, grazing by zooplankton (i.e., the formation of fecal pellets) is the most important pathway of POC production in ROMS-BEC (black arrows in Fig. 6, 9%/52% and 20%/37% of total POC production for *Phaeocystis*/diatoms between 30-90° S and 60-90° S, respectively). Yet, at high latitudes (60-90° S), aggregation of *Phaeocystis* biomass contributes *equally* to POC formation. "

Furthermore, we corrected a minor mistake in the caption of Fig. 6, where we falsely stated that the numbers describing the importance of the respective POC production pathway relative to total NPP were rounded to the nearest integer if they were >0.5%. Instead, this is only the case if the contribution of a respective pathway is >1%.

Cited literature

Garcia, H. E., Locarnini, R. A., Boyer, T. P., Antonov, J. I., Baranova, O. K., Zweng, M. M., … Johnson, D. R. (2013). *World Ocean Atlas 2013, Volume 4 : Dissolved Inorganic Nutrients (phosphate, nitrate, silicate)*. (S. (Ed. . Levitus & A. (Technical E. . Mishonov, Eds.) (Vol. 4). NOAA Atlas NESDIS 76.

Guidi, L., Legendre, L., Reygondeau, G., Uitz, J., Stemmann, L., & Henson, S. A. (2015). A new look at ocean carbon remineralization for estimating deepwater sequestration. *Global Biogeochemical Cycles*, *29*(7), 1044–1059. https://doi.org/10.1002/2014GB005063

Laufkötter, C., Vogt, M., Gruber, N., Aumont, O., Bopp, L., Doney, S. C., … Völker, C. (2016). Projected decreases in future marine export production: the role of the carbon flux through the upper ocean ecosystem. *Biogeosciences*, *13*(13), 4023–4047. https://doi.org/10.5194/bg-13-4023-2016

Lauvset, S. K., Key, R. M., Olsen, A., Van Heuven, S., Velo, A., Lin, X., … Watelet, S. (2016). A new global interior ocean mapped climatology: The 1° × 1° GLODAP version 2. *Earth System Science Data*, *8*(2), 325–340. https://doi.org/10.5194/essd-8-325-2016

Le Quéré, C., Buitenhuis, E. T., Moriarty, R., Alvain, S., Aumont, O., Bopp, L., … Vallina, S. M. (2016). Role of zooplankton dynamics for Southern Ocean phytoplankton biomass and global biogeochemical cycles. *Biogeosciences*, *13*(14), 4111–4133. https://doi.org/10.5194/bg-13-4111-2016

Lima, I. D., Lam, P. J., & Doney, S. C. (2014). Dynamics of particulate organic carbon flux in a global ocean model. *Biogeosciences*, *11*(4), 1177–1198. https://doi.org/10.5194/bg-11-1177-2014

Moore, J. K., Doney, S. C., Kleypas, J. A., Glover, D. M., & Fung, I. Y. (2002). An intermediate complexity marine ecosystem model for the global domain. *Deep Sea Research Part II: Topical Studies in Oceanography*, *49*(1–3), 403–462. https://doi.org/10.1016/S0967-0645(01)00108-4

Sailley, S. F., Vogt, M., Doney, S. C., Aita, M. N., Bopp, L., Buitenhuis, E. T., … Yamanaka, Y. (2013). Comparing food web structures and dynamics across a suite of global marine ecosystem models. *Ecological Modelling*, *261–262*, 43–57. https://doi.org/10.1016/j.ecolmodel.2013.04.006

Vallina, S. M., Ward, B. A., Dutkiewicz, S., & Follows, M. J. (2014). Maximal feeding with active prey-switching: A kill-the-winner functional response and its effect on global diversity and biogeography. *Progress in Oceanography*, *120*, 93–109. https://doi.org/10.1016/j.pocean.2013.08.001

Vallina, S. M., & Le Quéré, C. (2011). Stability of complex food webs: Resilience, resistance and the average interaction strength. *Journal of Theoretical Biology*, *272*(1), 160–173. https://doi.org/10.1016/j.jtbi.2010.11.043

Yang, S., Gruber, N., Long, M. C., & Vogt, M. (2017). ENSO-Driven Variability of Denitrification and Suboxia in the Eastern Tropical Pacific Ocean. *Global Biogeochemical Cycles*, *31*(10), 1470–1487. https://doi.org/10.1002/2016GB005596

Factors controlling the competition between *Phaeocystis* and diatoms in the Southern Ocean and implications for carbon export fluxes

Cara Nissen[1] and Meike Vogt[1]

[1]Institute for Biogeochemistry and Pollutant Dynamics, ETH Zürich, Universitätstrasse 16, 8092 Zürich, Switzerland

Correspondence: C. Nissen (cara.nissen@usys.ethz.ch)

Abstract. The high-latitude Southern Ocean phytoplankton community is shaped by the competition between *Phaeocystis* and silicifying diatoms, with the relative abundance of these two groups controlling primary and export production, the production of dimethylsulfide, the ratio of silicic acid and nitrate available in the water column, and the structure of the food web. Here, we investigate this competition using a regional physical-biogeochemical-ecological model (ROMS-BEC) configured at eddy-permitting resolution for the Southern Ocean south of 35° S. We extended ROMS-BEC by an explicit parameterization of *Phaeocystis* colonies, so that the model, together with the previous addition of an explicit coccolithophore type, now includes all biogeochemically relevant Southern Ocean phytoplankton types. We find that *Phaeocystis* contribute 46% and 40% to annual NPP and POC export south of 60° S, respectively, making them an important contributor to high-latitude carbon cycling. In our simulation, the relative importance of *Phaeocystis* and diatoms is mainly controlled by the temporal variability in temperature and iron availability. The higher light sensitivity of *Phaeocystis* at low irradiances promotes the succession from *Phaeocystis* to diatoms in more coastal areas, such as the Ross Sea. Still, differences in the biomass loss rates, such as aggregation or grazing by zooplankton, need to be considered to explain the simulated seasonal biomass evolution and carbon export fluxes.

1 Introduction

~~Unused nutrients from~~ Phytoplankton production in the Southern Ocean (SO) ~~fuel global primary and export production (e.g. Sarmiento et al., 2004; Palter et al., 2010), and the~~ regulates not only the uptake of anthropogenic carbon in marine food-webs, but also controls global primary production via the lateral export of nutrients to lower latitudes (e.g. Sarmiento et al., 2004; Palter et al., 201 The amount and stoichiometry of these laterally exported nutrients is determined by the combined action of multiple types of phytoplankton with ~~different~~ differing ecological niches and nutrient requirements. ~~As on-going climate change alters the~~ Yet, despite their important role, the drivers of phytoplankton biogeography and competition and the relative contribution of different phytoplankton groups to ~~total net primary production (NPP; IPCC, 2014; Constable et al., 2014; Deppeler and Davidson, 2017), this will hence have ramifications for global biogeochemical cycles and food web structure (Smetacek et al., 2004).~~ SO carbon cycling are still poorly quantified. Today, the SO phytoplankton community is largely dominated by silicifying diatoms ~~(e.g. Swan et al., 2016), but the contributions of~~ that efficiently fix and transport carbon from the surface ocean to depth (e.g. Swan et al., 2016) and have been suggested to be the major contributor to SO carbon export (Buesseler, 1998; Smetacek et al., 2012).

However, calcifying coccolithophores and dimethylsulfide (DMS) producing *Phaeocystis* ~~are substantial in the~~ have been found to contribute in a significant way to total phytoplankton biomass at subantarctic (Balch et al., 2016; Nissen et al., 2018) and ~~in the~~ at high latitudes, respectively (Smith and Gordon, 1997; Arrigo et al., 1999; DiTullio et al., 2000; Poulton et al., 2007), thus suggesting that the succession and competition of different plankton groups governs biogeochemical cycles at the (sub)regional scale. As climate change is expected to differentially impact the competitive fitness of different phytoplankton groups and ultimately their contribution to total net primary production (NPP; IPCC, 2014; Constable et al., 2014; Deppeler and Davidson, 2017), with a likely increase in the relative importance of ~~the latter two types~~ coccolithophores and *Phaeocystis* in a warming world ~~(Bopp et al., 2005; Winter et al., 2013; Rivero-Calle et al., 2015). On a global scale,~~ at the expense of diatoms (Bopp et al., 2005; Winter et the resulting change in SO phytoplankton community structure is likely to affect global nutrient and carbon distributions, ocean carbon uptake, and marine food web structure (Smetacek et al., 2004). While a number of recent studies have elucidated the importance of coccolithophores for subantarctic carbon cycling (e.g. Rosengard et al., 2015; Balch et al., 2016; Nissen et al., 2018; Rigual few estimates quantify the role of present and future high-latitude SO phytoplankton community structure for ecosystem services such as NPP and carbon export.

Phaeocystis ~~has been suggested to be a major player in the marine cycling of DMS (e.g. Keller et al., 1989; Liss et al., 1994) and to contribute 6-65% to total phytoplankton carbon biomass (Buitenhuis et al., 2013b). Yet, the contribution of~~ blooms in the SO have been regularly observed in early spring at high SO latitudes (especially in the Ross Sea, see e.g. Smith et al., 2011), thus preceding those of diatoms (Green and Sambrotto, 2006; Peloquin and Smith, 2007; Alvain et al., 2008; Arrigo et al., 2017; Ryan-Keogh e and *Phaeocystis* ~~to the export of particulate organic carbon (POC) is still subject to debate. While some have found blooms of~~ can dominate over diatoms in terms of carbon biomass at regional and sub-annual scales (e.g. Smith and Gordon, 1997; Alvain et al., 2008; Nevertheless, *Phaeocystis* ~~to be important vectors of carbon transfer to depth through the formation of aggregates (Asper and Smith, 1999; E others suggest their biomass losses to be efficiently degraded in the upper water column through bacterial and zooplankton activity, making *Phaeocystis* a minor contributor to POC export (Gowing et al., 2001; Accornero et al., 2003; Reigstad and Wassmann, 200~~

~~Possibly, the~~ is not routinely included as a phytoplankton functional type (PFT) in global biogeochemical models, possibly a result of the limited number of biomass validation data (Vogt et al., 2012) and its complex life cycle ~~of~~ (Schoemann et al., 2005). In particular, *Phaeocystis* ~~contributes to their apparent spatio-temporally varying relative importance for total biomass and POC export: Having a polymorphic life cycle, *Phaeocystis* alternates~~ is difficult to model because traits linked to biogeochemistry-related ecosystem services, such as size and carbon content, vary due to its complex multi-stage life cycle. Its alternation between solitary cells of a few μm in diameter and gelatinous colonies of several mm to cm in diameter ~~(e.g. Rousseau et al., 1994; Peperzak, 2000; Chen directly impacting~~ (e.g. Rousseau et al., 1994; Peperzak, 2000; Chen et al., 2002; Bender et al., 2018) directly impacts community biomass partitioning and the ~~fate of~~ relative importance of aggregation, viral lysis, and grazing for *Phaeocystis* biomass losses~~(Schoemann et al., 2005; Tang et al., 2008). While the factors controlling colony formation and disruption are still not fully clear (see review by Schoemann et al., 2005), the colonial form of~~, its susceptibility to zooplankton grazing relative to that of diatoms (Granéli et al., 1993; Smith et al., 2003), and ultimately the export of particulate organic carbon (POC; Schoemann et al., 20 With *Phaeocystis* ~~typically dominates~~ colonies typically dominating over solitary cells ~~in~~ during the SO growing season (Smith

et al., 2003)~~and regionally and temporarily over diatoms in terms of carbon biomass(e.g. Smith and Gordon, 1997; Leblanc et al., 2012; Vog~~ , *Phaeocystis* biomass loss via aggregation possibly increases in relative importance at the expense of grazing as more colonies are formed and colony size increases (Tang et al., 2008). Altogether, this implies a complex seasonal variability in the magnitude and pathways of carbon transfer to depth as the phytoplankton community changes throughout the year, which is difficult to comprehensively assess through in situ studies and therefore calls for marine ecosystem models.

~~To better quantify the effect~~ Across those marine ecosystem models including a *Phaeocystis* PFT, the representation of its life cycle differs in terms of complexity (Pasquer et al., 2005; Tagliabue and Arrigo, 2005; Wang and Moore, 2011; Le Quéré et al., 2016; Kauf While some models include rather sophisticated parametrizations to describe life cycle transitions (accounting for nutrient concentrations, li the majority includes rather simple transition functions (accounting for iron concentrations only, see Losa et al., 2019) or only the colonial life stage of *Phaeocystis* (Tagliabue and Arrigo, 2005; Wang and Moore, 2011; Le Quéré et al., 2016). Despite these differences, all of the models see improvements in the simulated SO phytoplankton biogeography as compared to observations upon the implementation of a *Phaeocystis* PFT. In particular, Wang and Moore (2011) find that *Phaeocystis* contributes substantially to SO integrated annual NPP and POC export (23% and 30% south of 60° S, respectively; Wang and Moore, 2011 implying that models not accounting for *Phaeocystis* possibly overestimate the role of diatoms for high-latitude phytoplankton biomass, NPP, and POC export (Laufkötter et al., 2016). Overall, the link between ecosystem composition, ecosystem function, and global biogeochemical cycling in general (e.g. Siegel et al., 2014; Guidi et al., 2016; Henson et al., 2019) and the contribution of *Phaeocystis* ~~on downward fluxes of carbon and nutrient distributions, factors controlling their biomass distributions need to be understood.~~ to SO export of POC in particular are still under debate. While some have found blooms of *Phaeocystis* to be important vectors of carbon transfer to depth through the formation of aggregates (Asper and Smith, 1999; DiTullio et al., 2000; Ducklow e others suggest their biomass losses to be efficiently degraded in the upper water column through bacterial and zooplankton activity, making *Phaeocystis* a minor contributor to SO POC export (Gowing et al., 2001; Accornero et al., 2003; Reigstad and Wassmann, This demonstrates the major existing uncertainty in how the high-latitude phytoplankton community structure impacts carbon export fluxes.

In general, the relative importance of different phytoplankton types for total phytoplankton biomass is controlled by a combination of ~~bottom-up, i.e. physical and biogeochemical variables impacting phytoplankton growth, and~~ top-down factors, i.e. processes impacting phytoplankton biomass loss such as grazing by zooplankton, aggregation of cells and subsequent sinking, or viral lysis~~(Le Quéré et al., 2016). Taking a bottom-up perspective, different phytoplankton types are often grouped in environmental niche space according to their preferred light and nutrient levels (Margalef, 1978; Reynolds, 2006). In the scheme by Reynolds (2006), R-strategists (low-light-high-nutrient) and S-strategists (high-light-low-nutrient) are found at opposite locations in the niche space.In this context, colonial and solitary cells of *Phaeocystis* can be grouped as R-~~ , and ~~S-strategists, respectively, as *Phaeocystis* colonies are known to have a significantly lower affinity for nutrients, such as iron, than solitary cells (Veldhuis et al., 1991). Accordingly, colonial *Phaeocystis* are more similar to large diatoms, growing fast under nutrient/iron-replete conditions at relatively low light levels (see review by Schoemann et al., 2005). Consequently, the~~ bottom-up factors, i.e. physical and biogeochemical variables impacting phytoplankton growth (Le Quéré et al., 2016). The observed spatio-temporal differences in the relative importance of *Phaeocystis* and diatoms in the SO are thought to be largely

controlled by differences in light and iron levels~~in the SO (Arrigo et al., 1998, 1999; Goffart et al., 2000; Sedwick et al., 2000; Garcia et al.~~ ~~A number of studies suggest *Phaeocystis* colonies to grow better than diatoms under low light levels (Garcia et al., 2009; Tang et al., 2009; N~~ ~~implying a seasonal succession from *Phaeocystis* to diatoms throughout the growing season as light levels increase (Green and Sambrotto, 2~~ ~~At the same time , in the Ross Sea, the large interannual variability in the~~ , but the relative importance of ~~*Phaeocystis* and~~ ~~diatoms has been suggested to be due to the large variability in iron availability in summer (for the years 2001-2010, between 39-87% of the~~ ~~Therefore, iron availability may be more important in controlling the magnitude of the summer diatom bloom than the spring~~ the different bottom-up factors appears to vary depending on the time and location of the sampling (Arrigo et al., 1998, 1999; Goffart et al., Concurrently, while available models agree with the observations on the general importance of light and iron levels, differences in the dominant bottom-up factors controlling the distribution of *Phaeocystis* ~~bloom (Peloquin and Smith, 2007; Smith et al., 2011).~~

~~Yet, other~~ at high SO latitudes across models are possibly a result of differences in how this phytoplankton type is parametrized (Tagliabue and Arrigo, 2005; Pasquer et al., 2005; Wang and Moore, 2011; Le Quéré et al., 2016; Kaufman et al., 2017; Losa et al., 2019) Besides bottom-up factors, some observational studies suggest that top-down factors ~~might be~~ are important in controlling the relative importance of *Phaeocystis* and diatoms as well. For instance, van Hilst and Smith (2002) suggest grazing by zooplankton to be an important factor explaining the observed distributions of these two phytoplankton types in the SO~~. In fact, grazing pressure has been shown to be lower~~ , likely resulting from the generally lower grazing pressure on *Phaeocystis* colonies than on diatoms ~~(Granéli et al., 1993; Smith et al., 2003; Tang et al., 2008), with cascading effects for food web structure (Smetacek et al., 2004). Furthermore, evidence also~~ (Granéli et al., 1993; Smith et al., 2003). Yet, further evidence suggests a role for other biomass loss processes such as aggregation and subsequent sinking ~~in controlling the relative abundance of *Phaeocystis* and diatoms (Asper and Smith, 1999)~~(Asper and Smith, 1999; Ducklow et al., 2015; Asper and Smith, 2019). Altogether, this ~~implies a complex interplay between bottom-up and top-down factors in controlling SO phytoplankton biomass levels in general and~~ calls for a comprehensive quantitative analysis of the relative importance of ~~diatoms and~~ bottom-up and top-down factors in controlling the competition between *Phaeocystis* ~~in particular, which is difficult to comprehensively assess through in situ studies.~~

~~Ecosystem models can be a useful tool to disentangle the controlling factors of SO phytoplankton biogeography over the course of the growing season and to quantify its biogeochemical implications (see e.g. Hashioka et al., 2013; Nissen et al., 2018). To date, some global (Wang and Moore, 2011; Le Quéré et al., 2016) or regional SO (Tagliabue and Arrigo, 2005; Pasquer et al., 2005; Ka~~ ~~exist that include an explicit representation of *Phaeocystis*, but these differ substantially in how they parameterize the life cycle of *Phaeocystis* (compare e.g. models including life cycle transitions such as Pasquer et al. (2005) and Kaufman et al. (2017) to Wang and Moore (2011) and Le Quéré et al. (2016), which only include the colonial stage of *Phaeocystis*). Using a 1D model setup for the Ross Sea, Kaufman et al. (2017) found light availability early in the growing season to critically impact the relative importance of diatoms and *Phaeocystis*. Similarly, in their study, Wang and Moore (2011) identify model parameters surrounding the light and iron sensitivity of growth by diatoms and *Phaeocystis* colonies to have the biggest impact on the relative importance of the two across the SO, with grazing by zooplankton playing only a minor role. While the models agree with the observations on the general importance of light and iron levels in controlling the relative importance of *Phaeocystis*~~ and

diatoms ~~in the SO, a detailed quantitative analysis of the factors controlling the competition of these two phytoplankton types~~ over the course of the ~~growing season is missing. In the past, some of the above-mentioned models have been used to relate the simulated spatio-temporal variability in the high-latitude phytoplankton community structure to the simulated variability in air-sea CO_2 fluxes (at KERFIX and for the Ross Sea, see Pasquer et al., 2005; Tagliabue and Arrigo, 2005) or to quantify the contribution of *Phaeocystis* to the SO integrated annual NPP or POC export (23% and 30% south of 60° S, respectively, see Wang and Moo Yet, none of these models has assessed the impacts of the seasonally varying phytoplankton community structure on basin-wide biogeochemical fluxes, such as POC export, and their implications for nutrient distributions~~SO growing season and its ramifications for carbon transfer to depth.

In this study, we investigate the competition between *Phaeocystis* and diatoms and its implications for carbon cycling using a regional coupled physical-biogeochemical-ecological model configured at eddy-permitting resolution for the SO (ROMS-BEC, Nissen et al., 2018). ~~In our previous work (Nissen et al., 2018), we had already extended the original BEC model (Moore et al., 2013) with an explicit parametrization of coccolithophores. Now, we are adding~~ To address the missing link between SO phytoplankton biogeography and the global carbon cycle, we have added *Phaeocystis* colonies as an additional ~~phytoplankton functional type~~PFT to the model, so that ~~the model includes all~~ it includes all major identified biogeochemically relevant phytoplankton types of the SO. We then assess the relative importance of bottom-up and top-down factors in controlling the relative importance of *Phaeocystis* colonies and diatoms over a complete annual cycle in the high-latitude SO~~and the imprint of the relative importance of *Phaeocystis* on SO nutrient distributions. Furthermore, we quantify the impact of the simulated spatio-temporal variability in phytoplankton community structure~~. We show that a correct representation of SO phytoplankton biogeography leaves a distinct imprint on upper ocean carbon cycling and POC export across the SO.

2 Methods

2.1 ROMS-BEC with explicit *Phaeocystis* colonies

We use a quarter-degree SO setup of the Regional Ocean Modeling System ROMS (latitudinal range from 24° S-78° S, 64 topography-following vertical levels, time step to solve the primitive equations is 1600 s; Shchepetkin and McWilliams, 2005; Haumann, 2016), coupled to the biogeochemical model BEC (Moore et al., 2013), which was recently extended to include an explicit represenation of coccolithophores and thoroughly validated in the SO setup (Nissen et al., 2018). BEC resolves the biogeochemical cycling of all macronutrients (C, N, P, Si), as well as the cycling of iron (Fe), the major micronutrient in the SO. The model includes four ~~phytoplankton functional types (PFT)~~ PFTs – diatoms, coccolithophores, small phytoplankton/SP, and N_2-fixing diazotrophs – and one zooplankton functional type (Moore et al., 2013; Nissen et al., 2018). Here, we extend the version of Nissen et al. (2018) to include an explicit parameterization of colonial *Phaeocystis antarctica*, which is the only species of *Phaeocystis* occurring in the SO (Schoemann et al., 2005). For the remainder of this manuscript, we will refer to the new PFT as "*Phaeocystis*". Generally, model parameters for *Phaeocystis* are chosen to represent the colonial form of *Phaeocystis* whenever information is available in the literature (see e.g. review by Schoemann et al., 2005). By only simulating the colonial form of *Phaeocystis*, we assume enough solitary cells of *Phaeocystis* to be available for colony formation at any time as part of the

SP PFT. As for the other phytoplankton PFTs, growth by *Phaeocystis* is limited by surrounding temperature, nutrient, and light conditions as outlined in the following ~~(for a complete description of the model equations describing phytoplankton growth, see Nissen et a~~ appendix B for a complete description of the model equations describing phytoplankton growth).

As the new PFT in ROMS-BEC represents a single species of *Phaeocystis*, we use an optimum function rather than an Eppley curve (Eppley, 1972) to describe its temperature-limited growth rate $\mu^{\mathrm{PA}}(T)$ (d^{-1}, Schoemann et al., 2005):

$$\mu^{\mathrm{PA}}(T) = \mu^{\mathrm{PA}}_{\mathrm{max}} \cdot e^{-\left(\frac{T-T_{\mathrm{opt}}}{\tau}\right)^2} \quad (1)$$

In the above equation, the maximum growth rate ($\mu^{\mathrm{PA}}_{\mathrm{max}}$) is 1.56 d^{-1} at an optimum temperature (T_{opt}) of 3.6° C and the temperature interval (τ) is 17.51° C and 1.17° C at temperatures below and above 3.6° C, respectively. With these parameters, the simulated growth rate of *Phaeocystis* in ROMS-BEC is zero at temperatures above ~8° C ~~(in agreement with laboratory experiments with *Phae*~~ higher than that of diatoms for temperatures between ~0-4° C (Fig. A1a). We acknowledge that the range of temperatures for which the growth of *Phaeocystis* exceeds that of diatoms is possibly ~~too small~~underestimated, as the temperature-limited growth rate by diatoms in ROMS-BEC is ~~too high~~ overestimated at low temperatures compared to available laboratory data (see Fig. A1a & Eq. B5). Yet, we note that temperature-limited growth by diatoms in the model is tuned to fit the data at the global range of temperatures, in particular for the competition with coccolithophores at subantarctic latitudes (Nissen et al., 2018).

Half-saturation constants for macronutrient limitation are scarce for *P. antarctica* (Schoemann et al., 2005), and macronutrient limitation of *Phaeocystis* is therefore chosen to be identical to that of diatoms in ROMS-BEC (Table 1). As the availability of the micronutrient Fe generally limits phytoplankton growth in the high-latitude SO (Martin et al., 1990a, b) and accordingly in ROMS-BEC (Fig. S1), this choice is not expected to significantly impact the simulated competition between diatoms and *Phaeocystis* in this area. In contrast, differences in the half-saturation constants with respect to dissolved Fe concentrations ($\mathrm{k_{Fe}}$) of *Phaeocystis* and diatoms ~~possibly~~ critically impact the competitive success of *Phaeocystis* relative to diatoms throughout the year (see e.g. Sedwick et al., 2000, 2007). Here, due to their larger size, we assume a higher $\mathrm{k_{Fe}}$ for *Phaeocystis* (0.2 μmol m^{-3}) than for diatoms (0.15 μmol m^{-3}, Table 1). We note however, that the $\mathrm{k_{Fe}}$ of *Phaeocystis* has been reported to vary over one order magnitude depending on the ambient light level (0.045-0.45 μmol m^{-3}, see Fig. A1b and Garcia et al., 2009), with lowest values at optimum light levels of around 80 W m^{-2}. Due to the limited number (3) of reported light levels in Garcia et al. (2009) and the associated uncertainty when fitting the data, we refrain from using this $\mathrm{k_{Fe}}$-light-dependency in the *Baseline* simulation, but explore the sensitivity of the simulated seasonality of *Phaeocystis* and diatom biomass to a polynomial fit describing the $\mathrm{k_{Fe}}$ of *Phaeocystis* as a function of the light intensity (see Fig. A1b and section 2.2). As a result of the tuning exercise aiming to maximize the fit of *all* simulated PFT biomass fields to available observations, the $\mathrm{k_{Fe}}$ of the other PFTs in ROMS-BEC are increased by 25% in this study as compared to in Nissen et al. (2018, see Table 1). For diatoms, this change leads to a better agreement of the $\mathrm{k_{Fe}}$ used in ROMS-BEC with values suggested for large SO diatoms by Timmermans et al. (2004), but we acknowledge that the chosen value here is still at the lower end of their suggested range (0.19-1.14 μmol m^{-3}). We note that we currently do not include any luxury uptake of Fe by *Phaeocystis* into their gelatinous matrix (Schoemann et al., 2001). Serving as a storage of additional Fe accessible to the *Phaeocystis* colony when Fe in the seawater gets low, this

Table 1. BEC parameters controlling phytoplankton growth and loss for the five phytoplankton PFTs diatoms (D), *Phaeocystis* (PA), coccolithophores (C), small phytoplankton (SP), and diazotrophs (N). Z=zooplankton, P=phytoplankton, PI=photosynthesis-irradiance. If not given in section 2.1, the model equations describing phytoplankton growth and loss rates are given in Nissen et al. (2018).

Parameter	Unit	Description	D	PA	C	SP	N†
μ_{max}	d^{-1}	max. growth rate at 30° C	4.6	‡	3.8	3.6	0.9
Q_{10}		temperature sensitivity	1.55	‡	1.45	1.5	1.5
k_{NO3}	mmol m^{-3}	half-saturation constant for NO_3	0.5	0.5	0.3	0.1	1.0
k_{NH4}	mmol m^{-3}	half-saturation constant for NH_4	0.05	0.05	0.03	0.01	0.15
k_{PO4}	mmol m^{-3}	half-saturation constant for PO_4	0.05	0.05	0.03	0.01	0.02
k_{DOP}	mmol m^{-3}	half-saturation constant for DOP	0.9	0.9	0.3	0.26	0.09
k_{Fe}	μmol m^{-3}	half-saturation constant for Fe	0.15	0.2	0.125	0.1	0.5
k_{SiO3}	mmol m^{-3}	half-saturation constant for SiO_3	1.0	-	-	-	-
α_{PI}	$\frac{\text{mmol C m}^2}{\text{mg Chl W s}}$	initial slope of PI-curve	0.44	0.63	0.4	0.44	0.38
$\gamma_{g,max}$	d^{-1}	max. growth rate of Z grazing on P	3.8	3.6	4.4	4.4	3.0
z_{grz}	mmol m^{-3}	half-saturation constant for ingestion	1.0	1.0	1.05	1.05	1.2
$\gamma_{m,0}$	d^{-1}	linear non-grazing mortality	0.12	0.18	0.12	0.12	0.15
$\gamma_{a,0}$	~~d^{-1}~~ $\frac{m^3}{\text{mmol C d}}$	quadratic loss rate in aggregation	0.001	0.005	0.001	0.001	-
r_g	-	fraction of grazing routed to POC	0.3	0.42	0.2	0.05	0.05

† Compared to Nissen et al. (2018), the k_{Fe} of diazotrophs in ROMS-BEC is higher than for all other PFTs, consistent with literature reporting high Fe requirements of *Trichodesmium* (Berman-Frank et al., 2001). Furthermore, the maximum grazing rate on diazotrophs is lowest in the model (Capone, 1997). Still, diazotrophs continue to be a minor player in the SO phytoplankton community, contributing <1% to domain-integrated NPP in ROMS-BEC.

‡ The temperature-limited growth rate of *Phaeocystis* is calculated based on an optimum function according to Eq. 1 (see also Fig. A1a).

luxury uptake is thought to relieve it from Fe limitation when Fe concentrations become growth limiting (see discussion in Schoemann et al., 2005). We therefore probably overestimate the Fe limitation of *Phaeocystis* growth in ROMS-BEC.

P. antarctica blooms are typically found where and when waters are ~~comparatively~~ turbulent and the mixed layer is ~~comparatively~~ deep (in comparison to blooms dominated by diatoms, see e.g. Arrigo et al., 1999; Alvain et al., 2008), suggesting that *Phaeocystis* is better in coping with low light levels than diatoms (e.g. Arrigo et al., 1999). In agreement with laboratory experiments (Tang et al., 2009; Mills et al., 2010; Feng et al., 2010), we therefore choose a higher α_{PI}, i.e. a higher sensitivity of growth to increases of photosynthetically active radiation (PAR) at low PAR levels, for *Phaeocystis* than for diatoms in ROMS-BEC (see Table 1). Our value (0.63 mmol C m^2 (mg Chl W s)$^{-1}$) corresponds to the average value compiled from available laboratory experiments (Schoemann et al., 2005).

In addition to environmental conditions directly impacting phytoplankton growth rates, loss processes such as grazing, non-grazing mortality, and aggregation impact the simulated biomass levels at any point and time (Moore et al., 2002). Grazing

on *Phaeocystis* varies across zooplankton size classes, as a consequence of *Phaeocystis* life forms spanning several orders of magnitude in size ~~(few μm to cm, Schoemann et al., 2005)~~(Schoemann et al., 2005). Furthermore, *Phaeocystis* colonies are surrounded by a ~~skin~~ membrane (Hamm et al., 1999), potentially serving as protection from zooplankton grazing. While small copepods have been shown to graze less on *Phaeocystis* once they form colonies, other larger zooplankton appear to continue grazing on *Phaeocystis* colonies at unchanged rates (Granéli et al., 1993; Schoemann et al., 2005; Nejstgaard et al., 2007). Based on a size-mismatch assumption of the single grazer in ROMS-BEC and *Phaeocystis* colonies, we assume a lower maximum grazing rate on *Phaeocystis* than on diatoms (3.6 d^{-1} and 3.8 d^{-1}, respectively, see $\gamma_{g,max}$ in Table 1). Upon grazing, we assume the fraction of the grazed phytoplankton biomass that is transformed to sinking POC via zooplankton fecal pellet production to be higher for larger and ballasted cells than for small, unballasted cells. Consequently, the fraction of grazing routed to POC increases from grazing on SP or diazotrophs to coccolithophores, *Phaeocystis*, and diatoms (r_g in Table 1). Consistent with Nissen et al. (2018), we keep a Holling Type II ingestion functional response here (Holling, 1959) and compute grazing on each prey separately ~~.~~ (Eq. B12). We refer to Nissen et al. (2018) for a discussion of the relative merits and pitfalls for using Holling Type II versus III.

Non-grazing mortality (such as viral lysis) has been shown to increase under environmental stress for *Phaeocystis* colonies, causing colony disruption and ultimately cell death (van Boekel et al., 1992; Schoemann et al., 2005). To account for processes causing colony disintegration and for grazing by higher trophic levels not explicitly included in ROMS-BEC, *Phaeocystis* in ROMS-BEC experience a higher mortality rate than diatoms (0.18 d^{-1} and 0.12 d^{-1}, respectively, see $\gamma_{m,0}$ in Table 1 & Eq. B14). Thereby, the chosen non-grazing mortality rate of *Phaeocystis* assumed in the model is still lower than the estimated rate of viral lysis for *Phaeocystis* in the North Sea by van Boekel et al. (1992, 0.25 d^{-1}), but we note that data on non-grazing mortality of *P. antarctica* are currently lacking (Schoemann et al., 2005). Furthermore, based on the assumption that for a given biomass concentration, larger cells are more likely than smaller cells to form aggregates and ~~subsequently~~ to subsequently stop photosynthesizing and sink as POC, we use a higher quadratic ~~mortality~~ loss rate for *Phaeocystis* (0.005 d^{-1}) than for diatoms (0.001 d^{-1}) in the model (see $\gamma_{a,0}$ in Table 1 & Eq. B16).

In summary, the spatio-temporal variability of the relative importance of *Phaeocystis* and diatoms in ROMS-BEC is controlled by the interplay of the environmental conditions and loss processes, which differentially impact the growth and loss rates of these two PFTs and consequently their competitive fitness in the model. In the following, we will describe the model setup and the simulations that were performed to assess the competition between *Phaeocystis* and diatoms throughout the year in the high-latitude SO. The simulations include a set of sensitivity experiments, with the aim to assess the impact of choices of single parameters or parameterizations on the simulated *Phaeocystis* biogeography.

2.2 Model setup and sensitivity simulations

With few exceptions, we use the same ROMS-BEC model setup as described in detail in Nissen et al. (2018): At the open northern boundary, we use monthly climatological fields for all tracers (Carton and Giese, 2008; Locarnini et al., 2013; Zweng et al., 2013; Garcia et al., 2014b, a; Lauvset et al., 2016; Yang et al., 2017), and the same data sources are used to initialize the model simulations. At the ocean surface, the model is forced with a 2003-normal year forcing for momentum, heat, and

Table 2. Overview of sensitivity experiments aiming to assess the sensitivity of the simulated *Phaeocystis*-diatom competition to chosen parameter values and parameterizations of *Phaeocystis*. See Table 1 and section 2.1 for parameter values and parameterizations of *Phaeocystis* in the reference simulation. PA=*Phaeocystis*, D=diatoms.

	Run Name	**Description**
1	TEMPERATURE	Use $\mu^{\mathrm{D}}_{\max}$, $\mathrm{Q}^{\mathrm{D}}_{10}$, and $\mu^{\mathrm{PA}}_{\mathrm{T}} = \mu^{\mathrm{D}}_{\max} \cdot \mathrm{Q}^{\mathrm{D}}_{10}{}^{\frac{\mathrm{T}-\mathrm{T}_{\mathrm{ref}}}{10^\circ\,\mathrm{C}}}$ to compute the temperature-limited growth rate of *Phaeocystis* instead of Eq. 1
2	$\mathrm{ALPHA_{PI}}$	Set $\alpha^{\mathrm{PA}}_{\mathrm{PI}}$ to $\alpha^{\mathrm{D}}_{\mathrm{PI}}$
3	IRON	Set $\mathrm{k}^{\mathrm{PA}}_{\mathrm{Fe}}$ to $\mathrm{k}^{\mathrm{D}}_{\mathrm{Fe}}$
4	GRAZING	Set $\gamma^{\mathrm{PA}}_{\mathrm{g,max}}$ to $\gamma^{\mathrm{D}}_{\max}$
5	AGGREGATION	Set $\gamma^{\mathrm{PA}}_{\mathrm{a},0}$ to $\gamma^{\mathrm{D}}_{\mathrm{a},0}$
6	MORTALITY	Set $\gamma^{\mathrm{PA}}_{\mathrm{m},0}$ to $\gamma^{\mathrm{D}}_{\mathrm{m},0}$
7	VARYING_kFE	Use $\mathrm{k}^{\mathrm{PA}}_{\mathrm{Fe}}(\mathrm{I}) = 2.776 \cdot 10^{-5} \cdot (\mathrm{I}+20)^2$ - 0.00683 $\cdot$ (I + 20) + 0.46 (with the irradiance I in W m^{-2}) instead of a constant $\mathrm{k}^{\mathrm{PA}}_{\mathrm{Fe}}$

freshwater fluxes (Dee et al., 2011). Satellite-derived climatological total chlorophyll concentrations are used to initialize phytoplankton biomass and to constrain it at the open northern boundary in the model (NASA-OBPG, 2014b), and the fields are extrapolated to depth following Morel and Berthon (1989). Due to the addition of *Phaeocystis*, the partitioning of total chlorophyll onto the different phytoplankton PFTs is adjusted compared to Nissen et al. (2018): 90% is attributed to small phytoplankton, 4% to diatoms and coccolithophores, respectively, and 1% to diazotrophs and *Phaeocystis*, respectively. This partitioning is motivated by the phytoplankton community structure at the open northern boundary at 24° S, where small phytoplankton typically dominate and *P. ~~Antarctica~~antarctica* are only a minor contributor to phytoplankton biomass (see e.g. Schoemann et al., 2005; Swan et al., 2016). *Phaeocystis* is initialized with a carbon-to-chlorophyll ratio of 60 mg C (mg chl)$^{-1}$ (same as small phytoplankton and coccolithophores), whereas diatoms are initialized with a ratio of 36 mg C (mg chl)$^{-1}$ (Sathyendranath et al., 2009).

We first run a 30 year long physics-only spin-up, followed by a 10 year long spin-up in the coupled ROMS-BEC setup. Our *Baseline* simulation for this study is then run for an additional 10 years, of which we analyze a daily climatology over the last 5 full seasonal cycles. i.e. from 1 July of year 5 until 30 June of year 10. Apart from having added *Phaeocystis* and adjusted the parameters of the other PFTs as described in section 2.1, the setup of the *Baseline* simulation in this study is thereby identical to the *Baseline* simulation in Nissen et al. (2018). We will evaluate the model's performance with respect to the simulated phytoplankton biogeography in section 3.1 and in the supplementary material.

Furthermore, we perform seven sensitivity experiments, in order to assess the sensitivity of the simulated *Phaeocystis* biogeography and the competition of *Phaeocystis* and diatoms to chosen parameters and parameterizations (Table 2). To do so, we set the parameters and parameterizations of *Phaeocystis* to those used for diatoms in ROMS-BEC (runs 1-6 in Table 2). Generally, the differences in parameters between *Phaeocystis* and diatoms affect either the simulated growth rates (runs TEMPERATURE,

ALPHA$_{PI}$, and IRON) or loss rates (runs GRAZING, AGGREGATION, and MORTALITY). By successively eradicating the differences between *Phaeocystis* and diatoms, these simulations allow us to directly quantify the impact of ~~differences in parameters~~ parameter differences on the simulated relative importance of *Phaeocystis* for total phytoplankton biomass. To assess the impact of iron-light interactions on the competitive success of *Phaeocystis* at high SO latitudes, we ultimately run a simulation in which the half-saturation constant of iron (k_{Fe}) of *Phaeocystis* is a function of the light intensity, following a polynomial fit of available laboratory data ~~(VARYING_kFE, see Fig. A1b and Garcia et al., 2009)~~(VARYING_kFE, Fig. A1b; Garcia et al., 2009). All sensitivity experiments use the same physical and biogeochemical spin-up as the *Baseline* simulation and start from the end of year 10 of the ~~*Baseline* simulation~~coupled ROMS-BEC spin-up. Each simulation is then run for an additional 10 years, of which the average over the last 5 full seasonal cycles is analyzed in this study.

2.3 Analysis framework

2.3.1 Evaluating the simulated phytoplankton community structure

We compare the simulated spatio-temporal variability in phytoplankton biomass and community structure to available observations of phytoplankton carbon biomass concentrations from the MAREDAT initiative (O'Brien et al., 2013; Leblanc et al., 2012; Vogt et al., 2012), satellite-derived total chlorophyll concentrations (Fanton d'Andon et al., 2009; Maritorena et al., 2010), DMS measurements (Curran and Jones, 2000; Lana et al., 2011), the ecological niches suggested for SO phytoplankton taxa (Brun et al., 2015), and the CHEMTAX climatology based on high performance liquid chromatography (HPLC) pigment data (Swan et al., 2016). The latter provides seasonal estimates of the mixed layer average community composition, which we compare to the seasonally and top 50 m averaged model output of each phytoplankton's contribution to total chlorophyll biomass. The CHEMTAX analysis splits the phytoplankton community into diatoms, nitrogen fixers (such as *Trichodesmium*), pico-phytoplankton (such as *Synechococcus* and *Prochlorococcus*), dinoflagellates, cryptophytes, chlorophytes (all three combined into the single group "Others" here), and haptophytes (such as coccolithophores and *Phaeocystis*). As noted in Swan et al. (2016), the differentiation between coccolithophores and *Phaeocystis* in the CHEMTAX analysis is difficult and prone to error. Possibly, this is due to the large variability in pigment composition of *Phaeocystis* ~~as a~~ in response to varying environmental conditions, especially regarding light and iron levels (Smith et al., 2010; Wright et al., 2010). Coccolithophores have been reported to only grow very slowly at low temperatures (below ~8° C, Buitenhuis et al., 2008), and in the SO, their abundance in the high latitudes south of the polar front is very low (Balch et al., 2016). Therefore, whenever the climatological temperature in the World Ocean Atlas 2013 (Locarnini et al., 2013) is below 2° C at the time and location of the respective HPLC observation, we re-assign data points identified as "Hapto-6" (hence e.g. *Emiliania huxleyi*) in the CHEMTAX analysis to "Hapto-8" (hence e.g. *Phaeocystis* ~~*Antarctica*~~*antarctica*). Throughout the manuscript, this new category ("Hapto-8 re-assigned") is indicated separately in the respective figures, and leads to a better correspondence of the functional types included in the CHEMTAX-based climatology by Swan et al. (2016) and the PFTs in ROMS-BEC.

To assess the controlling factors of the simulated PFT distributions in our model, we analyze the simulated ~~December-March (~~summer (December-March; DJFM) top 50 m average biomass distribution of the different model PFTs south of 40° S

in environmental niche space. To that aim, we bin the simulated carbon biomass concentrations of *Phaeocystis*, diatoms, and coccolithophores in ROMS-BEC as a function of the temperature [° C], nitrate concentration [mmol m^{-3}], iron concentration [μmol m^{-3}], and mixed layer photosynthetically active radiation (MLPAR; W m^{-2}). Subsequently, we compare the simulated ecological niche to that observed for ~~example taxa from the SO~~ abundant SO species of each model PFT ~~(such as *Phaeocystis Antarctica*, *Fragilariopsis kerguelensis*, *Thalassiosira* sp., or *Emiliania huxleyi*, see Brun et al., 2015).~~ (such as *Phae*

In section 3.3 of this manuscript, only the results for *Phaeocystis* and diatoms will be shown, the corresponding figures for coccolithophores can be found in the supplementary material (Fig. S8 & S9). While this analysis informs on possible links between the competitive fitness of a PFT and the environmental conditions it lives in, the assessment is ~~hindered~~ limited to a qualitative inter-comparison due to difficulties in comparing a model PFT to individual phytoplankton species, a sampling bias towards the summer months and the low latitudes, and the neglect of loss processes such as zooplankton grazing to explain biomass distributions. As a consequence, the ecological niche analysis does not allow for the assessment of any temporal variability in PFT biomass concentrations.

In order to assess the simulated seasonality and the seasonal succession of *Phaeocystis* and diatoms, we identify the bloom peak as the day of peak chlorophyll concentrations throughout the year. Besides the timing of the bloom peak, phytoplankton phenology is typically characterized by metrics such as the day of bloom initiation or the day of bloom end (see e.g. Soppa et al., 2016). In this regard, the timing of the bloom start is known to be sensitive to the chosen identification methodology (Thomalla et al., 2015). At high latitudes, the identification of the bloom start based on remotely sensed chlorophyll concentrations is additionally impaired by the large number of missing data in all seasons (even in the summer months, a large part of the SO is sampled by the satellite in less than 5 of the 21 available years, see Fig. S2), complicating any comparison of the high-latitude satellite-derived bloom start with output from models such as ROMS-BEC. To minimize the uncertainty due to the low data coverage in the region of interest for this study, and as the seasonal succession of *Phaeocystis* and diatoms in the high-latitude SO is mostly inferred from the timing of observed maximum abundances in the literature (e.g. Peloquin and Smith, 2007; Smith et al., 2011), we focus our discussion of the simulated bloom phenology on the timing of the bloom peak (Hashioka et al., 2013). To evaluate the model's performance, we compare the timing of the total chlorophyll bloom peak in the *Baseline* simulation of ROMS-BEC to the bloom timing derived from climatological daily chlorophyll data from Globcolor (climatology from 1998-2018 based on the daily 25 km chlorophyll product, see Fanton d'Andon et al., 2009; Maritorena et al., 2010).

~~The release of dimethylsulfoniopropionate (DMSP) via zooplankton grazing, cell lysis, and exudation and the subsequent transformation to DMS by bacterial activity are the major sources of DMS in seawater (e.g. Stefels et al., 2007). With *Phaeocystis* being the major DMSP producer in the SO (Keller et al., 1989; Liss et al., 1994), the timing of observed peak seawater DMS concentrations (Curran et al., 1998; Curran and Jones, 2000) will allow us to assess the simulated seasonality of *Phaeocystis* in the model. Though not explicitly including the biogeochemical cycling of sulphur, we can nevertheless use model output from ROMS-BEC to obtain an estimate of DMS production by *Phaeocystis* through a simple back-of-the-envelope calculation. To this aim, we use the model-based *Phaeocystis* biomass loss rates via zooplankton grazing and non-grazing mortality to get the DMSP release from this PFT (integrated annually over the top 10 m; we neglect exudation here), a molar DMSP:C ratio for~~

Phaeocystis of 0.011 (Stefels et al., 2007), and a DMSP-to-DMS conversion efficiency between 0.2-0.7 (the DMS yield depends on the loca
By comparing the resulting model-based estimates to previously published global estimates of marine DMS emissions (Lana et al., 2011),
we obtain an estimate of the importance of SO *Phaeocystis* for global sulphur cycling.

2.3.2 Assessing phytoplankton Phytoplankton competition throughout the yearand succession

In ROMS-BEC, phytoplankton biomass P^{i} (mmol C m^{-3}, $i \in \{PA, D, C, SP, N\}$) is determined by the balance between growth (μ^{i}) and loss terms (grazing by zooplankton $\gamma_{\mathrm{g}}^{\mathrm{i}}$, non-grazing mortality $\gamma_{\mathrm{m}}^{\mathrm{i}}$, and aggregation $\gamma_{\mathrm{a}}^{\mathrm{i}}$, see appendix in Nissen et al. (2018) B for a full description of the model equations). Here, in order to disentangle the factors controlling the relative importance of *Phaeocystis* and diatoms for total phytoplankton biomass throughout the year, we use the metrics first introduced by Hashioka et al. (2013) and then applied to assess the competition of diatoms and coccolithophores in ROMS-BEC in Nissen et al. (2018). Same as in Nissen et al. (2018), the relative growth ratio $\mu_{\mathrm{rel}}^{\mathrm{ij}}$ of phytoplankton i and j (e.g. diatoms and *Phaeocystis*) is defined as the ratios of their specific growth rates (μ^{i}, d^{-1}), which in turn depends on environmental dependencies regarding the temperature T, nutrients N, and irradiance I, following:

$$\begin{aligned}\mu_{\mathrm{rel}}^{\mathrm{DPA}} &= \log \frac{\mu^{\mathrm{D}}}{\mu^{\mathrm{PA}}} \\ &= \underbrace{\log \frac{\mathrm{f}^{\mathrm{D}}(\mathrm{T}) \cdot \mu_{\mathrm{max}}^{\mathrm{D}}}{\mu_{\mathrm{T}}^{\mathrm{PA}}}}_{\beta_T} + \underbrace{\log \frac{\mathrm{g}^{\mathrm{D}}(\mathrm{N})}{\mathrm{g}^{\mathrm{PA}}(\mathrm{N})}}_{\beta_{\mathrm{N}} \sim \beta_{\mathrm{Fe}}} + \underbrace{\log \frac{\mathrm{h}^{\mathrm{D}}(\mathrm{I})}{\mathrm{h}^{\mathrm{PA}}(\mathrm{I})}}_{\beta_{\mathrm{I}}}\end{aligned} \tag{2}$$

In the above equation, the specific growth rate μ^{i} of each phytoplankton i is calculated as a multiplicative function of a temperature-limited growth rate ($\mathrm{f}^{\mathrm{D}}(\mathrm{T}) \cdot \mu_{\mathrm{max}}^{\mathrm{D}}$ for diatoms and $\mu_{\mathrm{T}}^{\mathrm{PA}}$ for *Phaeocystis*, ; see Eq. B5 & Eq. 1), a nutrient limitation term ($\mathrm{g}^{\mathrm{i}}(\mathrm{N})$, limitation of each nutrient is calculated using a Michaelis-Menten function, and the most-limiting one is then used here; see Eq. B8), and a light limitation term ($\mathrm{h}^{\mathrm{i}}(\mathrm{I})$, Geider et al., 1998). For a detailed description of the underlying functions $f(T)$, $g(N)$, and $h(I)$, the reader is referred to the appendix in Nissen et al. (2018). ($\mathrm{h}^{\mathrm{i}}(\mathrm{I})$; see Eq. B9 and Geider et al., 1998). At high-latitudes south of 60° S, the ratio of the nutrient limitation of growth β_{N} corresponds to that of the iron limitation β_{Fe} in our model (Fig. S1). Consequently, environmental conditions regarding temperature, iron, and light decide whether the relative growth ratio is positive or negative at a given location and point in time, i.e., which of the two phytoplankton types has a higher specific growth rate and hence a competitive advantage over the other regarding growth.

Similarly, the relative grazing ratio $\gamma_{\mathrm{g,rel}}^{\mathrm{ij}}$ of phytoplankton i and j (e.g. diatoms and *Phaeocystis*) is defined as the ratio of their specific grazing rates ($\gamma_{\mathrm{g}}^{\mathrm{i}}$, d^{-1}) following:

$$\gamma_{\mathrm{g,rel}}^{\mathrm{DPA}} = \log \frac{\frac{\gamma_{\mathrm{g}}^{\mathrm{PA}}}{P^{\mathrm{PA}}}}{\frac{\gamma_{\mathrm{g}}^{\mathrm{D}}}{P^{\mathrm{D}}}} \tag{3}$$

In ROMS-BEC, grazing on each phytoplankton i is calculated using a Holling Type II ingestion function (Nissen et al., 2018). As described in section 2.1, *Phaeocystis* and diatoms in ROMS-BEC do not only differ in parameters describing the zooplankton grazing pressure they experience, but in parameters describing their non-grazing mortality and aggregation losses as well.

Therefore, in accordance with the relative grazing ratio defined above, we define the relative mortality ratio ($\gamma^{\mathrm{ij}}_{\mathrm{m,rel}}$) and the relative aggregation ratio ($\gamma^{\mathrm{ij}}_{\mathrm{a,rel}}$) of phytoplankton i and j (e.g. diatoms and *Phaeocystis*) as the ratio of their specific non-grazing mortality rates ($\gamma^{\mathrm{i}}_{\mathrm{m}}$, d^{-1}) and aggregation rates ($\gamma^{\mathrm{i}}_{\mathrm{a}}$, d^{-1}), respectively, following:

$$\gamma^{\mathrm{DPA}}_{\mathrm{m,rel}} = \log \frac{\frac{\gamma^{\mathrm{PA}}_{\mathrm{m}}}{P^{\mathrm{PA}}}}{\frac{\gamma^{\mathrm{D}}_{\mathrm{m}}}{P^{\mathrm{D}}}} \tag{4}$$

$$\gamma^{\mathrm{DPA}}_{\mathrm{a,rel}} = \log \frac{\frac{\gamma^{\mathrm{PA}}_{\mathrm{a}}}{P^{\mathrm{PA}}}}{\frac{\gamma^{\mathrm{D}}_{\mathrm{a}}}{P^{\mathrm{D}}}} \tag{5}$$

Since the total specific loss rate ($\gamma^{\mathrm{ij}}_{\mathrm{total}}$, d^{-1}) of phytoplankton i is the addition of its specific grazing, non-grazing mortality, and aggregation loss rates, the relative total loss ratio $\gamma^{\mathrm{ij}}_{\mathrm{total,rel}}$ of phytoplankton i and j (e.g. diatoms and *Phaeocystis*) is defined as

$$\gamma^{\mathrm{DPA}}_{\mathrm{total,rel}} = \log \frac{\frac{\gamma^{\mathrm{PA}}_{\mathrm{g}}}{P^{\mathrm{PA}}} + \frac{\gamma^{\mathrm{PA}}_{\mathrm{m}}}{P^{\mathrm{PA}}} + \frac{\gamma^{\mathrm{PA}}_{\mathrm{a}}}{P^{\mathrm{PA}}}}{\frac{\gamma^{\mathrm{D}}_{\mathrm{g}}}{P^{\mathrm{D}}} + \frac{\gamma^{\mathrm{D}}_{\mathrm{m}}}{P^{\mathrm{D}}} + \frac{\gamma^{\mathrm{D}}_{\mathrm{a}}}{P^{\mathrm{D}}}} \tag{6}$$

If $\gamma^{\mathrm{DPA}}_{\mathrm{total,rel}}$ is positive, the specific total loss rate of *Phaeocystis* is larger than that of diatoms (and accordingly for the individual loss ratios in Eq. 3-5), and loss processes promote the accumulation of diatom biomass relative to that of *Phaeocystis*. While the maximum grazing rate on *Phaeocystis* is lower than that of diatoms, their non-grazing mortality and aggregation losses are higher (see section 2.1 and Table 1). Ultimately, at any given location and point in time, the interaction between the phytoplankton biomass concentrations (impacting the respective loss rates) and environmental conditions (impacting the respective growth rate) will determine the relative contribution of each phytoplankton type i to total phytoplankton biomass. Here, we use these metrics to assess the controls on the simulated seasonal evolution of the relative importance of *Phaeocystis* and diatoms in the high-latitude SO.

3 Results

3.1 Phytoplankton biogeography and community composition in the SO

In the 5-PFT *Baseline* simulation of ROMS-BEC, total summer chlorophyll is highest close to the Antarctic continent (>10 mg chl m^{-3}) and decreases northwards to values <1 mg chl m^{-3} close to the open northern boundary (Fig. 1a). While this south-north gradient is in broad agreement with remotely sensed chlorophyll concentrations (Fig. 1b), our model generally overestimates high-latitude chlorophyll levels, which has already been noted for the 4-PFT setup of ROMS-BEC (Nissen et al., 2018). With *Phaeocystis* added, the model overestimates annual mean satellite derived surface chlorophyll biomass estimates by 18% (40.8 Gg chl in ROMS-BEC between 30-90° S compared to 34.5 Gg chl in the MODIS Aqua chlorophyll product, Table 3, NASA-OBPG, 2014a; Johnson et al., 2013) and satellite derived NPP by 38-42% (17.2 compared to 12.1-12.5 Pg C yr^{-1}, Table 3, Behrenfeld and Falkowski, 1997; O'Malley, last access: 16 May 2016; Buitenhuis et al., 2013a). This bias is

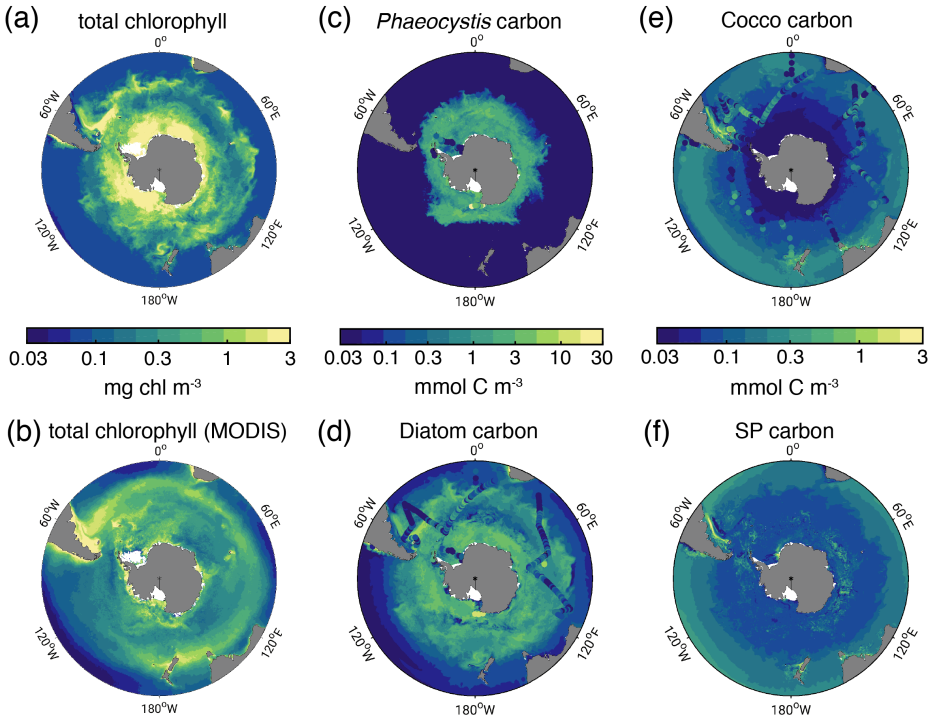

Figure 1. Biomass distributions for December-March (DJFM). Total surface chlorophyll [mg chl m^{-3}] in a) ROMS-BEC and b) MODIS-Aqua climatology (NASA-OBPG, 2014a), using the chlorophyll algorithm by Johnson et al. (2013). c)-f) Mean top 50 m c) *Phaeocystis*, d) diatom, e) coccolithophore, and f) small phytoplankton carbon biomass concentrations [mmol C m^{-3}] in ROMS-BEC. *Phaeocystis*, diatom, and coccolithophore biomass observations from the top 50 m are indicated by colored dots in c), d), and e), respectively (Balch et al., 2016; Saavedra-Pellitero et al., 2014; O'Brien et al., 2013; Vogt et al., 2012; Leblanc et al., 2012; Tyrrell and Charalampopoulou, 2009; Gravalosa et al., 2008; Cubillos et al., 2007). For more details on the biomass evaluation, see Nissen et al. (2018).

largest south of 60° S, where NPP and surface chlorophyll are overestimated by a factor 1.8-4.4 and 1.8, respectively (Table 3), and the bias is likely due to a combination of underestimated high-latitude chlorophyll concentrations in satellite-derived products (Johnson et al., 2013) and the missing complexity in the zooplankton compartment in ROMS-BEC, as biases in the simulated physical fields (temperature, light) have been shown to only explain a minor fraction of the simulated high-latitude biomass overestimation (Nissen et al., 2018).

The simulated carbon biomass distributions of colonial *Phaeocystis*, diatoms, coccolithophores, and SP are distinctly different in the model (Fig. 1c-f, showing top 50 m averages). The simulated summer *Phaeocystis* biomass is highest south of 50° S~~(top 50 m mean)~~, with highest concentrations of 10 mmol C m^{-3} at ∼74° S. In the model, average *Phaeocystis* biomass concentrations quickly decline to levels <0.1 mmol C m^{-3} north of 50° S (Fig. 1c), a direct result of the restriction of *Phaeocystis* growth to temperatures < ∼8° C in the model (Fig. A1a). This is in broad agreement with in situ observations, which suggest highest concentrations (>20 mmol C m^{-3}) south of ∼75° S, and concentrations <5 mmol C m^{-3} north of ∼65° S

Table 3. Comparison of ROMS-BEC based phytoplankton biomass, production, and export estimates with available observations (given in parentheses). Data sources are given below the Table.

		ROMS-BEC (Data)	
		30-90° S	**60-90° S**
Surface chlorophyll biomass	total, annual mean [Gg chl]	40.8 (34.5[a])	17.1 (9.5[a])
Diatom carbon biomass	0-200m, annual mean [Pg C]	0.059 (global[b]: 0.10-0.94)	0.015
Phaeocystis carbon biomass	0-200m, annual mean [Pg C]	0.019 (global[b]: 0.11-0.71)	0.010
Coccolithophore carbon biomass	0-200m, annual mean [Pg C]	0.012 (global[b]: 0.001-0.03)	0.001
NPP	Pg C yr^{-1}	17.2 (12.1-12.5[c])	3.0 (0.68-1.7[c])
	Diatoms [%]	52.0	49.1
	Phaeocystis [%]	15.3	45.8
	Coccolithophores [%]	14.6	0.7
	SP [%]	17.2	4.5
POC export at 100m	Pg C yr^{-1}	3.1 (2.3-2.96[d])	0.62 (0.21-0.24[d])

[a] Monthly climatology from MODIS Aqua (2002-2016, NASA-OBPG, 2014a), SO algorithm (Johnson et al., 2013)

[b] The reported estimates from the MAREDAT data base in Buitenhuis et al. (2013) are global estimates of phytoplankton biomass.

[c] Monthly climatology from MODIS Aqua VGPM (2002-2016, Behrenfeld and Falkowski, 1997; O'Malley, last access: 16 May 2016), NPP climatology from Buitenhuis et al. (2013a, 2002-2016)

[d] Monthly output from a biogeochemical inverse model (Schlitzer, 2004) and a data-assimilated model (DeVries and Weber, 2017).

(Fig. 1c & Fig. S3a & b). As a response to the addition of *Phaeocystis* to ROMS-BEC, the simulated high-latitude diatom biomass concentrations decrease compared of the 4-PFT setup of the model (Nissen et al., 2018). In the 5-PFT setup, the model simulates highest diatom biomass south of 60° S with maximum concentrations of ~7 mmol C m^{-3} at 72° S (top 50 m mean; ~17 mmol C m^{-3} in 4-PFT setup) and rapidly declining concentrations north of 60° S (Fig. 1d). Nevertheless, the simulated summer diatom biomass levels are still overestimated compared to carbon biomass estimates (Fig. S3c, Leblanc et al., 2012) and satellite derived diatom chlorophyll estimates (Soppa et al., 2014, comparison not shown). In contrast to both *Phaeocystis* and diatoms, the simulated biomass levels of coccolithophores are highest in the subantarctic (highest concentrations of 3 mmol C m^{-3} on the Patagonian Shelf, Fig. 1e & S3d), and their simulated SO biogeography remains largely unchanged compared to the 4-PFT setup (Nissen et al., 2018).

Taken together, the model simulates a phytoplankton community with substantial contributions of coccolithophores and *Phaeocystis* in the subantarctic and high-latitude SO, respectively (Fig. 2a). CHEMTAX data generally support this latitudinal trend ~~(CHEMTAX is based on high performance liquid chromatography pigment data, see Fig. 2b-d and section 2.3.1, Swan et al., 2016)~~(Averaged over 30-90° S (60-90° S), the simulated relative contributions of *Phaeocystis*, diatoms, and coccolithophores to total chlorophyll in summer are 20% (33%), 68% (64%), and 5% (<1%), respectively, in good agreement with the CHEMTAX climatology (28% (27%), 46% (48%), and 3% (1%), respectively, Fig. 2b & c). Acknowledging the uncertainty in the attribution of the group "Other" in the CHEMTAX data to a model PFT ("Other" includes dinoflagellates, cryptophytes, and chlorophytes

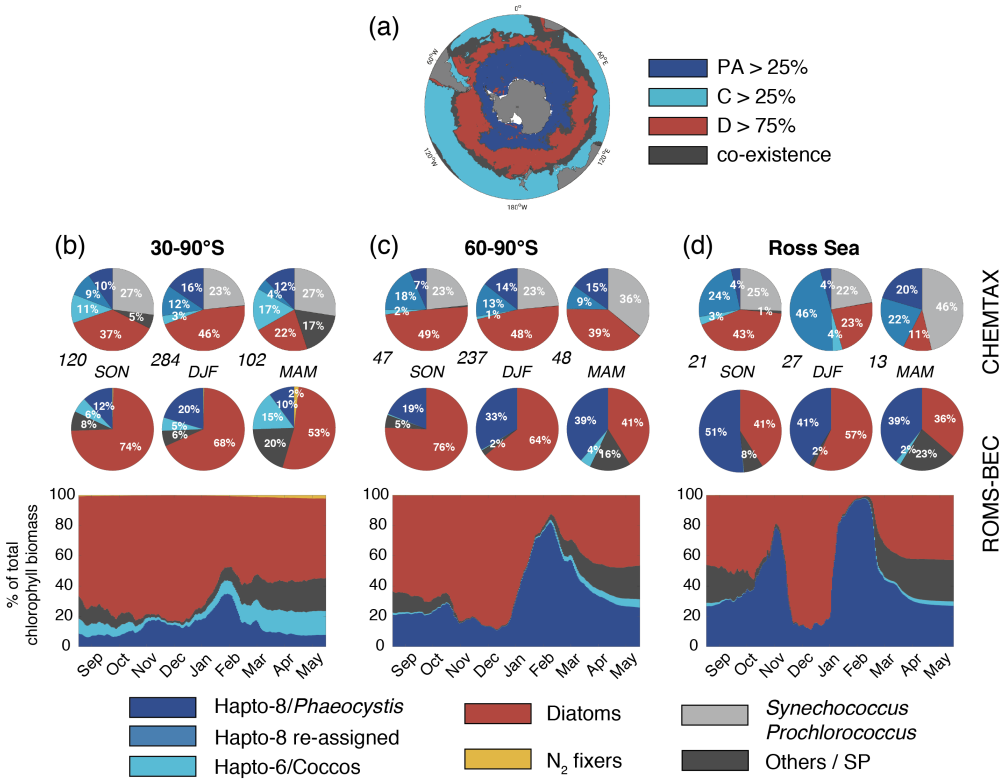

Figure 2. Spatio-temporal distribution of phytoplankton communities in the SO. a) Diatom-dominated phytoplankton community vs. mixed communities with substantial contributions of *Phaeocystis*, coccolithophores and small phytoplankton in ROMS-BEC. Communities in which neither *Phaeocystis* (PA, dark blue) or coccolithophores (C, light blue) contribute >25 % nor diatoms (D, red) contribute >75 % to total annual NPP are classified as ~~mixed~~ co-existence communities (grey). b)-d) Relative contribution of the five phytoplankton PFTs to total chlorophyll biomass [mg chl m^{-3}] for b) 30-90° S, c) 60-90° S, and d) the Ross Sea. The top pie charts denote the climatological mixed layer average community composition suggested by CHEMTAX analysis of HPLC pigments for spring, summer, and fall, respectively (the total number of available observations for a given region and season is given at the lower left side, Swan et al., 2016), and the lower pie charts denote the corresponding community structure in the top 50 m in ROMS-BEC. Note that the categories in the CHEMTAX analysis are not 100% equivalent to the model PFTs. Here, "others" in the CHEMTAX fractions corresponds to dinoflagellates, cryptophytes, and ~~here~~chlorophytes, and "Hapto-8 reassigned" corresponds to the contribution of Hapto-6 where the temperature is <2° C (see also section 2.3.1). The panels at the bottom denote the daily contribution of each PFT in ROMS-BEC to total surface chlorophyll biomass.

here, see section 2.3.1), the model also captures the seasonal evolution of the relative importance of *Phaeocystis* and diatoms
415 reasonably well, both averaged over 30-90° S (Fig. 2b) and at high SO latitudes (Fig. 2c-d). The model overestimates the contribution of *Phaeocystis* in fall (39% as compared to 24% in CHEMTAX) and spring (51% as compared to 28%) between 60-90° S and in the Ross Sea, respectively (Fig. 2c-d), but the limited number of data points available in the CHEMTAX cli-

matology in this area and the uncertainty in the attribution of pigments in CHEMTAX to the *Phaeocystis* PFT in ROMS-BEC have to be noted (see section 2.3.1).

In the 4-PFT setup of ROMS-BEC, the simulated summer phytoplankton community south of 60° S was often almost solely composed of diatoms (Fig. S4 and Nissen et al., 2018), suggesting that the implementation of *Phaeocystis* led to a substantial improvement in the representation of the observed high-latitude community structure (Fig. 2). Concurrently, as the distribution of silicic acid and nitrate is directly impacted by the relative importance of silicifying and non-silicifying phytoplankton, such as *Phaeocystis*, in the community, the addition of *Phaeocystis* to the model led to an improvement in the simulated high-latitude nutrient distributions when comparing to climatological data from the World Ocean Atlas (WOA, Fig. S5d-f, Garcia et al., 2014b). Upon the addition of *Phaeocystis*, the zonal average location of the silicate front, i.e., the latitude at which nitrate and silicic acid concentrations are equal (Freeman et al., 2018), is shifted northward by ∼7° C in ROMS-BEC (from 57.1° S in 4-PFT setup to 50° S in 5-PFT setup, see Fig. S6). While this is further north than suggested by WOA data (56.5° S, Fig. S6b and Garcia et al., 2014b), this can certainly be expected to affect the competitive fitness of individual phytoplankton types in the subantarctic and possibly at lower latitudes, which we did not assess further in this study. Overall, our model suggests that *Phaeocystis* is an important member of the high-latitude phytoplankton community. In the remainder of the manuscript, we will therefore explore the temporal variability in the relative importance of diatoms and *Phaeocystis* and its implications for SO carbon cycling in more detail.

3.2 ~~Bloom characteristics &~~ Patterns of phytoplankton phenology and seasonal succession

Maximum total chlorophyll concentrations are simulated for the first half of December across latitudes in ROMS-BEC (solid blue line in Fig. 3a). At high SO latitudes south of 60° S, this is 1-2 months earlier than suggested by satellite estimates (black line in Fig. 3a). Yet, compared to the 4-PFT setup (dashed blue line in Fig. 3a), the simulated timing of peak chlorophyll levels improved in this study, with peak chlorophyll delayed by on average a week in the model upon the implementation of *Phaeocystis*. The simulated physical biases (i.e., generally too high temperatures and too shallow mixed layer depths, both favoring an earlier onset of the phytoplankton bloom, see Nissen et al., 2018) only partially explain the bias in the simulated timing of maximum chlorophyll levels (see red and green dashed lines in Fig. S7a), suggesting that biological factors must explain the difference between ROMS-BEC and the satellite product. As diatoms dominate the phytoplankton community at peak total chlorophyll concentrations everywhere in the model domain (compare their bloom timing in Fig. 3c to Fig. 3a and to the simulated community composition in Fig. 2b-d), the mismatch in timing is likely related to the representation of this PFT in the model, and is possibly at least partly caused by their comparatively high growth rates at low temperatures (see Fig. A1a).

In contrast to diatoms, maximum chlorophyll concentrations of *Phaeocystis* are simulated for late November or early December across most latitudes in the model (only around 70° S a peak in late January is simulated, Fig. 3b). Overall, the timing of simulated peak *Phaeocystis* chlorophyll levels corresponds well to the suggested timing of observed maximum seawater DMSP concentrations (peak in November/December in Curran et al., 1998; Curran and Jones, 2000) and the delayed maximum atmospheric DMS concentrations (January/February, e.g. Nguyen et al., 1990; Ayers et al., 1991). This further corroborates the hypothesis that the bias in the timing of maximum total chlorophyll levels in ROMS-BEC is likely caused by how diatoms

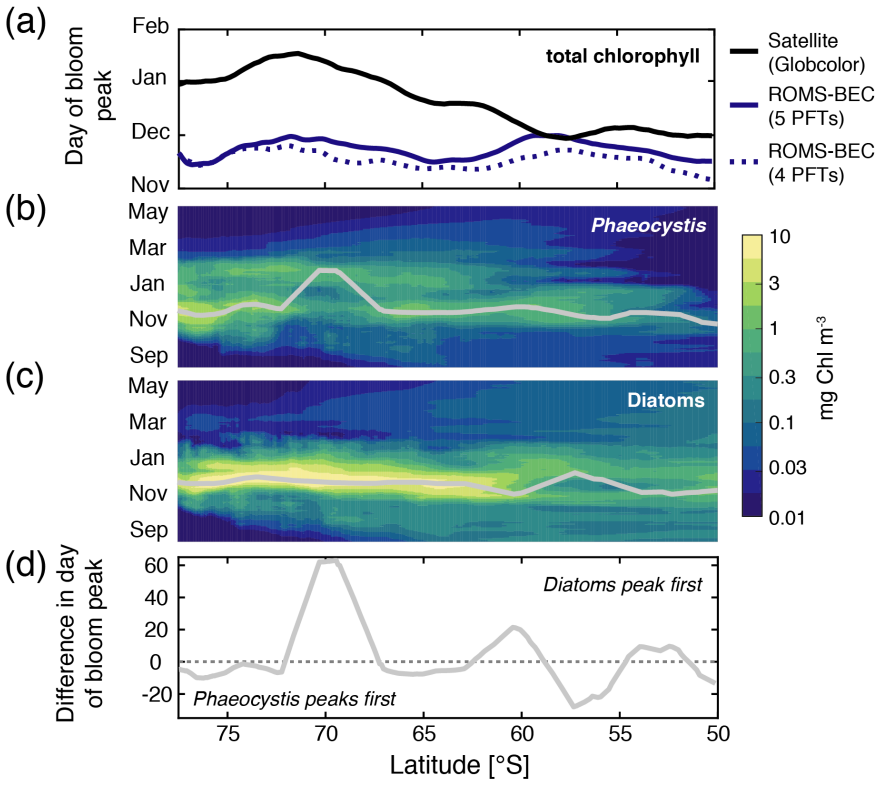

Figure 3. Hovmoller plots south of 50° S of a) the day of maximum total chlorophyll concentrations in a satellite product (black line, Globcolor climatology from 1998-2018 based on the daily 25 km chlorophyll product, see Fanton d'Andon et al., 2009; Maritorena et al., 2010), the *Baseline* simulation of this study (solid blue line), and the *Baseline* simulation of Nissen et al. (2018, dashed blue line; without *Phaeocystis*), and daily surface b) diatom and c) *Phaeocystis* chlorophyll biomass concentrations [mg chl m^{-3}]. Overlain are the average day of the peak concentrations for each latitude (see also section 2.3.1). Panel d) denotes the difference in days in the timing of the bloom peak of diatoms and *Phaeocystis* for each latitude, with negative values denoting a succession from *Phaeocystis* to diatoms throughout the season.

are parameterized in the model. Taken together, the model simulates a succession from *Phaeocystis* to diatoms close to the Antarctic continent (south of 72° S, see also Fig. S7b) and in some parts of the open ocean north of 68° S (Fig. 3d & Fig. S7b). The difference in the timing of the bloom peak between the two PFTs is largely <10 days when averaged zonally, but locally exceeds 30 days when looking at individual grid cells in the model (Fig. S7b), in broad agreement with observations, which suggest up to 2 months between the peak chlorophyll concentrations of *Phaeocystis* and diatoms in the Ross Sea (see e.g. Peloquin and Smith, 2007; Smith et al., 2011). Subsequently, we will assess how environmental conditions and biomass loss processes interact to control the ~~SO phytoplankton biogeography and in particular the~~ competition between *Phaeocystis* and diatoms at high SO latitudes.

3.3 ~~Analyzing ecological niches: A bottom-up perspective on~~ Drivers of SO phytoplankton biogeography, phenology, and succession patterns

~~Simulated DJFM average top 50 m average a) & d) *Phaeocystis*, b) & e) diatom, and c) & f) coccolithophore carbon biomass concentrations mmol C m^{-3}south of 40° S as a function of the simulated concurrent a)-c) nitrate concentrations mmol N m^{-3}and temperature (° C) and d)-f) temperature ° Cand mixed layer PAR levels (W m^{-2}). Overlain are the observed ecological niche centers (median) and breadths (inter quartile ranges) for example taxa of the three functional types from Brun et al. (2015, circles and solid l as simulated in ROMS-BEC (triangles and dashed lines; area and biomass weighted). The red bars on the axes indicate the simulated range of the respective environmental condition in ROMS-BEC between 60-90° S and averaged over DJFM and the top 50 m.~~

Relating the observed or simulated ~~biomass concentrations of a PFT~~ PFT biomass concentrations to the concurrent environmental conditions allows for an assessment of the ecological niche of the PFT in question. In ROMS-BEC, ~~in~~ *Phaeocystis* and diatoms occupy distinct ecological niches in the *Baseline* simulation, in agreement with their distinct ~~simulated geographical~~ geographic distributions in summer (Fig. 1~~e-e), *Phaeocystis*, diatoms, and coccolithophores also occupy distinct ecological niches in the model~~c-d). Between 40-90° S, the niche center of DJFM average *Phaeocystis* biomass is simulated at a nitrate concentration of 18.8 mmol m^{-3} (inter quartile range (IQR) 16.6~~-20.6~~-20.5 mmol m^{-3}), a temperature of 1.1° C (IQR -0.2-2.6° C), and MLPAR of 27.8 W m^{-2} (IQR 24.3-32 W m^{-2}, Fig. 4a & ~~d). In comparison~~c). Since the diatom PFT in ROMS-BEC represents multiple species (in contrast to the *Phaeocystis* PFT), diatoms occupy a wider niche in temperature (~~inter quartile range~~ IQR 0.8-8.5° C, niche center at 5° C~~, Fig. 4b) . While the niche center is at lower nitrate concentrations for diatoms (15.5)~~ and nitrate (IQR 11-19.5 mmol m^{-3}~~) than for *Phaeocystis* (18.8~~, niche center at 15.5 mmol m^{-3}) ~~, maximum diatom biomass at high SO latitudes, i.e., where DJFM average temperatures are <5° C, is simulated at higher nitrate concentrations than maximum~~ in the model, which is in agreement with the ecological niches of important SO diatom and *Phaeocystis* ~~biomass~~ species derived by Brun et al. (2015) based on presence/absence observations and species distribution models (Fig. 4a & b). In ~~the model, averaged over the summer, the difference in biomass concentrations across MLPAR between diatoms and~~ ROMS-BEC, the niche center is only at marginally higher MLPAR for diatoms than for *Phaeocystis* ~~is rather small (niche center at~~ (28.9 W m^{-2} ~~and~~ compared to 27.8 W m^{-2}, respectively, Fig. 4~~d & e) . In agreement with their maximum simulated biomass concentrations in the subantarctic (section 3.1), the niche center of coccolithophore biomass~~ c & d) and is at higher ~~temperatures (10.4° C), higher light levels (35.8~~ MLPAR for both PFTs than available observations for important SO species suggest (~10 W m^{-2} ~~), and lower nitrate concentrations (8.8 mmol m^{-3})than the niche center of the other~~ and ~20 W m^{-2} for *Phaeocystis* and diatoms, respectively, see Fig. 4c & d). While this bias in the MLPAR niche is consistent with the mixed layer depth bias in ROMS-BEC (~10 m; Nissen et al., 2018), the small difference in the MLPAR niche center between *Phaeocystis* and diatoms implies a minor role for MLPAR in controlling the differences in DJFM average biomass concentrations of these two PFTs (Fig. ~~4c & f). Regarding~~ 1c-d). With regard to iron, the ~~three~~ two PFTs do not occupy distinct ecological niches in ROMS-BEC (niche centers at 0.32 μmol m^{-3} ~~, 0.32 μmol m^{-3}, and 0.34 μmol m^{-3} for *Phaeocystis*, diatoms, and coccolithophores, respectively,~~ for both PFTs, see Fig. ~~S8). Given that~~ S9). Yet, as all simulated phytoplankton growth is limited by iron

availability in the high-latitude SO ~~in the model~~ (Fig. S1), this suggests that the spatio-temporal averaging applied for the niche analysis here potentially precludes the assessment of the ~~ecological niche in iron space (by averaging over DJFM here if iron were to matter~~ role of iron in the competition between *Phaeocystis* and diatoms, especially on a sub-seasonal scale~~).~~

~~In comparison to the~~ . We conclude that the simulated ecological niches of ~~important SO phytoplankton taxa derived by Brun et al. (2015) based on global presence/absence observations of phytoplankton and species distribution models, the niche centers of all PFTs are simulated at higher MLPAR in the model (~30 W m^{-2}~~ *Phaeocystis* and diatoms are largely in agreement with available observations, ~~~30 W m^{-2}, and ~35 W m^{-2}) than in available observations(~10 W m^{-2}, ~20 W m^{-2} and ~30 W m^{-2} for *Phaeocystis*, diatoms, and coccolithophores, respectively, Fig. 4d-f). Yet, the 5-20 W m^{-2} higher model-based estimates are consistent with the mixed layer depth bias in ROMS-BEC (see Nissen et al., 2018). While the simulated niche of diatoms regarding temperature and nitrate is in broad agreement with that observed for example SO taxa (Fig. 4b), the simulated niches are wider for *Phaeocystis* (Fig. 4a) and generally centered around lower temperatures for coccolithophores (Fig. 4c). Acknowledging the difficulties comparing a~~ but acknowledge the difficulties in comparing the ecological niche of a model PFT to ~~individual phytoplankton taxa~~those of individual phytoplankton species or groups, a sampling bias towards temperate and tropical species/strains ~~,~~ and the overall low data coverage in the high-latitude SO ~~, we conclude that the simulated ecological niches of *Phaeocystis*, diatoms, and coccolithophores are largely in agreement with available observations. Since the analysis of the summer average ecological niches does not inform about sub-seasonal environmental variability and neglects~~ in Brun et al. (2015), and the limitation of this niche analysis to inform about the role of top-down factors and sub-seasonal environmental variability in controlling the simulated ~~distributions~~ biogeography of phytoplankton types~~, we will assess these in more detail for the simulated competition between *Phaeocystis* and diatoms in the following~~.

3.4 ~~High-latitude competition of *Phaeocystis* and diatoms: An assessment of bottom-up and top-down factors~~

The temporal evolution of the relative growth ratio, i.e., the ratio of the specific growth rates of diatoms and *Phaeocystis*~~(Eq. 2)~~, informs about the competitive advantage of one PFT over the other throughout the year ~~. In~~ due to bottom-up factors and can be broken down into the different environmental contributors for each phytoplankton type at any point in time (Eq. 2). In the 5-PFT *Baseline* simulation of ROMS-BEC, the relative growth ratio is ~~negative throughout spring and fall between 60-90° S (μ^{PA} is on average 5%/6% larger than μ^{D} in spring/fall) and only positive~~ only positive ($\mu^{D} > \mu^{PA}$) between early December and early February between 60-90° S (μ^{D} is on average 5% larger than μ^{PA} in summer, but 5-6% smaller in the other seasons, Fig. 5a & c) ~~. Hence, bottom-up factors promote the accumulation of *Phaeocystis* (diatom) relative to diatom (*Phaeocystis*) biomass in spring/fall (summer) in this area in our model. In comparison, the relative growth ratio is positive for a shorter time period in the~~ and only between mid-December and mid-January in the Ross Sea (μ^{D}~~>~~μ^{PA} ~~between mid-December and mid-January, Fig. 5b). In fact, averaged seasonally, the specific growth rate of *Phaeocystis* is larger than that of diatoms for all seasons (μ_{rel}^{DPA}~~<0), being~~ is up to 38% larger ~~in spring (~~than μ^{D} in spring, Fig. 5~~d), suggesting that~~ b & d). Hence, bottom-up factors ~~are particularly favorable for~~ promote the accumulation of *Phaeocystis* ~~biomass~~ relative to diatom biomass over much of the year, particularly in the Ross Sea.

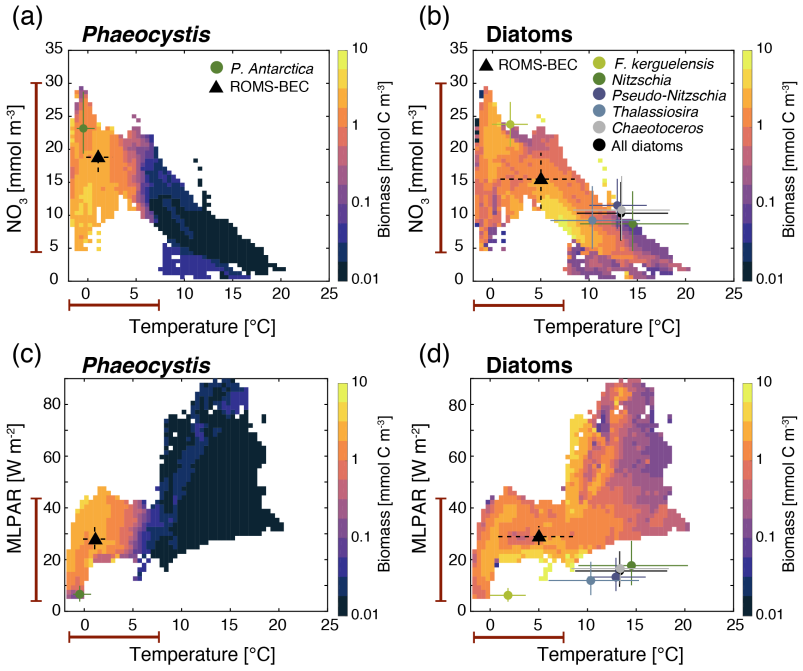

Figure 4. Simulated DJFM average top 50 m average a) & c) *Phaeocystis* and b) & d) diatom carbon biomass concentrations (mmol C m^{-3}) south of 40° S as a function of the simulated temperature (° C) and a)-b) nitrate concentrations (mmol N m^{-3}) and c)-d) mixed layer PAR levels (W m^{-2}). Overlain are the observed ecological niche centers (median) and breadths (inter quartile ranges) for example taxa of the two functional types from Brun et al. (2015, circles and solid lines) and as simulated in ROMS-BEC (triangles and dashed lines; area and biomass weighted). The red bars on the axes indicate the simulated range of the respective environmental condition in ROMS-BEC between 60-90° S and averaged over DJFM and the top 50 m.

~~To understand the controls of the spatio-temporal differences in the specific growth rates, the relative growth ratio can be broken down into the environmental factors contributing to the simulated specific growth rate of each phytoplankton type at any point in time (Eq. 2, colors in Fig. 5a-d). As a direct result of the higher k_{Fe} of *Phaeocystis* in the model (~~In both areas, as expected from the chosen half-saturation constants ($k^{PA}_{Fe} > k^{D}_{Fe}$; Table 1), the iron limitation of ~~their~~ *Phaeocystis* growth is stronger than that of diatoms in the model, and iron availability ~~, i.e., β_{Fe} in Eq. 2,~~ is an advantage for diatoms ~~both between 60-90° S and in the Ross Sea~~ at all times (~~blue area is positive, $\beta_{Fe} > 0$;~~ up to 14% stronger iron limitation of *Phaeocystis* in both areas in summer, ~~see~~ blue areas in Fig. 5a-d). Yet, the two subareas differ in the simulated temperature and light limitation of growth of *Phaeocystis* and diatoms. Overall, temperature is limiting diatom growth more than *Phaeocystis* growth in both subareas throughout the year ($\beta_T < \beta_T < 0$~~; up to 16% and~~), but this difference is rather small in summer between 60-90° S (5%, but up to 19% stronger growth limitation ~~between 60-90° S and~~ in the Ross Sea, ~~respectively, see~~ red areas in Fig. 5a-d~~). While the growth advantage of *Phaeocystis* regarding temperature is rather constant over time in the Ross Sea (Fig. 5b & d), their advantage is substantially smaller in summer between 60-90° S (5%,~~ , see also Fig. ~~5a & c). Additionally~~ A1). Similarly, the dif-

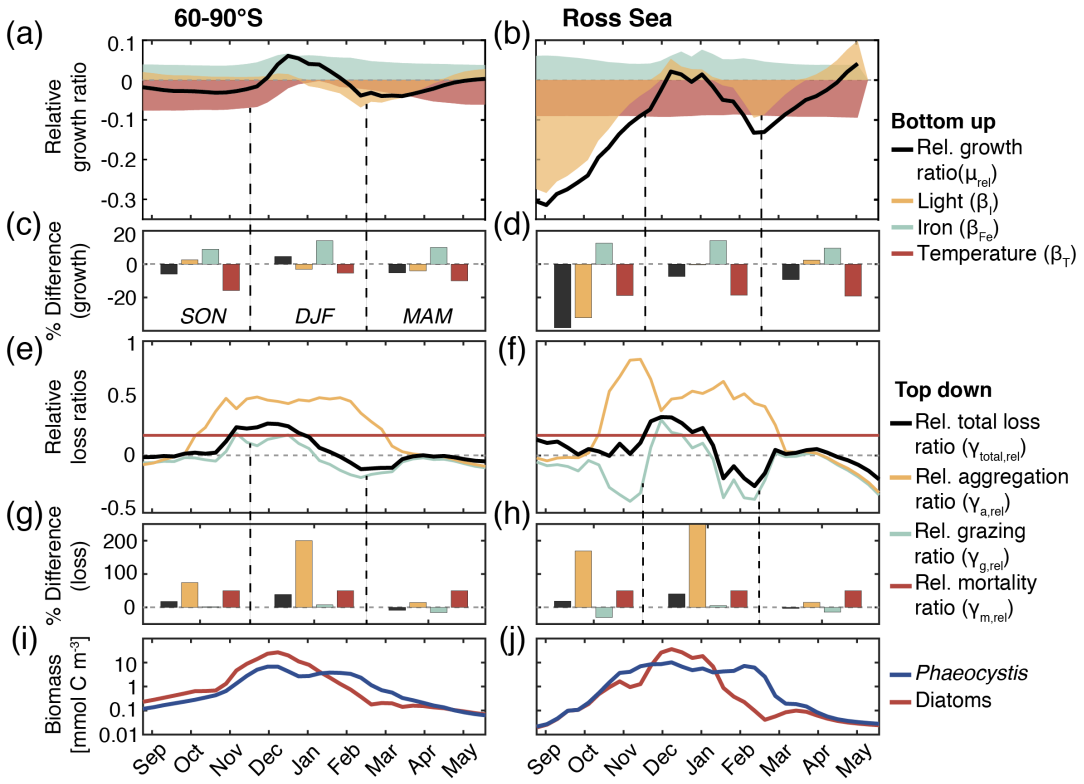

Figure 5. a) & b) Relative growth ratio (black) of diatoms vs. *Phaeocystis*. The colored areas are the contributions of the limitation of growth by light (yellow, β_{I}), iron (blue, β_{Fe}), and temperature (red, β_{T}, see Eq. 2). c) & d) Seasonally averaged percent difference between diatoms and *Phaeocystis* in the specific growth rate (black), light limitation (yellow), iron limitation (blue), and temperature limitation (red). Calculated from non-log-transformed ratios, i.e., e.g. black bar corresponds to $10^{\mu_{\mathrm{rel}}^{\mathrm{DPA}}}$ (see Eq. 2). e) & f) Relative total loss ratio (black) of diatoms vs. *Phaeocystis*, with contributions of the relative grazing ratio (blue), relative non-grazing loss ratio (red), and relative aggregation ratio (yellow, see Eq. 3-6). g) & h) Seasonally averaged percent difference between diatoms and *Phaeocystis* in the total specific loss rate (black), specific aggregation rate (yellow), specific grazing rate (blue), and specific mortality rate (red), calculated from non-log-transformed ratios. i) & j) *Phaeocystis* (blue) and diatom (red) surface carbon biomass concentrations [mmol C m^{-3}]. For all metrics, the left panels are ~~averaged~~ surface averages over 60-90° S and those on the right for the Ross Sea.

ference in light limitation between diatoms and *Phaeocystis* is rather small ~~in this area~~ between 60-90° S (3-4% throughout the year, yellow areas in Fig. 5a & c), implying that their differences in α_{PI} (43% higher for *Phaeocystis*, see Table 1) are balanced by differences in photoacclimation in ROMS-BEC ~~(Geider et al., 1998; Nissen et al., 2018). Consequently, the combination of the comparatively large advantage in iron limitation and the rather small disadvantage in temperature limitation results in the higher specific growth rates of diatoms in summer between 60-90° S~~in this area (see Eq. B9 and Geider et al., 1998). In contrast, in the Ross Sea, differences in light limitation between diatoms and *Phaeocystis* are large, ~~with a maximum advantage for *Phaeocystis*~~ especially in spring (~~their growth~~ the growth of diatoms is 32% ~~less~~ more light limited; Fig. 5b & d). Therefore,

the difference in light limitation predominantly controls the seasonality of the relative growth ratio (Fig. 5b) and promotes the dominance of *Phaeocystis* over diatoms early in the growing season in this area in our model (Fig. 5j), which is not simulated when averaging over 60-90° S (Fig. 5i). Nevertheless, acknowledging the sensitivity of the simulated *Phaeocystis* and diatom biomass levels to all chosen model parameters describing the growth of the respective PFT (the annual mean biomass changes by >17% and >14% for *Phaeocystis* and diatoms, respectively, in the experiments TEMPERATURE, ALPHA$_{PI}$, and IRON, Fig. A2 & Fig. S11), the sensitivity simulations support the importance of light in controlling the annual mean high-latitude phytoplankton community structure for both subareas, as the elimination of the differences in α_{PI} between the PFTs results in the largest biomass changes both between 60-90° S (-76% and +52% for *Phaeocystis* and diatoms, respectively) and in the Ross Sea (-87% and +86%, Fig. A2). Altogether, in ROMS-BEC, differences in growth between diatoms and *Phaeocystis* are mostly controlled by seasonal differences in iron/temperature (60-90° S) and iron/light conditions (Ross Sea), respectively. Still, given the simulated growth advantage of *Phaeocystis* throughout much of the growing season in both subareas, bottom-up factors alone cannot explain why *Phaeocystis* only dominates over diatoms temporarily (Fig. 5i & j), implying that top-down factors need to be considered to explain their biomass evolution in our model.

In both subareas, the simulated relative total loss ratio is positive throughout spring and summer, implying that the specific total loss rate of *Phaeocystis* is higher than that of diatoms (γ^{PA}_{total}>γ^{D}_{total}, see Eq. 6), which favors the accumulation of diatom biomass relative to that of *Phaeocystis* (Fig. 5e-h). In fact, the total loss rate of *Phaeocystis* is on average 17%/38% (60-90° S) and 18%/40% (Ross Sea) higher than that of diatoms in spring/summer ~~in ROMS-BEC~~ (Fig. 5g & h), despite the higher prescribed maximum grazing rate on *Phaeocystis* in ROMS-BEC (Table 1). In the model, the relative total loss ratio is only negative in early fall in both subareas (γ^{D}_{total}>γ^{PA}_{total}, Fig. 5e & f), but ~~in this season,~~ the difference between diatoms and *Phaeocystis* in their specific total loss rates is ~~overall smaller than in the other seasons~~ rather small in this season (9% and 3% between 60-90° S and in the Ross Sea, respectively, Fig. 5g & h). In all top-down sensitivity experiments, the simulated change in *Phaeocystis* biomass levels is larger than for the bottom-up experiments (>20% for experiments GRAZING, AGGREGATION, and MORTALITY, see Fig. A2), and the dominance of *Phaeocystis* over diatoms increases in magnitude and duration both between 60-90° S and in the Ross Sea if disadvantages of *Phaeocystis* in the loss processes are eliminated (Fig. S11). The simulated seasonality of the total loss ratio is the result of the interplay between losses through grazing, aggregation, and non-grazing mortality of each phytoplankton type in ROMS-BEC (Eq. 6, colors in Fig. 5e-h). Of all three loss pathways, differences in aggregation losses in the *Baseline* simulation are largest between *Phaeocystis* and diatoms both between 60-90° S (up to 200% higher aggregation losses for *Phaeocystis* in summer, yellow in Fig. 5e & g) and in the Ross Sea (up to 250% higher in summer, Fig. 5f & h). In comparison, differences between *Phaeocystis* and diatoms in grazing (up to 16% and 14% between 60-90° S and in the Ross Sea, respectively) and mortality losses (50% everywhere) are considerably smaller (see blue and red areas in Fig. 5e-h, respectively), suggesting that aggregation losses predominantly contribute to the simulated differences in the total loss rates between *Phaeocystis* and diatoms.

In summary, between 60-90° S, the simulated growth advantage of *Phaeocystis* early in the season (facilitated by advantages in the temperature limitation of their growth) are not large enough to outweigh the disadvantages in iron limitation of their growth and in the biomass losses they experience. As a result, in spring and summer, *Phaeocystis* do not accumulate substantial

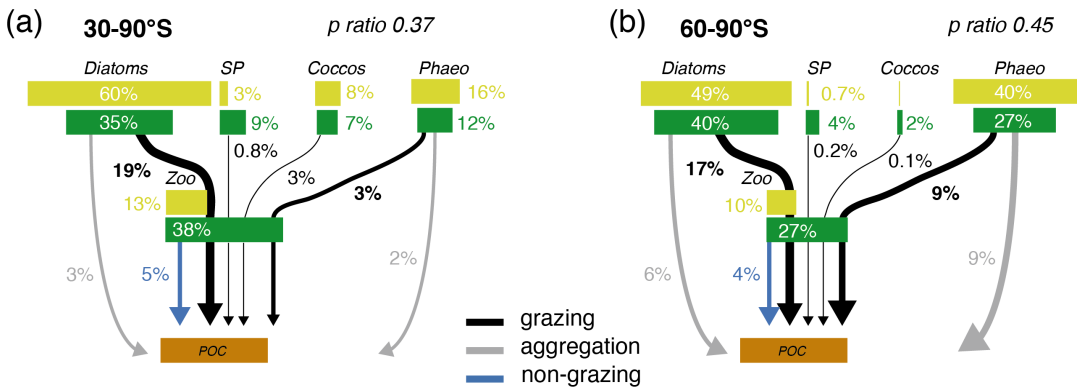

Figure 6. Pathways of particulate organic carbon (POC) formation in the *Baseline* simulation of ROMS-BEC averaged annually over a) 30-90° S and b) 60-90° S. The green and yellow boxes show the relative contribution (%) of *Phaeocystis*, diatoms, coccolithophores, small phytoplankton (SP), and zooplankton (Zoo) to the combined phytoplankton and zooplankton biomass (green) and total POC production (yellow) in the top 100 m, respectively. The arrows denote the relative contribution of the different POC production pathways associated with each PFT (black = grazing by zooplankton, grey = aggregation, blue = non-grazing mortality), given as % of total NPP in the top 100 m. Numbers are printed if ≥0.1% and rounded to the nearest integer if >~~0.5~~1%. The sum of all arrows gives the POC production efficiency (p ratio). Note that diazotrophs are not included in this figure due to their minor contribution to NPP in the model domain.

biomass relative to (or even dominate over) diatoms in this subarea in ROMS-BEC. In the Ross Sea, however, the simulated growth advantages of *Phaeocystis* (resulting from advantages in the light and temperature limitation of their growth) are large enough to outweigh the disadvantages in iron limitation and specific biomass loss rates, allowing them to dominate over diatoms early in the growing season in our model and explaining the simulated succession from *Phaeocystis* to diatoms close to the Antarctic continent (see also section 3.2). Ultimately, this simulated spatio-temporal variability in the relative importance of *Phaeocystis* and diatoms has implications for ~~both SO and global~~ SO carbon cycling, which we will assess ~~subsequently~~in the following.

3.4 Quantifying the importance of *Phaeocystis* for the ~~cycling of~~ SO carbon cycle

Phaeocystis is an important member of the SO phytoplankton community in our model, particularly south of 60°S, where it contributes 46% and 40% to total annual NPP and POC formation, respectively ~~.~~(Table 3 & Fig. 6). Even when considering the entire region south of 30°S, the contribution of *Phaeocystis* to NPP (15%) and POC production (16%) is sizeable. The simulated spatial differences in phytoplankton community structure have direct implications for the fate of organic carbon upon biomass loss, and Fig. 6 illustrates the annually integrated importance of different pathways of POC formation ~~for~~ related to each PFT in ROMS-BEC. Overall, in our model, the p ratio, i.e., the fraction of NPP that is transformed to sinking POC (Laufkötter et al., 2016), is higher at high latitudes south of 60° S (45%) than the domain average (37%, Fig. 6). This is a direct result of the higher fraction of large phytoplankton types, i.e., *Phaeocystis* and diatoms, in the ~~phytoplankton community in this area (~~ecosystem south of 60° S (67% of total carbon biomass) than between 30-90° S (47%; Fig. 6, but see also Fig. 2), facilitating more carbon

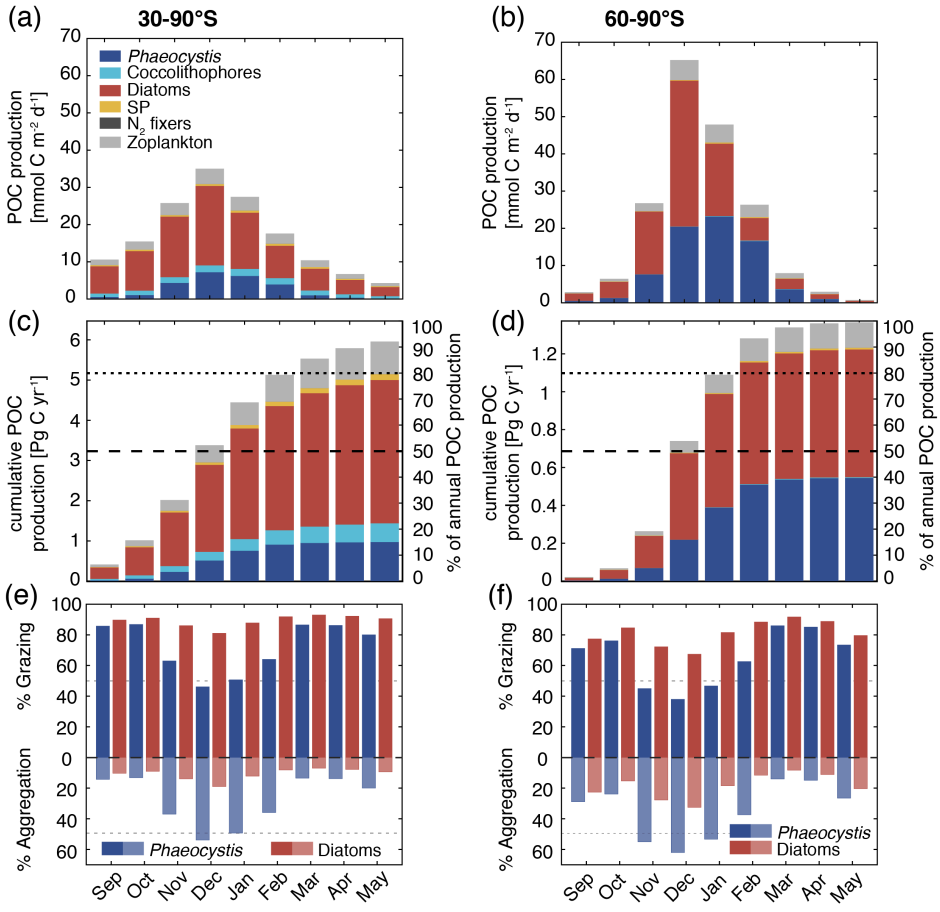

Figure 7. Simulated vertically integrated production of particulate organic carbon (POC) a) & b) as a function of time [mmol C m^{-2} d^{-1}], c) & d) cumulative over time (absolute production in Pg C yr^{-1} on the left axis and relative to annually integrated production on the right axis), and e) & f) as a function of time via grazing and aggregation, respectively. The colors correspond to the different PFTs in ROMS-BEC, and the panels correspond to averages or integrals over 30-90° S (left) and 60-90° S (right), respectively.

export relative to NPP in the model. In fact, our model results suggest that these two large phytoplankton types contribute more to POC formation than to total biomass (76% and 89% of total POC formation between 30-90° S and 60-90° S, respectively; compare yellow and green boxes in Fig. 6). Integrated annually, diatoms contribute most of all PFTs to POC formation in our model (60% and 49% between 30-90° S and 60-90° S, respectively, Fig. 6). For both diatoms and *Phaeocystis*, grazing by zooplankton (i.e., the formation of fecal pellets) is the most important pathway of POC production in ROMS-BEC (black arrows in Fig. 6, ~~13~~9%/52% and ~~29~~20%/37% of total POC production for *Phaeocystis*/diatoms between 30-90° S and 60-90° S, respectively). Yet, at high latitudes (60-90° S), aggregation of *Phaeocystis* biomass contributes significantly to POC formation (20% of total POC production, 9% of NPP, grey arrows in Fig. 6b). Given that the loss of biomass via a given pathway is a function of the local biomass concentrations of each PFT at any given point in time ~~(see section 2.1 and Nissen et al., 2018)~~(see

section 2.1 and appendix B), the relative importance of any PFT or biomass loss pathway for total POC formation and hence the total POC produced vary throughout the year.

The seasonal variability in total POC formation is governed by the variability in total chlorophyll concentrations both between 30-90° S and 60-90° S, and peak POC formation rates of 35 mmol m^{-2} d^{-1} (30-90° S) and 65 mmol m^{-2} d^{-1} (60-90° S) are simulated for December in ROMS-BEC (Fig. 7a & b; compare to Fig. 3a). Similarly, the contribution of *Phaeocystis* and diatoms to total POC formation closely follows their contribution to total biomass over the year, with the contribution of *Phaeocystis* peaking in January (23%) and February (63%) for 30-90° S and 60-90° S, respectively (Fig. 7a & b; compare timing to Fig. 2b & c). As a result of the close link between POC formation and chlorophyll concentrations in ROMS-BEC, the majority of the annual POC formation occurs between November and February in our model (64% and 88% south of 30° S and 60° S, respectively, Fig. 7c & d). During these months, the simulated pathways of POC formation differ from the annually integrated perspective in Fig. 6, especially for *Phaeocystis*. While grazing is the most important pathway throughout the year for diatoms in both subareas in our model (red bars in Fig. 7e & f), aggregation of *Phaeocystis* is as important as grazing in December and January between 30-90° S (blue bars in Fig. 7e) and even dominantly contributes to POC formation between November and January at high SO latitudes (up to 65%, blue bars in Fig. 7f). Altogether, this implies that both spatial and temporal variations in SO phytoplankton community structure critically impact the fate of carbon beyond the upper ocean.

4 Discussion

~~Our simulated contribution of~~ and the competition between *Phaeocystis* ~~to SO NPP and net POC formation is higher than that found in the previous modeling study by Wang and Moore (2011), particularly at higher latitudes: They diagnosed a contribution of 13% and 23% to NPP south of 40° S and 60° S, respectively, compared to our estimates of 15% for south of 30° S and 46% for the region south of 60° S. We interpret the difference to stem primarily from differences in parameter choices of the PFTs between the two models. As an example, the half-saturation constant of iron of *Phaeocystis* is 125% larger than that of diatoms in the model by Wang and Moore (2011, 0.18 μmol m^{-3} for *Phaeocystis* as compared to 0.08 μmol m^{-3} for diatoms), but only 33% larger in ours (Table 1). The resulting smaller difference in the growth limitation by iron in ROMS-BEC leads to more competitive *Phaeocystis* relative to diatoms in the iron-depleted SO and can at least partially explain the higher relative importance of *Phaeocystis* in our model. In fact, differences in model parameters between *Phaeocystis* and diatoms in ROMS-BEC can alter the simulated contribution of *Phaeocystis* to total NPP from 5-32% and 17-63% between 30-90° S and 60-90° S, respectively (see section A1, as well as section 2.2 and Table 2). This illustrates how single model parameters sensitively impact the competitive success of *Phaeocystis* in the SO. Still, the simulated community structure in the *Baseline* simulation with ROMS-BEC is supported by available observations (see section 3.1), giving us confidence in our estimates.~~

~~The simulated contribution of *Phaeocystis* to POC export in ROMS-BEC (16% and 40% south of 30° S and 60° S) is in broad agreement with the previous estimate from Wang and Moore (2011, 19% and 30% south of 40° S and 60° S, respectively). This is despite the differences in phytoplankton community structure between the two models (see above) and demonstrates our on-going limited quantitative understanding of the fate of biomass losses (see also Laufkötter et al., 2016). Across the parameter~~

sensitivity runs in ROMS-BEC (section 2.2), the contribution of *Phaeocystis* to POC production and export varies from 4-23% and 13-59% south of 30° S and 60° S, respectively. In addition to this uncertainty resulting only from the growth and loss parameters of *Phaeocystis* in the model (Table 2), further uncertainty arises from parameters describing the partitioning of biomass losses amongst dissolved and particulate carbon species, which we did not assess in this study. Acknowledging that the exact numbers are highly sensitive to parameter choices in the model, our analysis reveals how the pathways of POC production, in particular the relative importance of fecal pellets from zooplankton and aggregated phytoplankton cells, are impacted by the simulated spatio-temporal variability in phytoplankton community structure throughout the year (Fig. 7). In this regard, the simulated strong temporal coupling between POC fluxes and biomass distributions in ROMS-BEC is a direct result of the model formulations describing particle sinking (Lima et al., 2014). This coupling is supported by observations, e.g., from the Ross Sea, where the POC flux from the upper ocean has been found to be closely linked to biomass levels in the overlying surface layer (with aggregates being an important vector for POC export when *Phaeocystis* dominated the community, Asper and Smith, 1999). Yet, the coupling in our model is potentially too strong in other areas, where reprocessing of POC by zooplankton in the upper ocean or lateral advection of POC could decouple the seasonal evolution of phytoplankton biomass and POC export (e.g. Lam and Bishop, 2007; Stange et al., 2017), the effect of which we can currently not assess. Given the possibly large importance of different POC production pathways for carbon and nutrient cycling through their impact on the remineralization depth of organic matter, these processes should be better constrained in the future, in order to further quantify the imprint of spatio-temporal variations in the relative importance of *Phaeocystis* for the high-latitude cycling of carbon. Despite these uncertainties, *Phaeocystis* is clearly a substantial player on the global scale. Comparing the model-simulated integrated NPP and POC export across the entire model domain with data-based estimates of global NPP and POC export suggests that SO *Phaeocystis* alone contribute about 5% to globally integrated NPP (58 ± 7 Pg C yr^{-1}, Buitenhuis et al., 2013a), and about the same percentage to global POC export (9.1 ± 0.2 Pg C yr^{-1}, DeVries and Weber, 2017).

Besides its impact on the carbon cycle, *Phaeocystis* is the major contributor to the marine sulphur cycle in the SO through its production of DMSP (Keller et al., 1989; Liss et al., 1994; Stefels et al., 2007). Integrating the modeled *Phaeocystis* biomass loss rates via zooplankton grazing and non-grazing mortality and making assumptions regarding the corresponding DMS(P) release (see section 2.3.1), our estimated annual DMS production by *Phaeocystis* in ROMS-BEC amounts to 3.3-11.5 Tg S and 1.8-6.4 Tg S south of 30° S and 60° S, respectively. Consequently, assuming that all of this DMS production quickly escapes to the atmosphere, our estimates correspond to 11.6-40.1% (30-90° S) and 6.5-22.7% (60-90° S) of the global flux of DMS to the atmosphere previously estimated by Lana et al. (2011, 28.1 Tg S yr^{-1}). Our estimate is an upper bound, however, as not all DMS produced in seawater is readily released to the atmosphere. In fact, a fraction is likely broken down by bacteria, by photolysis, or is mixed down in the water column (see e.g. Simó and Pedrós-Alló, 1999; Stefels et al., 2007). Still, given that other phytoplankton types also produce DMS(P) (Keller et al., 1989; Stefels et al., 2007), the ROMS-BEC-based contribution of SO *Phaeocystis* alone (3.3-11.5 Tg S yr^{-1}) to the global flux of DMS to the atmosphere is in agreement with the flux suggested in Lana et al. (2011, 8.1 Tg S yr^{-1} south of 30° S, i.e., 29% of their global estimate), and the substantial contribution of SO *Phaeocystis* underpins its major role for the global cycling of sulphur.

4.1 Drivers of phytoplankton biogeography and the competition between *Phaeocystis* and diatoms

In ROMS-BEC, the interplay of iron availability with temperature (60-90° S) and light levels (Ross Sea), respectively, largely controls the competitive fitness of *Phaeocystis* relative to diatoms in the high-latitude SO. Yet, differences in the simulated biomass loss rates between the two PFTs (in particular via aggregation) need to be considered in order to explain why peak *Phaeocystis* biomass levels precede those of diatoms only close to the Antarctic continent in the model. In the literature, the spatial distribution of *Phaeocystis* and diatoms and the temporal succession from *Phaeocystis* to diatoms is almost exclusively discussed in terms of light and iron availability (see e.g. Arrigo et al., 1999; Smith et al., 2014). In this context, regions/times of low light and/or high mixed layer depth are typically associated with high *Phaeocystis* abundance (Alvain et al., 2008; Smith et al., 2014), explaining their bloom in spring, whereas iron availability has been suggested to largely control the magnitude of the summer diatom bloom (Peloquin and Smith, 2007; Smith et al., 2011). This is in agreement with the simulated dynamics and parameters chosen in ROMS-BEC, in which the difference in light limitation between growth of *Phaeocystis* and diatoms facilitates early *Phaeocystis* blooms in the Ross Sea. Yet, it has to be noted that advantages in temperature limitation contribute to the growth advantage of *Phaeocystis* in the high-latitude SO in ROMS-BEC as well ~~.~~ and without it, *Phaeocystis* would contribute substantially less to high-latitude phytoplankton biomass (Fig. A2). Currently, this growth advantage of *Phaeocystis* at temperatures $<4°$ C is possibly underestimated in the model, as diatom growth at low temperatures is currently overestimated when comparing to available laboratory measurements (Fig. A1a). Nevertheless, in agreement with Peloquin and Smith (2007) and Smith et al. (2011), when diatoms reach peak chlorophyll levels in summer in our model, the simulated difference in iron limitation between the two PFTs is largest across the high-latitude SO (Fig. 5a & b), suggesting that any change in summer iron availability will indeed strongly impact peak diatom and hence total chlorophyll levels in ROMS-BEC.

~~Still, an~~ An important limitation in the assessment of the role of iron in controlling the relative importance of *Phaeocystis* in the high-latitude phytoplankton community is the assumption of a constant k_{Fe} of *Phaeocystis* in the model (0.2 μmol m^{-3}, Table 1). In laboratory experiments, the affinity of *Phaeocystis* for iron has been shown to be sensitive to light (Garcia et al., 2009), which is not accounted for in the *Baseline* simulation of ROMS-BEC. In order to assess the possible effect of a varying k_{Fe} on the competition between *Phaeocystis* and diatoms, we fit a polynomial function to describe the k_{Fe} of *Phaeocystis* as a function of the light level (VARYING_kFE simulation in Table 2, Fig. A1b, Garcia et al., 2009). Acknowledging the ~~substantial~~ uncertainty in the fit, our model simulates k_{Fe} <0.2 μmol m^{-3} ~~and even k_{Fe} <0.15 μmol m^{-3} (corresponding to the k_{Fe} of diatoms in the *Baseline* simulation)~~ only at highest light intensities in summer and mostly close to the surface, and 0.2 μmol m^{-3} $< k_{Fe} \leq$ 0.26 μmol m^{-3} elsewhere as a result of low light levels (Fig. ~~S9a~~ S10a & b). While the contribution of *Phaeocystis* to total NPP is only affected to a lesser extent as a consequence (37% and 13% south of 60° S and 30° S, respectively, instead of 46% and 15% in the *Baseline* simulation), the simulated phytoplankton seasonality is impacted substantially. The maximum chlorophyll levels of diatoms occur earlier than those of *Phaeocystis* in many more places of the SO compared to the *Baseline* simulation, both in coastal areas and in the open ocean (Fig. ~~S9c~~ S10c & d). Thus, in order to include light-iron interactions in future modeling efforts with *Phaeocystis* and to assess their impact on the competition of *Phaeocystis* with diatoms throughout the SO, additional measurements are needed for how k_{Fe} varies as a function of the

surrounding light level. Taken together, given the likely ~~lower k_{Fe}~~ underestimation of ~~*Phaeocystis* at high-latitude light levels in summer than what we currently assume in~~ the growth advantage of *Phaeocystis* in temperature and at least occasionally in iron in ROMS-BEC~~(Fig. A1b and Garcia et al., 2009) and given the likely underestimation of their growth advantage in temperature~~, we probably currently underestimate the competitive advantage in growth of *Phaeocystis* relative to diatoms in the model. However, such a potential underestimation in growth advantage does not automatically mean that the contribution of *Phaeocystis* to the phytoplankton community is underestimated as well. This is because of the important role of biomass loss processes to explain why *Phaeocystis* do not outcompete diatoms everywhere in the high latitudes in ROMS-BEC (Fig. 5). Furthermore, the simulated phytoplankton community structure is in good agreement with available observations (Fig. 2).

Loss processes, such as aggregation and grazing, clearly matter for the competitive advantage of one PFT over another, but these loss processes are generally not well quantified and often not studied with sufficient detail. For example, while the modeling study by Le Quéré et al. (2016) demonstrates the importance of such top-down control for total SO phytoplankton biomass concentrations, an analysis of the impact on phytoplankton community structure is ~~lacking~~yet to be done. In fact, in the literature, only few studies discuss the role of top-down factors for the relative importance of *Phaeocystis* and diatoms in the high-latitude SO (Granéli et al., 1993; van Hilst and Smith, 2002). In agreement with our results, aggregation has been suggested to be an important process facilitating high POC export when *Phaeocystis* biomass is high ~~(Asper and Smith, 1999)~~(Asper and Smith, 1999; Ducklow et al., 2015; Asper and Smith, 2019), but to what extent this process significantly contributes to the observed relative importance of *Phaeocystis* and diatoms throughout the year in the high-latitude SO remains largely unknown.

~~Here, our~~ Our findings suggest an important role for biomass loss processes in controlling the relative importance of *Phaeocystis* and diatoms in ROMS-BEC, but very little quantitative information exists to constrain model parameters (see section 2.1) or to validate the simulated ~~aggregation~~non-grazing mortality, grazing, or ~~non-grazing mortality~~ aggregation loss rates of *Phaeocystis* and diatoms over time. Certainly, the simulated aggregation rates in the model and their impact on spatio-temporal distributions of PFT biomass concentrations and rates of NPP are associated with substantial uncertainty due to the immediate conversion of biomass to sinking detritus in the model, the equal treatment of POC originating from all PFTs, the neglect of disaggregation, and due to the calculation of aggregation rates based on the biomass concentrations of individual PFTs rather than all PFTs or even particles combined (see e.g. Turner, 2015). Given that the simulated biomass distributions in ROMS-BEC are most sensitive to differences in parameters describing non-grazing mortality (e.g. viral lysis) and aggregation (Fig. A2 & S11), any changes in these loss processes will significantly impact the relative abundance of *Phaeocystis* and diatoms in the SO. Additionally, as discussed in Nissen et al. (2018), the lack of multiple zooplankton groups in the SO model (Le Quéré et al., 2016) and the parametrization of the single zooplankton grazer ~~is a major limitation~~ using fixed prey preferences and separate grazing on each prey using a Holling Type II function (Holling, 1959), which thus precludes a saturation of feeding at high total phytoplankton biomass, are major limitations of ROMS-BEC. To what extent accounting implicitly for grazing by higher ~~tropic~~ trophic levels in the non-grazing mortality term makes up for not including more zooplankton PFTs remains unclear. Nevertheless, by changing the overall coupling between phytoplankton and zooplankton and through the distinct grazing preferences of the different zooplankton types, the addition of larger zooplankton grazers would

likely change the simulated temporal evolution of *Phaeocystis* and diatom biomass in the model (Le Quéré et al., 2016). Therefore, the above mentioned uncertainties should be addressed by future in situ or laboratory measurements in order to better constrain the simulated biomass loss processes, as our findings suggest these to be necessary to explain the seasonal evolution of the relative importance of *Phaeocystis* and diatoms in the high-latitude SO.

4.2 Biogeochemical implications of high-latitude SO phytoplankton biogeography

Based on our model results, *Phaeocystis* is a substantial contributor to global NPP and POC export. Comparing the integrated NPP and POC export between 30-90° S in ROMS-BEC with data-based estimates of global NPP and POC export suggests that SO *Phaeocystis* alone contribute about 5% to globally integrated NPP (58±7 Pg C yr^{-1}, Buitenhuis et al., 2013a), and about the same percentage to global POC export (9.1±0.2 Pg C yr^{-1}, DeVries and Weber, 2017). Thereby, our simulated contribution of *Phaeocystis* to global NPP is higher than that found in the previous modeling study by Wang and Moore (2011), particularly at higher latitudes, where Wang and Moore (2011) diagnosed a contribution of 23% to NPP south of 60° S (46% in ROMS-BEC). We interpret the difference to stem primarily from differences in parameter choices of the PFTs between the two models. For example, the lower ratio of the half-saturation constants of iron of *Phaeocystis* and diatoms in our model (25%; Table 1) as compared to the one in Wang and Moore (2011, 125%) leads to a larger growth advantage of *Phaeocystis* over diatoms in our model. In fact, differences in model parameters between *Phaeocystis* and diatoms in ROMS-BEC can alter the simulated contribution of *Phaeocystis* to total NPP from 5-32% and 17-63% between 30-90° S and 60-90° S, respectively (see section 2.2 and also section A1). This illustrates how single model parameters sensitively impact the competitive success of *Phaeocystis* in the SO. Still, the simulated community structure in the *Baseline* simulation with ROMS-BEC is supported by available observations (see section 3.1), giving us confidence in our estimates.

The simulated contribution of *Phaeocystis* to POC export in ROMS-BEC (16% and 40% south of 30° S and 60° S) is in broad agreement with the previous estimate from Wang and Moore (2011, 19% and 30% south of 40° S and 60° S, respectively). This is despite the differences in high-latitude phytoplankton community structure between the two models (see above) and demonstrates our on-going limited quantitative understanding of the fate of biomass losses (see also Laufkötter et al., 2016). Across the parameter sensitivity runs in ROMS-BEC (section 2.2), the contribution of *Phaeocystis* to POC production and export varies from 4-23% and 13-59% south of 30° S and 60° S, respectively. In addition to this uncertainty resulting only from the growth and loss parameters of *Phaeocystis* in the model, further uncertainty arises from parameters describing the partitioning of biomass losses amongst dissolved and particulate carbon species, which we did not assess in this study. Acknowledging that the exact numbers are highly sensitive to parameter choices in the model, our analysis reveals how the pathways of POC production, in particular the relative importance of fecal pellets from zooplankton and aggregated phytoplankton cells, are impacted by the simulated spatio-temporal variability in phytoplankton community structure throughout the year (Fig. 7). In this regard, the simulated strong temporal coupling between POC fluxes and biomass distributions in ROMS-BEC is a direct result of the model formulations describing particle sinking (Lima et al., 2014). This coupling is supported by observations, e.g., from the Ross Sea, where the POC flux from the upper ocean has been found to be closely linked to biomass levels in the overlying surface layer (with aggregates being an important vector for POC export when *Phaeocystis* dominated the community, Asper and Smith, 1999).

Yet, the coupling in our model is potentially too strong in other areas, where reprocessing of POC by zooplankton in the upper ocean or lateral advection of POC could decouple the seasonal evolution of phytoplankton biomass and POC export (e.g. Lam and Bishop, 2007; Stange et al., 2017), the effect of which we can currently not assess. Given the possibly large importance of different POC production pathways for carbon and nutrient cycling through their impact on the remineralization depth of organic matter, these processes should be better constrained in the future, in order to further quantify the imprint of spatio-temporal variations in the relative importance of *Phaeocystis* for the high-latitude cycling of carbon.

Besides its impact on the carbon cycle, *Phaeocystis* is the major contributor to the marine sulphur cycle in the SO through its production of DMSP (Keller et al., 1989; Liss et al., 1994; Stefels et al., 2007). Though not explicitly including the biogeochemical cycling of sulphur, we can nevertheless use model output from ROMS-BEC to obtain an estimate of DMS production by *Phaeocystis* through a simple back-of-the-envelope calculation. Integrating the modeled *Phaeocystis* biomass loss rates via zooplankton grazing and non-grazing mortality over the top 10 m, assuming a molar DMSP:C ratio for *Phaeocystis* of 0.011 (Stefels et al., 2007), and a DMSP-to-DMS conversion efficiency between 0.2-0.7 (the DMS yield depends on the local sulphur demand of our estimated annual DMS production by *Phaeocystis* in ROMS-BEC amounts to 3.3-11.5 Tg S and 1.8-6.4 Tg S south of 30° S and 60° S, respectively. Consequently, assuming that all of this DMS production quickly escapes to the atmosphere, our estimates correspond to 11.6-40.1% (30-90° S) and 6.5-22.7% (60-90° S) of the global flux of DMS to the atmosphere previously estimated by Lana et al. (2011, 28.1 Tg S yr^{-1}). Our estimate is an upper bound, however, as not all DMS produced in seawater is readily released to the atmosphere. In fact, a fraction is likely broken down by bacteria, by photolysis, or is mixed down in the water column (see e.g. Simó and Pedrós-Alló, 1999; Stefels et al., 2007). Still, given that other phytoplankton types also produce DMS(P) (Keller et al., 1989; Stefels et al., 2007), the ROMS-BEC-based contribution of SO *Phaeocystis* alone (3.3-11.5 Tg S yr^{-1}) to the global flux of DMS to the atmosphere is in agreement with the flux suggested in Lana et al. (2011, 8.1 Tg S and the substantial contribution of SO *Phaeocystis* underpins its major role for the global cycling of sulphur.

4.3 Limitations & Caveats

Our results may be affected by several shortcomings regarding the parameterization of *Phaeocystis*, in particular the representation of its life cycle, the fate of its biomass losses, ~~and its~~ the temperature and light limitation of its growth, and its nutrient uptake stoichiometry. We considered here only colonial *Phaeocystis*, thereby implicitly assuming that a seed population of solitary cells is always available for colony formation. Not including an explicit parameterization for single cells and hence life cycle transitions might substantially impact both the seasonal *Phaeocystis* biomass evolution and the competition with diatoms, as solitary cells have been proposed to require less iron (Veldhuis et al., 1991) and are possibly subject to higher loss rates due to e.g. zooplankton grazing compared to colonies (Smith et al., 2003; Nejstgaard et al., 2007). The transition from solitary to colonial cells is a function of the seed population and light and nutrient levels ~~(Verity, 2000)~~(Verity, 2000; Bender et al., 2018), and transition models have been applied in SO marine ecosystem models ~~(e.g. Popova et al., 2007; Kaufman et al., 2017). Yet, implementing~~ (e.g. Popova et al., 2007; Kaufman et al., 2017; Losa et al., 2019). For example, in their higher complexity, self-organizing ecosystem model (Follows et al., 2007), Losa et al. (2019) include both life stages of *Phaeocystis* and two types of diatoms to simulate phytoplankton competition at high SO latitudes. While our model results suggest that this is

not required to reproduce the observed SO biogeography of *Phaeocystis* and diatoms in ROMS-BEC, it nevertheless highlights the need for further research on the impact of the chosen marine ecosystem complexity on the modeled biogeochemical fluxes (Ward et al., 2013). To date, the implementation of morphotype transitions of *Phaeocystis* into a basin-wide SO model such as ROMS-BEC is severely hindered by data availability. At the moment, 390 *Phaeocystis* biomass observations are included in the MAREDAT data base south of 30° S, and the distinction between solitary and colonial cells is often difficult (Vogt et al., 2012), impeding the basin-wide model evaluation of both *Phaeocystis* life stages. In addition, colonies of *Phaeocystis* are surrounded by a gelatinous matrix, which contains nutrients and carbon (Schoemann et al., 2005), leading to an underestimation of modeled *Phaeocystis* carbon biomass estimates if not accounting for this mucus (Vogt et al., 2012). In ROMS-BEC, this underestimation is likely small, as <20% of the total *Phaeocystis* biomass is reportedly encorporated into the mucus in the SO (Fig. 9 in Vogt et al., 2012). Nevertheless, through its function as a nutrient storage, the mucus promotes the accumulation of *Phaeocystis* biomass relative to other phytoplankton types when the latter become limited by low nutrient availability. While the gelatinous matrix is additionally thought to prevent grazing, the literature on grazing losses of *Phaeocystis* colonies is non-conclusive (Schoemann et al., 2005). This is possibly a result of the large range of sizes of both *Phaeocystis* and the respective grazers, with smaller zooplankton typically grazing less on *Phaeocystis* colonies than larger zooplankton (see reviews by Schoemann et al., 2005; Nejstgaard et al., 2007). As discussed above, the fate of biomass losses of *Phaeocystis* is still poorly constrained (this applies to all model PFTs, see also Laufkötter et al., 2016). Currently, ROMS-BEC treats POC from all formation pathways equal, i.e., once produced, there is no differentiation between POC originating from diatoms or *Phaeocystis* or from grazing or aggregation. In reality, *Phaeocystis* aggregates might be recycled more readily than those from diatoms. This could reconcile our model results, i.e., the substantial simulated contribution of *Phaeocystis* to POC export at 100 m, with observations which suggest that the contribution of *Phaeocystis* to the POC flux across 200 m is small (<5%, Gowing et al., 2001; Accornero et al., 2003; Reigstad and Wassmann, 2007). Furthermore, other functional relationships than those used in ROMS-BEC exist to describe the light and temperature dependent growth of *Phaeocystis* (e.g. Moisan and Mitchell, 2018). In comparison to the equations used in ROMS-BEC (see appendix B), the ones suggested by Moisan and Mitchell (2018) lead to generally lower *Phaeocystis* growth rates, especially at PAR<50 W m^{-2}, suggesting that our biomass estimates at high latitudes and early/late in the season are associated with substantial uncertainty. Ultimately, the C:P and N:P nutrient uptake ratios by *Phaeocystis* and diatoms are higher (147±26.7 and 19.2±0.61) and lower (94.3±20.1 and 9.67±0.33), respectively (Arrigo et al., 1999, 2000), than those originally suggested by Redfield and currently used in ROMS-BEC (117:16:1 for C:N:P uptake by *Phaeocystis* and diatoms, Anderson and Sarmiento, 1994). Consequently, this suggests that not accounting for the non-Redfield ratios in nutrient uptake by these PFTs leads to an over(under)estimation of carbon fixation per unit of P and hence POC export where/when *Phaeocystis* (diatoms) dominate the phytoplankton community.

5 Conclusions

In this modeling study, we present a thorough assessment of the factors controlling the relative importance of SO *Phaeocystis* and diatoms throughout the year and quantify the implications of the spatio-temporal variability in phytoplankton community

structure for POC export. In ROMS-BEC, *Phaeocystis* colonies are an important member of the SO phytoplankton community, contributing 15% (16%) to total annual NPP (POC export) south of 30° S. Moreover, their contribution is threefold higher south of 60° S in our model. Given that our results imply a contribution of approximately 5% of SO *Phaeocystis* colonies to total global NPP and POC export, respectively, we recommend the inclusion of an explicit representation of *Phaeocystis* in ecosystem models of the SO. This will allow for a more realistic representation of the SO phytoplankton community structure, in particular the relative importance of silicifying diatoms and non-silicifying phytoplankton, which we here find to significantly impact the simulated high-latitude carbon fluxes and nutrient distributions. ~~A follow-up study~~ Follow-up studies with both regional SO and global marine ecosystem models should more closely assess what the impact of this simulated change in the relative concentrations of silicic acid and nitrate in the high-latitude SO is on subantarctic and low latitude phytoplankton dynamics.

On a basin-scale, we find that the competition of *Phaeocystis* and diatoms is controlled by seasonal differences in temperature and iron availability, but that variations in light levels are critical on a local scale~~, e. g. facilitating early blooms by *Phaeocystis* in the Ross Sea, in agreement with previous studies.~~ . Yet, our model suggests that the relative importance of *Phaeocystis* and diatoms over a complete annual cycle is ultimately determined by differences in their biomass loss rates ~~(such as zooplankton grazing and aggregation)~~(such as zooplankton grazing and aggregation, Le Quéré et al., 2016), which in turn impacts the formation of sinking particles and hence carbon transfer to depth. Despite knowing of the importance of top-down factors for global phytoplankton biomass distributions (Behrenfeld, 2014) and for the formation of sinking particles (e.g. Steinberg and Landry, 2017), model parameters describing the fate of carbon after its fixation during photosynthesis are still surprisingly uncertain (Laufkötter et al., 2016), complicating the assessment of the role of biomass loss processes in regulating global biogeochemical cycles.

Environmental conditions in the SO have changed considerably in the last million years (see e.g. Martínez-García et al., 2014), as well as during the past decades (Constable et al., 2014), and are projected to change further during this century (IPCC, 2014). These changes will impact the competitive fitness of *Phaeocystis* and diatoms (see e.g. Hancock et al., 2018; Boyd, 2019) and hence affect the entire phytoplankton community with likely repercussions for the entire food web (Smetacek et al., 2004). Consequently, based on our results, future laboratory and modeling studies should assess how uncertainties in marine ecosystem models surrounding e.g. the parameterization of the life cycle of *Phaeocystis* and the fate of biomass losses impact the simulated relative importance of this phytoplankton type and carbon transfer to depth at high SO latitudes. Thereby, such studies will allow us to better constrain how potential future changes in the high-latitude phytoplankton community structure impact global biogeochemical cycles.

Data availability. Model data are available upon email request to the first author (cara.nissen@usys.ethz.ch) or in the ETH library archive (available at https://www.research-collection.ethz.ch/handle/20.500.11850/409193, last access: 2 May 2020; Nissen and Vogt, 2020).

Appendix A: Evaluating the simulated phytoplankton dynamics in ROMS-BEC

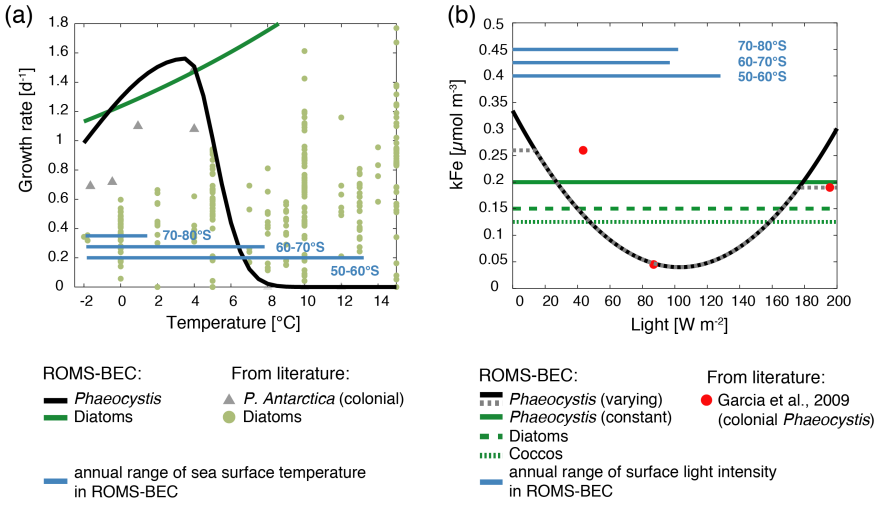

Figure A1. a) Growth rates of *Phaeocystis antarctica* colonies as a function of temperature (conditions of nutrients and light are non-limiting) in laboratory data (grey triangles, see compilation by Schoemann et al., 2005) and as used in ROMS-BEC (black line, see Eq. 1). Green circles and the green line show the temperature-limited growth rate of diatoms in laboratory data (see compilation by Le Quéré et al., 2016) and as used in ROMS-BEC, respectively (see also Table 1). b) Half-saturation constant of Fe (k_{Fe}) of *Phaeocystis* as a function of light intensity I (W m^{-2}) in laboratory data (red circles) and the polynomial fit ($k_{Fe}^{PA}(I) = 2.776 \cdot 10^{-5} \cdot (I + 20)^2$ - $0.00683 \cdot (I + 20) + 0.46$) without (black) and with (dashed grey, as used in ROMS-BEC in simulation VARYING_kFe, see Table 2) the correction at low and high light intensities to restrict k_{Fe} to the range measured in the laboratory experiments by Garcia et al. (2009). The green lines correspond to the half-saturation constants used for *Phaeocystis* (solid), diatoms (dashed), and coccolithophores (dotted) in the *Baseline* simulation in this study (see Table 1). In both panels, the blue lines correspond to the simulated annual range in a) sea surface temperature [° C] and b) light intensity [W m^{-2}] between 50-60° S, 60-70° S, and 70-80° S, respectively.

A1 Sensitivity of *Phaeocystis* biogeography to chosen parameter values

We assess the sensitivity of the simulated annual mean *Phaeocystis* biogeography to parameter choices by performing a set of sensitivity experiments (runs 1-6 in Table 2). Overall, the simulated surface *Phaeocystis* biomass concentrations change by $\gtrapprox$ $\pm$50% for each of the experiments in the high-latitude SO (Fig. A2). Between 60-90° S and in the Ross Sea, the largest increase in *Phaeocystis* biomass concentrations is simulated for AGGREGATION (+112% and +96%, respectively, Fig. A2b & c), whereas the strongest decline is simulated for $ALPHA_{PI}$ (-76% and -87%, respectively, Fig. A2b & c). As a response to changes in *Phaeocystis* parameters, diatom biomass changes overall more than that of SP on a basin scale, suggesting *Phaeocystis* is indeed mostly competing with diatoms for resources in the high-latitude SO. Between 60-90° S, the magnitude of change is similar for the experiments TEMPERATURE (-73%), $ALPHA_{PI}$ (-76%), and IRON (+70%), while in the Ross Sea, the response in IRON is substantially smaller (+17%) than that for the other two experiments (-82% and -87% for TEMPERATURE

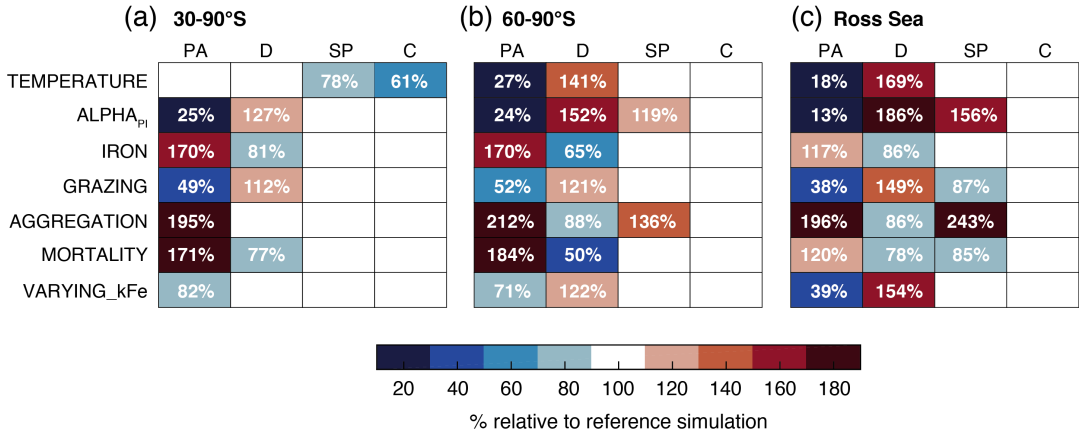

Figure A2. Annual mean surface chlorophyll concentrations of *Phaeocystis* (PA), diatoms (D), small phytoplankton (SP), and coccolithophores (C) in the parameter sensitivity simulations (see section 2.2 and Table 2) relative to the *Baseline* simulation. The model output is averaged over a) 30-90° S, b) 60-90° S, and c) the Ross Sea. Numbers are only printed if the relative change exceeds ±10%

and $\mathrm{ALPHA_{PI}}$, respectively; Fig. A2b & c). This supports our findings from section ??3.3, namely that the difference in light sensitivity between *Phaeocystis* and diatoms is more important in coastal areas than on a basin scale in controlling the relative importance of *Phaeocystis* for total phytoplankton biomass.

Appendix B: BEC equations: Phytoplankton growth & loss

Any change in phytoplankton biomass P [mmol C $\mathrm{m^{-3}}$] of phytoplankton i ($i \in \{PA, D, C, SP, N\}$) over time is determined by the balance of growth and loss terms:

$$\frac{\mathrm{dP^i}}{\mathrm{dt}} = \mathrm{Growth - Loss} \tag{B1}$$

$$= \mu^{\mathrm{i}} \cdot \mathrm{P^i} - \gamma^{\mathrm{i}}(\mathrm{P^i}) \cdot \mathrm{P^i} \tag{B2}$$

$$= \mu^{\mathrm{i}} \cdot \mathrm{P^i} - \gamma^{\mathrm{i}}_{\mathrm{g}}(\mathrm{P^i}) \cdot \mathrm{P^i} - \gamma^{\mathrm{i}}_{\mathrm{m}} \cdot \mathrm{P^i} - \gamma^{\mathrm{i}}_{\mathrm{a}}(\mathrm{P^i}) \cdot \mathrm{P^i} \tag{B3}$$

In the above equation, γ_{g} denotes the loss by zooplankton grazing, γ_{m} the loss by non-grazing mortality, and γ_{a} the loss by aggregation.

B1 Phytoplankton growth

The specific growth rate μ^{i} [$\mathrm{day^{-1}}$] of phytoplankton i ($i \in \{D, C, SP, N\}$, i.e., all but *Phaeocystis*) is determined by the maximum growth rate $\mu^{\mathrm{i}}_{\mathrm{max}}$ (Table 1) and modifications due to temperature (T), nutrients (N) and irradiance (I), following:

$$\mu^{\mathrm{i}} = \mu^{\mathrm{i}}_{\mathrm{max}} \cdot \mathrm{f^i(T)} \cdot \mathrm{g^i(N)} \cdot \mathrm{h^i(I)} \tag{B4}$$

The temperature function $f(T)$ is an exponential function, which is modified by the constant Q_{10} specific to every phytoplankton i (Table 1):

$$f^i(T) = Q_{10}^i \cdot \exp(\frac{T - T_{ref}}{10°C}) \tag{B5}$$

Note that for *Phaeocystis* in ROMS-BEC, an optimum temperature function is used (Eq. 1), as this PFT is parametrized to only represent *Phaeocystis antarctica* in the SO application of this study (see section 2.1).

First, the limitation of growth of phytoplankton i ($i \in \{PA, D, C, SP, N\}$) by the surrounding nutrient $L^i(N)$ is calculated individually for each nutrient (nitrogen, phosphorus, iron for all phytoplankton, silicate for diatoms only) following a Michaelis-Menten function (see Table 1 for half-saturation constants k_N^i). Accordingly, the limitation factor is calculated as follows for iron (Fe) and silicate (SiO3):

$$L^i(N) = \frac{N}{N + k_N^i} \tag{B6}$$

For nitrogen and phosphorus, the combined limitation by nutrient N and M (nitrate (NO3) and ammonium (NH4) for nitrogen, phosphate (PO4) and dissolved organic phosphorus (DOP) for phosphorus) is accounted for following:

$$L^i(N, M) = \frac{N}{k_N^i + N + M \cdot (k_N^i / k_M^i)} + \frac{M}{k_M^i + M + N \cdot (k_M^i / k_N^i)} \tag{B7}$$

In the model, the phytoplankton growth rate is then only limited by the most limiting nutrient:

$$g^i(N) = \min(L^i(NO3, NH4), L^i(PO4, DOP), L^i(Fe), L^i(SiO3)) \tag{B8}$$

The light limitation function $h^i(I)$ includes the effects of photoacclimation by including the chlorophyll-to-carbon ratio θ^i and the growth of the respective phytoplankton i ($i \in \{PA, D, C, SP, N\}$) limited by nutrients and temperature:

$$h^i(I) = 1 - \exp(-1 \cdot \frac{\alpha_{PI}^i \cdot \theta^i \cdot I}{\mu_{max}^i \cdot g^i(N) \cdot f^i(T)}) \tag{B9}$$

Here, same as in Nissen et al. (2018), growth by coccolithophores is set to zero at PAR levels <1 W m^{-2} (Zondervan, 2007) and is linearly reduced at temperatures $<6°C$ following:

$$\mu^C = \mu^C \cdot \frac{\max(T + 2°C), 0)}{8°C} \tag{B10}$$

Coccolithophore calcification amounts to 20% of their photosynthetic growth at any location and point in time in ROMS-BEC.

Diazotroph growth is zero at temperatures $<14°C$.

B2 Phytoplankton loss

In ROMS-BEC, the corrected phytoplankton biomass $\mathrm{P'^i}$ is used to compute loss rates of phytoplankton biomass, to prevent phytoplankton biomass loss at very low biomass levels:

$$\mathrm{P'^i} = \max(\mathrm{P^i} - c^{\mathrm{i}}_{\mathrm{loss}}, 0) \tag{B11}$$

In this equation, $c^{\mathrm{i}}_{\mathrm{loss}}$ is the threshold of phytoplankton biomass $\mathrm{P^i}$ below which no losses occur ($c^{\mathrm{N}}_{\mathrm{loss}}$=0.022 mmol C m^{-3} and $c^{\mathrm{PA,D,C,SP}}_{\mathrm{loss}}$=0.04 mmol C m^{-3}).

The single zooplankton grazer Z [mmol C m^{-3}] feeds on the respective phytoplankton $\mathrm{P'^i}$ [mmol C m^{-3}] at a grazing rate $\gamma^{\mathrm{i}}_{\mathrm{g}}$ [mmol C m^{-3} day^{-1}] that is given by:

$$\gamma^{\mathrm{i}}_{\mathrm{g}} = \gamma^{\mathrm{i}}_{\mathrm{max}} \cdot \mathrm{f^Z(T)} \cdot \mathrm{Z} \cdot \frac{\mathrm{P'^i}}{\mathrm{z}^{\mathrm{i}}_{\mathrm{grz}} + \mathrm{P'^i}} \tag{B12}$$

with

$$\mathrm{f^Z(T)} = 1.5 \cdot \exp\left(\frac{\mathrm{T} - T_{\mathrm{ref}}}{10°\mathrm{C}}\right) \tag{B13}$$

The non-grazing mortality rate $\gamma^{\mathrm{i}}_{\mathrm{m}}$ [mmol C m^{-3} day^{-1}] of phytoplankton i [mmol C m^{-3}] is the product of a maximum mortality rate $\mathrm{m}^{\mathrm{i}}_0$ [day^{-1}] scaled by the temperature function $f^{\mathrm{i}}(T)$ with the modified phytoplankton biomass P'^{i}:

$$\gamma^{\mathrm{i}}_{\mathrm{m}} = \mathrm{m}^{\mathrm{i}}_0 \cdot \mathrm{f^i(T)} \cdot \mathrm{P'^i} \tag{B14}$$

with $\mathrm{m}^{\mathrm{i}}_0$ being 0.15 day^{-1} for diazotrophs and 0.12 day^{-1} for all other phytoplankton.

Phytoplankton $\mathrm{P'^i}$ [mmol C m^{-3}] aggregate at an aggregation rate $\gamma^{\mathrm{i}}_{\mathrm{a}}$ [mmol C m^{-3} day^{-1}] which is computed with the quadratic mortality rate constants $\gamma^{\mathrm{i}}_{\mathrm{a,0}}$ ([m^3 (mmol C)$^{-1}$ d^{-1}], Table 1) and :

$$\gamma^{\mathrm{i}}_{\mathrm{a}} = \min(\gamma^{\mathrm{i}}_{\mathrm{a,max}} \cdot \mathrm{P'^i}, \gamma^{\mathrm{i}}_{\mathrm{a,0}} \cdot \mathrm{P'^i} \cdot \mathrm{P'^i}) \tag{B15}$$

$$\gamma^{\mathrm{i}}_{\mathrm{a}} = \max(\gamma^{\mathrm{i}}_{\mathrm{a,min}} \cdot \mathrm{P'^i}, \gamma^{\mathrm{i}}_{\mathrm{a}}) \tag{B16}$$

In ROMS-BEC, $\gamma^{\mathrm{i}}_{\mathrm{a,min}}$ is 0.01 day^{-1} for small phytoplankton and coccolithophores and 0.02 day^{-1} for *Phaeocystis* and diatoms, and with $\gamma^{\mathrm{i}}_{\mathrm{a,max}}$ being 0.9 day^{-1} for *Phaeocystis*, diatoms, coccolithophores, and small phytoplankton. Note that phytoplankton immediately stop photosynthesizing upon aggregation and that aggregation losses do not occur for diazotrophs in ROMS-BEC.

Author contributions. MV and CN conceived the study. CN set up the model simulations, performed the analysis, and wrote the paper. MV contributed to the interpretation of the results and the writing of the paper.

Competing interests. The authors declare that they have no conflict of interest.

Acknowledgements. We acknowledge all the scientists who contributed phytoplankton and zooplankton cell count data to the MAREDAT initiative and William Balch, Helen Smith, Mariem Saavedra-Pellitero, Gustaaf Hallegraeff, José-Abel Flores, and Alex Poulton for providing additional cell count data. Furthermore, GlobColour data (http://globcolour.info) used in this study has been developed, validated, and distributed by ACRI-ST, France. We would like to thank Nicolas Gruber, Matthias Münnich, and Domitille Louchard for valuable discussions and Damian Loher for technical support. Additionally, we would like to thank Gianna Ferrari for the analysis of early ROMS-BEC simulations with *Phaeocystis*. Ultimately, we thank two reviewers for their valuable reviews and comments, which have improved the quality of the manuscript. This research was financially supported by the Swiss Federal Institute of Technology Zürich (ETH Zürich) and the Swiss National Science Foundation (project SOGate, grant no. 200021_153452). The simulations were performed at the HPC cluster of ETH Zürich, Euler, which is located in the Swiss Supercomputing Center (CSCS) in Lugano and operated by ETH ITS Scientific IT Services in Zürich. Model output is available upon request to the corresponding author, Cara Nissen (cara.nissen@usys.ethz.ch).

References

Accornero, A., Manno, C., Esposito, F., and Gambi, M. C.: The vertical flux of particulate matter in the polynya of Terra Nova Bay. Part II. Biological components, Antarctic Science, 15, S0954102003001 214, https://doi.org/10.1017/S0954102003001214, 2003.

Alvain, S., Moulin, C., Dandonneau, Y., and Loisel, H.: Seasonal distribution and succession of dominant phytoplankton groups in the global ocean: A satellite view, Global Biogeochemical Cycles, 22, GB3001, https://doi.org/10.1029/2007GB003154, 2008.

Anderson, L. A. and Sarmiento, J. L.: Redfield ratios of remineralization determined by nutrient data analysis, Global Biogeochemical Cycles, 8, 65–80, https://doi.org/10.1029/93GB03318, 1994.

Arrigo, K. R., Weiss, A. M., and Smith, W. O.: Physical forcing of phytoplankton dynamics in the southwestern Ross Sea, Journal of Geophysical Research: Oceans, 103, 1007–1021, https://doi.org/10.1029/97JC02326, 1998.

Arrigo, K. R., Robinson, D. H., Worthen, D. L., Dunbar, R. B., DiTullio, G. R., VanWoert, M. L., and Lizotte, M. P.: Phytoplankton community structure and the drawdown of nutrients and CO_2 in the Southern Ocean, Science, 283, 365–367, https://doi.org/10.1126/science.283.5400.365, 1999.

Arrigo, K. R., DiTullio, G. R., Dunbar, R. B., Robinson, D. H., VanWoert, M., Worthen, D. L., and Lizotte, M. P.: Phytoplankton taxonomic variability in nutrient utilization and primary production in the Ross Sea, Journal of Geophysical Research: Oceans, 105, 8827–8846, https://doi.org/10.1029/1998JC000289, 2000.

Arrigo, K. R., van Dijken, G. L., Alderkamp, A.-C., Erickson, Z. K., Lewis, K. M., Lowry, K. E., Joy-Warren, H. L., Middag, R., Nash-Arrigo, J. E., Selz, V., and van de Poll, W.: Early Spring Phytoplankton Dynamics in the Western Antarctic Peninsula, Journal of Geophysical Research: Oceans, 122, 9350–9369, https://doi.org/10.1002/2017JC013281, 2017.

Asper, V. L. and Smith, W. O.: Particle fluxes during austral spring and summer in the southern Ross Sea, Antarctica, Journal of Geophysical Research: Oceans, 104, 5345–5359, https://doi.org/10.1029/1998JC900067, 1999.

Asper, V. L. and Smith, W. O.: Variations in the abundance and distribution of aggregates in the Ross Sea, Antarctica, Elem Sci Anth, 7, 23, https://doi.org/10.1525/elementa.355, https://www.elementascience.org/article/10.1525/elementa.355/, 2019.

Ayers, G. P., Ivey, J. P., and Gillett, R. W.: Coherence between seasonal cycles of dimethyl sulphide, methanesulphonate and sulphate in marine air, Nature, 349, 404–406, https://doi.org/10.1038/349404a0, 1991.

Balch, W. M., Bates, N. R., Lam, P. J., Twining, B. S., Rosengard, S. Z., Bowler, B. C., Drapeau, D. T., Garley, R., Lubelczyk, L. C., Mitchell, C., and Rauschenberg, S.: Factors regulating the Great Calcite Belt in the Southern Ocean and its biogeochemical significance, Global Biogeochemical Cycles, 30, 1199–1214, https://doi.org/10.1002/2016GB005414, 2016.

Behrenfeld, M. J.: Climate-mediated dance of the plankton, Nature Climate Change, 4, 880–887, https://doi.org/10.1038/nclimate2349, 2014.

Behrenfeld, M. J. and Falkowski, P. G.: Photosynthetic rates derived from satellite-based chlorophyll concentration, Limnology and Oceanography, 42, 1–20, https://doi.org/10.4319/lo.1997.42.1.0001, 1997.

Ben Mustapha, Z. B., Alvain, S., Jamet, C., Loisel, H., and Dessailly, D.: Automatic classification of water-leaving radiance anomalies from global SeaWiFS imagery: Application to the detection of phytoplankton groups in open ocean waters, Remote Sensing of Environment, 146, 97–112, https://doi.org/10.1016/j.rse.2013.08.046, 2014.

Bender, S. J., Moran, D. M., McIlvin, M. R., Zheng, H., McCrow, J. P., Badger, J., DiTullio, G. R., Allen, A. E., and Saito, M. A.: Colony formation in *Phaeocystis antarctica*: connecting molecular mechanisms with iron biogeochemistry, Biogeosciences, 15, 4923–4942, https://doi.org/10.5194/bg-15-4923-2018, 2018.

Berman-Frank, I., Cullen, J. T., Shaked, Y., Sherrell, R. M., and Falkowski, P. G.: Iron availability, cellular iron quotas, and nitrogen fixation in Trichodesmium, Limnology and Oceanography, 46, 1249–1260, https://doi.org/10.4319/lo.2001.46.6.1249, 2001.

Bopp, L., Aumont, O., Cadule, P., Alvain, S., and Gehlen, M.: Response of diatoms distribution to global warming and potential implications: A global model study, Geophysical Research Letters, 32, 1–4, https://doi.org/10.1029/2005GL023653, 2005.

Boyd, P. W.: Physiology and iron modulate diverse responses of diatoms to a warming Southern Ocean, Nature Climate Change, 9, 148–152, https://doi.org/10.1038/s41558-018-0389-1, 2019.

Brun, P., Vogt, M., Payne, M. R., Gruber, N., O'Brien, C. J., Buitenhuis, E. T., Le Quéré, C., Leblanc, K., and Luo, Y.-W.: Ecological niches of open ocean phytoplankton taxa, Limnology and Oceanography, 60, 1020–1038, https://doi.org/10.1002/lno.10074, 2015.

Buesseler, K. O.: The decoupling of production and particulate export in the surface ocean, Global Biogeochemical Cycles, 12, 297–310, https://doi.org/10.1029/97GB03366, 1998.

Buitenhuis, E. T., Pangerc, T., Franklin, D. J., Le Quéré, C., and Malin, G.: Growth rates of six coccolithophorid strains as a function of temperature, Limnology and Oceanography, 53, 1181–1185, https://doi.org/10.4319/lo.2008.53.3.1181, 2008.

Buitenhuis, E. T., Hashioka, T., and Le Quéré, C.: Combined constraints on global ocean primary production using observations and models, Global Biogeochemical Cycles, 27, 847–858, https://doi.org/10.1002/gbc.20074, 2013a.

Buitenhuis, E. T., Vogt, M., Moriarty, R., Bednaršek, N., Doney, S. C., Leblanc, K., Le Quéré, C., Luo, Y. W., O'Brien, C., O'Brien, T., Peloquin, J., Schiebel, R., and Swan, C.: MAREDAT: Towards a world atlas of MARine Ecosystem DATa, Earth System Science Data, 5, 227–239, https://doi.org/10.5194/essd-5-227-2013, 2013b.

Buma, A. G. J., Bano, N., Veldhuis, M. J. W., and Kraay, G. W.: Comparison of the pigmentation of two strains of the prymnesiophyte *Phaeocystis* sp., Netherlands Journal of Sea Research, 27, 173–182, https://doi.org/10.1016/0077-7579(91)90010-X, 1991.

Capone, D. G.: Trichodesmium, a Globally Significant Marine Cyanobacterium, Science, 276, 1221–1229, https://doi.org/10.1126/science.276.5316.1221, 1997.

Carton, J. A. and Giese, B. S.: A reanalysis of ocean climate using Simple Ocean Data Assimilation (SODA), Monthly Weather Review, 136, 2999–3017, https://doi.org/10.1175/2007MWR1978.1, 2008.

Chen, Y.-Q., Wang, N., Zhang, P., Zhou, H., and Qu, L.-H.: Molecular evidence identifies bloom-forming *Phaeocystis* (Prymnesiophyta) from coastal waters of southeast China as *Phaeocystis globosa*, Biochemical Systematics and Ecology, 30, 15–22, https://doi.org/10.1016/S0305-1978(01)00054-0, 2002.

Constable, A. J., Melbourne-Thomas, J., Corney, S. P., Arrigo, K. R., Barbraud, C., Barnes, D. K. A., Bindoff, N. L., Boyd, P. W., Brandt, A., Costa, D. P., Davidson, A. T., Ducklow, H. W., Emmerson, L., Fukuchi, M., Gutt, J., Hindell, M. A., Hofmann, E. E., Hosie, G. W., Iida, T., Jacob, S., Johnston, N. M., Kawaguchi, S., Kokubun, N., Koubbi, P., Lea, M.-A., Makhado, A., Massom, R. A., Meiners, K., Meredith, M. P., Murphy, E. J., Nicol, S., Reid, K., Richerson, K., Riddle, M. J., Rintoul, S. R., Smith, W. O., Southwell, C., Stark, J. S., Sumner, M., Swadling, K. M., Takahashi, K. T., Trathan, P. N., Welsford, D. C., Weimerskirch, H., Westwood, K. J., Wienecke, B. C., Wolf-Gladrow, D., Wright, S. W., Xavier, J. C., and Ziegler, P.: Climate change and Southern Ocean ecosystems I: how changes in physical habitats directly affect marine biota, Global Change Biology, 20, 3004–3025, https://doi.org/10.1111/gcb.12623, 2014.

Cubillos, J. C., Wright, S. W., Nash, G., de Salas, M. F., Griffiths, B., Tilbrook, B., Poisson, A., and Hallegraeff, G. M.: Calcification morphotypes of the coccolithophorid *Emiliania huxleyi* in the Southern Ocean: changes in 2001 to 2006 compared to historical data, Marine Ecology Progress Series, 348, 47–54, https://doi.org/10.3354/meps07058, 2007.

Curran, M. A. J. and Jones, G. B.: Dimethyl sulfide in the Southern Ocean: Seasonality and flux, Journal of Geophysical Research: Atmospheres, 105, 20 451–20 459, https://doi.org/10.1029/2000JD900176, 2000.

Curran, M. A. J., Jones, G. B., and Burton, H.: Spatial distribution of dimethylsulfide and dimethylsulfoniopropionate in the Australasian sector of the Southern Ocean, Journal of Geophysical Research: Atmospheres, 103, 16 677–16 689, https://doi.org/10.1029/97JD03453, 1998.

Dee, D. P., Uppala, S. M., Simmons, A. J., Berrisford, P., Poli, P., Kobayashi, S., Andrae, U., Balmaseda, M. A., Balsamo, G., Bauer, P., Bechtold, P., Beljaars, A. C. M., van de Berg, L., Bidlot, J., Bormann, N., Delsol, C., Dragani, R., Fuentes, M., Geer, A. J., Haimberger, L., Healy, S. B., Hersbach, H., Hólm, E. V., Isaksen, L., Kållberg, P., Köhler, M., Matricardi, M., McNally, A. P., Monge-Sanz, B. M., Morcrette, J.-J., Park, B.-K., Peubey, C., de Rosnay, P., Tavolato, C., Thépaut, J.-N., and Vitart, F.: The ERA-Interim reanalysis: configuration and performance of the data assimilation system, Quarterly Journal of the Royal Meteorological Society, 137, 553–597, https://doi.org/10.1002/qj.828, 2011.

Deppeler, S. L. and Davidson, A. T.: Southern Ocean phytoplankton in a changing climate, Frontiers in Marine Science, 4, 40, https://doi.org/10.3389/fmars.2017.00040, 2017.

DeVries, T. and Weber, T.: The export and fate of organic matter in the ocean: New constraints from combining satellite and oceanographic tracer observations, Global Biogeochemical Cycles, 31, 535–555, https://doi.org/10.1002/2016GB005551, 2017.

DiTullio, G. R., Grebmeier, J. M., Arrigo, K. R., Lizotte, M. P., Robinson, D. H., Leventer, A., Barry, J. P., VanWoert, M. L., and Dunbar, R. B.: Rapid and early export of *Phaeocystis antarctica* blooms in the Ross Sea, Antarctica, Nature, 404, 595–598, https://doi.org/10.1038/35007061, 2000.

Ducklow, H. W., Wilson, S. E., Post, A. F., Stammerjohn, S. E., Erickson, M., Lee, S., Lowry, K. E., Sherrell, R. M., and Yager, P. L.: Particle flux on the continental shelf in the Amundsen Sea Polynya and Western Antarctic Peninsula, Elementa: Science of the Anthropocene, 3, 000 046, https://doi.org/10.12952/journal.elementa.000046, 2015.

Eppley, R. W.: Temperature and phytoplankton growth in the sea, Fishery Bulletin, 70, 1972.

Fanton d'Andon, O., Mangin, A., Lavender, S., Antoine, D., Maritorena, S., Morel, A., Barrot, G., Demaria, J., and Pinnock, S.: GlobColour - the European Service for Ocean Colour, in: Proceedings of the 2009 IEEE International Geoscience & Remote Sensing Symposium, IEEE International Geoscience & Remote Sensing Symposium (IGARSS), ISBN: 9781424433957, 2009.

Feng, Y., Hare, C. E., Rose, J. M., Handy, S. M., DiTullio, G. R., Lee, P. A., Smith, W. O., Peloquin, J., Tozzi, S., Sun, J., Zhang, Y., Dunbar, R. B., Long, M. C., Sohst, B., Lohan, M., and Hutchins, D. A.: Interactive effects of iron, irradiance and CO_2 on Ross Sea phytoplankton, Deep Sea Research Part I: Oceanographic Research Papers, 57, 368–383, https://doi.org/10.1016/j.dsr.2009.10.013, 2010.

Follows, M. J., Dutkiewicz, S., Grant, S., and Chisholm, S. W.: Emergent biogeography of microbial communities in a model ocean, Science, 315, 1843–6, https://doi.org/10.1126/science.1138544, 2007.

Freeman, N. M., Lovenduski, N. S., Munro, D. R., Krumhardt, K. M., Lindsay, K., Long, M. C., and Maclennan, M.: The variable and changing Southern Ocean silicate front: Insights from the CESM large ensemble, Global Biogeochemical Cycles, 32, 752–768, https://doi.org/10.1029/2017GB005816, 2018.

Garcia, H. E., Locarnini, R. A., Boyer, T. P., Antonov, J. I., Baranova, O., Zweng, M., Reagan, J., and Johnson, D.: World Ocean Atlas 2013, Volume 3: Dissolved oxygen, apparent oxygen utilization, and oxygen saturation, NOAA Atlas NESDIS 75, 3, 27 pp, 2014a.

Garcia, H. E., Locarnini, R. A., Boyer, T. P., Antonov, J. I., Baranova, O. K., Zweng, M. M., Reagan, J. R., and Johnson, D. R.: World Ocean Atlas 2013, Volume 4 : Dissolved inorganic nutrients (phosphate, nitrate, silicate), NOAA Atlas NESDIS 76, 4, 25 pp, 2014b.

Garcia, N. S., Sedwick, P. N., and DiTullio, G. R.: Influence of irradiance and iron on the growth of colonial *Phaeocystis antarctica*: implications for seasonal bloom dynamics in the Ross Sea, Antarctica, Aquatic Microbial Ecology, 57, 203–220, https://doi.org/10.3354/ame01334, 2009.

Geider, R. J., MacIntyre, H. L., and Kana, T. M.: A dynamic regulatory model of phytoplanktonic acclimation to light, nutrients, and temperature, Limnology and Oceanography, 43, 679–694, https://doi.org/10.4319/lo.1998.43.4.0679, 1998.

Goffart, A., Catalano, G., and Hecq, J.: Factors controlling the distribution of diatoms and *Phaeocystis* in the Ross Sea, Journal of Marine Systems, 27, 161–175, https://doi.org/10.1016/S0924-7963(00)00065-8, 2000.

Gowing, M. M., Garrison, D. L., Kunze, H. B., and Winchell, C. J.: Biological components of Ross Sea short-term particle fluxes in the austral summer of 1995–1996, Deep Sea Research Part I: Oceanographic Research Papers, 48, 2645–2671, https://doi.org/10.1016/S0967-0637(01)00034-6, 2001.

Granéli, E., Granéli, W., Rabbani, M. M., Daugbjerg, N., Fransz, G., Roudy, J. C., and Alder, V. A.: The influence of copepod and krill grazing on the species composition of phytoplankton communities from the Scotia Weddell sea, Polar Biology, 13, 201–213, https://doi.org/10.1007/BF00238930, 1993.

Gravalosa, J. M., Flores, J.-A., Sierro, F. J., and Gersonde, R.: Sea surface distribution of coccolithophores in the eastern Pacific sector of the Southern Ocean (Bellingshausen and Amundsen Seas) during the late austral summer of 2001, Marine Micropaleontology, 69, 16–25, https://doi.org/10.1016/j.marmicro.2007.11.006, 2008.

Green, S. E. and Sambrotto, R. N.: Plankton community structure and export of C, N, P and Si in the Antarctic Circumpolar Current, Deep Sea Research Part II: Topical Studies in Oceanography, 53, 620–643, https://doi.org/10.1016/j.dsr2.2006.01.022, 2006.

Guidi, L., Chaffron, S., Bittner, L., Eveillard, D., Larhlimi, A., Roux, S., Darzi, Y., Audic, S., Berline, L., Brum, J. R., Coelho, L. P., Espinoza, J. C. I., Malviya, S., Sunagawa, S., Dimier, C., Kandels-Lewis, S., Picheral, M., Poulain, J., Searson, S., Stemmann, L., Not, F., Hingamp, P., Speich, S., Follows, M., Karp-Boss, L., Boss, E., Ogata, H., Pesant, S., Weissenbach, J., Wincker, P., Acinas, S. G., Bork, P., de Vargas, C., Iudicone, D., Sullivan, M. B., Raes, J., Karsenti, E., Bowler, C., and Gorsky, G.: Plankton networks driving carbon export in the oligotrophic ocean, Nature, 532, 465–470, https://doi.org/10.1038/nature16942, 2016.

Hamm, C. E., Simson, D. A., Merkel, R., and Smetacek, V.: Colonies of *Phaeocystis globosa* are protected by a thin but tough skin, Marine Ecology Progress Series, 187, 101–111, https://doi.org/10.3354/meps187101, 1999.

Hancock, A. M., Davidson, A. T., McKinlay, J., McMinn, A., Schulz, K. G., and van den Enden, R. L.: Ocean acidification changes the structure of an Antarctic coastal protistan community, Biogeosciences, 15, 2393–2410, https://doi.org/10.5194/bg-15-2393-2018, 2018.

Hashioka, T., Vogt, M., Yamanaka, Y., Le Quéré, C., Buitenhuis, E. T., Aita, M. N., Alvain, S., Bopp, L., Hirata, T., Lima, I., Sailley, S., and Doney, S. C.: Phytoplankton competition during the spring bloom in four plankton functional type models, Biogeosciences, 10, 6833–6850, https://doi.org/10.5194/bg-10-6833-2013, 2013.

Haumann, F. A.: Southern Ocean response to recent changes in surface freshwater fluxes, PhD Thesis, ETH Zürich, https://doi.org/10.3929/ethz-b-000166276, 2016.

Henson, S. A., Le Moigne, F., and Giering, S.: Drivers of Carbon Export Efficiency in the Global Ocean, Global Biogeochemical Cycles, p. 2018GB006158, https://doi.org/10.1029/2018GB006158, 2019.

Holling, C. S.: The components of predation as revealed by a study of small-mammal predation of the European pine sawfly, The Canadian Entomologist, 91, 293–320, https://doi.org/10.4039/Ent91293-5, 1959.

IPCC: Climate change 2013 - The physical science basis: Working group I contribution to the fifth assessment report of the Intergovernmental Panel on Climate Change, Cambridge University Press, https://doi.org/10.1017/CBO9781107415324, 2014.

Johnson, R., Strutton, P. G., Wright, S. W., McMinn, A., and Meiners, K. M.: Three improved satellite chlorophyll algorithms for the Southern Ocean, Journal of Geophysical Research-Oceans, 118, 3694–3703, https://doi.org/10.1002/jgrc.20270, 2013.

Kaufman, D. E., Friedrichs, M. A. M., Smith, W. O., Hofmann, E. E., Dinniman, M. S., and Hemmings, J. C. P.: Climate change impacts on southern Ross Sea phytoplankton composition, productivity, and export, Journal of Geophysical Research: Oceans, 122, 2339–2359, https://doi.org/10.1002/2016JC012514, 2017.

Keller, M. D., Bellows, W. K., and Guillard, R. R. L.: Dimethyl sulfide production in marine phytoplankton, in: Biogenic Sulfur in the Environment, edited by Saltzman, E. S. and Cooper, W. J., vol. 393 of *ACS Symposium Series*, pp. 167–182, American Chemical Society, https://doi.org/10.1021/bk-1989-0393, ISBN: 0-8412-1612-6, 1989.

Lam, P. J. and Bishop, J. K. B.: High biomass, low export regimes in the Southern Ocean, Deep Sea Research Part II: Topical Studies in Oceanography, 54, 601–638, https://doi.org/10.1016/j.dsr2.2007.01.013, 2007.

Lana, A., Bell, T. G., Simó, R., Vallina, S. M., Ballabrera-Poy, J., Kettle, A. J., Dachs, J., Bopp, L., Saltzman, E. S., Stefels, J., Johnson, J. E., and Liss, P. S.: An updated climatology of surface dimethlysulfide concentrations and emission fluxes in the global ocean, Global Biogeochemical Cycles, 25, 1–17, https://doi.org/10.1029/2010GB003850, 2011.

Laufkötter, C., Vogt, M., Gruber, N., Aumont, O., Bopp, L., Doney, S. C., Dunne, J. P., Hauck, J., John, J. G., Lima, I. D., Seferian, R., and Völker, C.: Projected decreases in future marine export production: the role of the carbon flux through the upper ocean ecosystem, Biogeosciences, 13, 4023–4047, https://doi.org/10.5194/bg-13-4023-2016, 2016.

Lauvset, S. K., Key, R. M., Olsen, A., Van Heuven, S., Velo, A., Lin, X., Schirnick, C., Kozyr, A., Tanhua, T., Hoppema, M., Jutterström, S., Steinfeldt, R., Jeansson, E., Ishii, M., Perez, F. F., Suzuki, T., and Watelet, S.: A new global interior ocean mapped climatology: The 1°x1° GLODAP version 2, Earth System Science Data, 8, 325–340, https://doi.org/10.5194/essd-8-325-2016, 2016.

Le Quéré, C., Buitenhuis, E. T., Moriarty, R., Alvain, S., Aumont, O., Bopp, L., Chollet, S., Enright, C., Franklin, D. J., Geider, R. J., Harrison, S. P., Hirst, A. G., Larsen, S., Legendre, L., Platt, T., Prentice, I. C., Rivkin, R. B., Sailley, S., Sathyendranath, S., Stephens, N., Vogt, M., and Vallina, S. M.: Role of zooplankton dynamics for Southern Ocean phytoplankton biomass and global biogeochemical cycles, Biogeosciences, 13, 4111–4133, https://doi.org/10.5194/bg-13-4111-2016, 2016.

Leblanc, K., Arístegui, J., Armand, L., Assmy, P., Beker, B., Bode, A., Breton, E., Cornet, V., Gibson, J., Gosselin, M.-P., Kopczynska, E., Marshall, H., Peloquin, J., Piontkovski, S., Poulton, A. J., Quéguiner, B., Schiebel, R., Shipe, R., Stefels, J., van Leeuwe, M. A., Varela, M., Widdicombe, C., and Yallop, M.: A global diatom database - abundance, biovolume and biomass in the world ocean, Earth System Science Data, 4, 149–165, https://doi.org/10.5194/essd-4-149-2012, 2012.

Lima, I. D., Lam, P. J., and Doney, S. C.: Dynamics of particulate organic carbon flux in a global ocean model, Biogeosciences, 11, 1177–1198, https://doi.org/10.5194/bg-11-1177-2014, 2014.

Liss, P. S., Malin, G., Turner, S. M., and Holligan, P. M.: Dimethyl sulphide and *Phaeocystis*: A review, Journal of Marine Systems, 5, 41–53, https://doi.org/10.1016/0924-7963(94)90015-9, 1994.

Locarnini, R. A., Mishonov, A. V., Antonov, J. I., Boyer, T. P., Garcia, H. E., Baranova, O. K., Zweng, M. M., Paver, C. R., Reagan, J. R., Johnson, D. R., Hamilton, M., and Seidov, D.: World Ocean Atlas 2013, Volume 1: Temperature, NOAA Atlas NESDIS 73, 1, 40 pp, 2013.

Losa, S. N., Dutkiewicz, S., Losch, M., J., O., Soppa, M. A., Trimborn, S., Xi, H., , and Bracher, A.: On modeling the Southern Ocean Phytoplankton Functional Types, Biogeosciences Discussion, https://doi.org/10.5194/bg-2019-289, 2019.

Margalef, R.: Life-forms of phytoplankton as survival alternatives in an unstable environment, Oceanologica Acta, 1, 493–509, 1978.

Maritorena, S., Fanton D'Andon, O., Mangin, A., and Siegel, D. A.: Merged satellite ocean color data products using a bio-optical model: Characteristics, benefits and issues, Remote Sensing of Environment, 114, 1791–1804, https://doi.org/10.1016/j.rse.2010.04.002, 2010.

Martin, J. H., Fitzwater, S. E., and Gordon, R. M.: Iron deficiency limits phytoplankton growth in Antarctic waters, Global Biogeochemical Cycles, 4, 5–12, https://doi.org/10.1029/GB004i001p00005, 1990a.

Martin, J. H., Gordon, R. M., and Fitzwater, S. E.: Iron in Antarctic waters, Nature, 345, 156–158, https://doi.org/10.1038/345156a0, 1990b.

Martínez-García, A., Sigman, D. M., Ren, H., Anderson, R. F., Straub, M., Hodell, D. a., Jaccard, S. L., Eglinton, T. I., and Haug, G. H.: Iron fertilization of the Subantarctic ocean during the last ice age., Science, 343, 1347–50, https://doi.org/10.1126/science.1246848, 2014.

Mills, M. M., Kropuenske, L. R., van Dijken, G. L., Alderkamp, A.-C., Berg, G. M., Robinson, D. H., Welschmeyer, N. A., and Arrigo, K. R.: Photophysiology in two Southern Ocean phytoplankton taxa: photosynthesis of *Phaeocystis Antarctica* (Prymnesiophyceae) and *Fragilariopsis cylindrus* (Bacillariophyceae) under simulated mixed-layer irradiance, Journal of Phycology, 46, 1114–1127, https://doi.org/10.1111/j.1529-8817.2010.00923.x, 2010.

Moisan, T. A. and Mitchell, B. G.: Modeling Net Growth of *Phaeocystis antarctica* Based on Physiological and Optical Responses to Light and Temperature Co-limitation, Frontiers in Marine Science, 4, 1–15, https://doi.org/10.3389/fmars.2017.00437, 2018.

Moore, J. K., Doney, S. C., Kleypas, J. A., Glover, D. M., and Fung, I. Y.: An intermediate complexity marine ecosystem model for the global domain, Deep-Sea Research Part II, 49, 403–462, https://doi.org/10.1016/S0967-0645(01)00108-4, 2002.

Moore, J. K., Lindsay, K., Doney, S. C., Long, M. C., and Misumi, K.: Marine ecosystem dynamics and biogeochemical cycling in the Community Earth System Model [CESM1(BGC)]: Comparison of the 1990s with the 2090s under the RCP4.5 and RCP8.5 scenarios, Journal of Climate, 26, 9291–9312, https://doi.org/10.1175/JCLI-D-12-00566.1, 2013.

Morel, A. and Berthon, J.-F.: Surface pigments, algal biomass profiles, and potential production of the euphotic layer: Relationships reinvestigated in view of remote-sensing applications, Limnology and Oceanography, 34, 1545–1562, https://doi.org/10.4319/lo.1989.34.8.1545, 1989.

NASA-OBPG: NASA Goddard Space Flight Center, Ocean Ecology Laboratory, Ocean Biology Processing Group, Moderate-resolution Imaging Spectroradiometer (MODIS) Aqua Chlorophyll Data, https://doi.org/10.5067/AQUA/MODIS/L3M/CHL/2014, 2014a.

NASA-OBPG: NASA Goddard Space Flight Center, Ocean Ecology Laboratory, Ocean Biology Processing Group, Sea-viewing Wide Field-of-view Sensor (SeaWiFS) Chlorophyll Data, https://doi.org/10.5067/ORBVIEW-2/SEAWIFS/L3M/CHL/2014, 2014b.

Nejstgaard, J. C., Tang, K. W., Steinke, M., Dutz, J., Koski, M., Antajan, E., and Long, J. D.: Zooplankton grazing on *Phaeocystis*: a quantitative review and future challenges, in: *Phaeocystis*, major link in the biogeochemical cycling of climate-relevant elements, vol. 83, pp. 147–172, Springer Netherlands, https://doi.org/10.1007/s10533-007-9098-y, 2007.

Nguyen, B. C., Mihalopoulos, N., and Belviso, S.: Seasonal variation of atmospheric dimethylsulfide at Amsterdam Island in the southern Indian Ocean, Journal of Atmospheric Chemistry, 11, 123–141, https://doi.org/10.1007/BF00053671, 1990.

Nissen, C. and Vogt, M.: ROMS-BEC model data: Factors controlling the competition between *Phaeocystis* and diatoms in the Southern Ocean and implications for carbon export fluxes, https://doi.org/10.3929/ethz-b-000409193, 2020.

Nissen, C., Vogt, M., Münnich, M., Gruber, N., and Haumann, F. A.: Factors controlling coccolithophore biogeography in the Southern Ocean, Biogeosciences, 15, 6997–7024, https://doi.org/10.5194/bg-15-6997-2018, 2018.

O'Brien, C. J., Peloquin, J. A., Vogt, M., Heinle, M., Gruber, N., Ajani, P., Andruleit, H., Arístegui, J., Beaufort, L., Estrada, M., Karentz, D., Kopczyńska, E., Lee, R., Poulton, A. J., Pritchard, T., and Widdicombe, C.: Global marine plankton functional type biomass distributions: coccolithophores, Earth System Science Data, 5, 259–276, https://doi.org/10.5194/essd-5-259-2013, 2013.

O'Malley, R.: Ocean Productivity website, data downloaded from http://www.science.oregonstate.edu/ocean.productivity/index.php, last access: 16 May 2016.

Palter, J. B., Sarmiento, J. L., Gnanadesikan, A., Simeon, J., and Slater, R. D.: Fueling export production: nutrient return pathways from the deep ocean and their dependence on the Meridional Overturning Circulation, Biogeosciences, 7, 3549–3568, https://doi.org/10.5194/bg-7-3549-2010, 2010.

Pasquer, B., Laruelle, G., Becquevort, S., Schoemann, V., Goosse, H., and Lancelot, C.: Linking ocean biogeochemical cycles and ecosystem structure and function: results of the complex SWAMCO-4 model, Journal of Sea Research, 53, 93–108, https://doi.org/10.1016/j.seares.2004.07.001, 2005.

Peloquin, J. A. and Smith, W. O.: Phytoplankton blooms in the Ross Sea, Antarctica: Interannual variability in magnitude, temporal patterns, and composition, Journal of Geophysical Research, 112, C08 013, https://doi.org/10.1029/2006JC003816, 2007.

Peperzak, L.: Observations of flagellates in colonies of *Phaeocystis globosa* (Prymnesiophyceae); a hypothesis for their position in the life cycle, Journal of Plankton Research, 22, 2181–2203, https://doi.org/10.1093/plankt/22.12.2181, 2000.

Popova, E. E., Pollard, R. T., Lucas, M. I., Venables, H. J., and Anderson, T. R.: Real-time forecasting of ecosystem dynamics during the CROZEX experiment and the roles of light, iron, silicate, and circulation, Deep Sea Research Part II: Topical Studies in Oceanography, 54, 1966–1988, https://doi.org/10.1016/j.dsr2.2007.06.018, 2007.

Poulton, A. J., Moore, M. C., Seeyave, S., Lucas, M. I., Fielding, S., and Ward, P.: Phytoplankton community composition around the Crozet Plateau, with emphasis on diatoms and *Phaeocystis*, Deep Sea Research Part II: Topical Studies in Oceanography, 54, 2085–2105, https://doi.org/10.1016/j.dsr2.2007.06.005, 2007.

Reigstad, M. and Wassmann, P.: Does *Phaeocystis* spp. contribute significantly to vertical export of organic carbon?, in: *Phaeocystis*, major link in the biogeochemical cycling of climate-relevant elements, vol. 83, pp. 217–234, Springer Netherlands, https://doi.org/10.1007/978-1-4020-6214-8_16, http://link.springer.com/10.1007/978-1-4020-6214-8_16, 2007.

Reynolds, C. S.: The Ecology of Phytoplankton, Cambridge University Press, Cambridge, https://doi.org/10.1017/CBO9780511542145, https://www.cambridge.org/core/product/identifier/9780511542145/type/book, ISBN: 9780511542145, 2006.

Rigual Hernández, A. S., Trull, T. W., Nodder, S. D., Flores, J. A., Bostock, H., Abrantes, F., Eriksen, R. S., Sierro, F. J., Davies, D. M., Ballegeer, A.-M., Fuertes, M. A., and Northcote, L. C.: Coccolithophore biodiversity controls carbonate export in the Southern Ocean, Biogeosciences, 17, 245–263, https://doi.org/10.5194/bg-17-245-2020, 2020.

Rivero-Calle, S., Gnanadesikan, A., Del Castillo, C. E., Balch, W. M., and Guikema, S. D.: Multidecadal increase in North Atlantic coccolithophores and the potential role of rising CO_2, Science, 350, 1533–1537, https://doi.org/10.1126/science.aaa8026, 2015.

Rosengard, S. Z., Lam, P. J., Balch, W. M., Auro, M. E., Pike, S., Drapeau, D., and Bowler, B.: Carbon export and transfer to depth across the Southern Ocean Great Calcite Belt, Biogeosciences, 12, 3953–3971, https://doi.org/10.5194/bg-12-3953-2015, 2015.

Rousseau, V., Vaulot, D., Casotti, R., Cariou, V., Lenz, J., Gunkel, J., and Baumann, M.: The life cycle of *Phaeocystis* (Prymnesiophycaea): evidence and hypotheses, Journal of Marine Systems, 5, 23–39, https://doi.org/10.1016/0924-7963(94)90014-0, 1994.

Ryan-Keogh, T. J., DeLizo, L. M., Smith, W. O., Sedwick, P. N., McGillicuddy, D. J., Moore, C. M., and Bibby, T. S.: Temporal progression of photosynthetic-strategy in phytoplankton in the Ross Sea, Antarctica, Journal of Marine Systems, 166, 87–96, https://doi.org/10.1016/j.jmarsys.2016.08.014, http://dx.doi.org/10.1016/j.jmarsys.2016.08.014https://linkinghub.elsevier.com/retrieve/pii/S0924796316302688, 2017.

Saavedra-Pellitero, M., Baumann, K.-H., Flores, J.-A., and Gersonde, R.: Biogeographic distribution of living coccolithophores in the Pacific sector of the Southern Ocean, Marine Micropaleontology, 109, 1–20, https://doi.org/10.1016/j.marmicro.2014.03.003, 2014.

Sarmiento, J. L., Gruber, N., Brzezinski, M. A., and Dunne, J. P.: High-latitude controls of thermocline nutrients and low latitude biological productivity., Nature, 427, 56–60, https://doi.org/10.1038/nature02127, 2004.

Sathyendranath, S., Stuart, V., Nair, A., Oka, K., Nakane, T., Bouman, H., Forget, M. H., Maass, H., and Platt, T.: Carbon-to-chlorophyll ratio and growth rate of phytoplankton in the sea, Marine Ecology Progress Series, 383, 73–84, https://doi.org/10.3354/meps07998, 2009.

Schlitzer, R.: Export production in the Equatorial and North Pacific derived from dissolved oxygen, nutrient and carbon data, J. Oceanogr., 60, 53–62, https://doi.org/10.1023/B:JOCE.0000038318.38916.e6, 2004.

Schoemann, V., Wollast, R., Chou, L., and Lancelot, C.: Effects of photosynthesis on the accumulation of Mn and Fe by *Phaeocystis* colonies, Limnology and Oceanography, 46, 1065–1076, https://doi.org/10.4319/lo.2001.46.5.1065, 2001.

Schoemann, V., Becquevort, S., Stefels, J., Rousseau, V., and Lancelot, C.: *Phaeocystis* blooms in the global ocean and their controlling mechanisms: a review, Journal of Sea Research, 53, 43–66, https://doi.org/10.1016/j.seares.2004.01.008, 2005.

Sedwick, P. N., DiTullio, G. R., and Mackey, D. J.: Iron and manganese in the Ross Sea, Antarctica: Seasonal iron limitation in Antarctic shelf waters, Journal of Geophysical Research, 105, 11 321, https://doi.org/10.1029/2000JC000256, 2000.

Sedwick, P. N., Garcia, N. S., Riseman, S. F., Marsay, C. M., and DiTullio, G. R.: Evidence for high iron requirements of colonial *Phaeocystis antarctica* at low irradiance, in: *Phaeocystis*, major link in the biogeochemical cycling of climate-relevant elements, vol. 83, pp. 83–97, Springer Netherlands, https://doi.org/10.1007/978-1-4020-6214-8_8, 2007.

Shchepetkin, A. F. and McWilliams, J. C.: The regional oceanic modeling system (ROMS): a split-explicit, free-surface, topography-following-coordinate oceanic model, Ocean Modeling, 9, 347–404, https://doi.org/10.1016/j.ocemod.2004.08.002, 2005.

Siegel, D. A., Buesseler, K. O., Doney, S. C., Sailley, S. F., Behrenfeld, M. J., and Boyd, P. W.: Global assessment of ocean carbon export by combining satellite observations and food-web models, Global Biogeochemical Cycles, 28, 181–196, https://doi.org/10.1002/2013GB004743, 2014.

Simó, R. and Pedrós-Alló, C.: Role of vertical mixing in controlling the oceanic production of dimethyl sulphide, Nature, 402, 396–399, https://doi.org/10.1038/46516, 1999.

Smetacek, V., Assmy, P., and Henjes, J.: The role of grazing in structuring Southern Ocean pelagic ecosystems and biogeochemical cycles, Antarct. Sci., 16, 541–558, https://doi.org/10.1017/S0954102004002317, 2004.

Smetacek, V., Klaas, C., Strass, V. H., Assmy, P., Montresor, M., Cisewski, B., Savoye, N., Webb, A., D'Ovidio, F., Arrieta, J. M., Bathmann, U., Bellerby, R., Berg, G. M., Croot, P., Gonzalez, S., Henjes, J., Herndl, G. J., Hoffmann, L. J., Leach, H., Losch, M., Mills, M. M., Neill, C., Peeken, I., Röttgers, R., Sachs, O., Sauter, E., Schmidt, M. M., Schwarz, J., Terbrüggen, A., and Wolf-Gladrow, D.: Deep carbon export from a Southern Ocean iron-fertilized diatom bloom, Nature, 487, 313–319, https://doi.org/10.1038/nature11229, 2012.

Smith, W. O. and Gordon, L. I.: Hyperproductivity of the Ross Sea (Antarctica) polynya during austral spring, Geophysical Research Letters, 24, 233–236, https://doi.org/10.1029/96GL03926, 1997.

Smith, W. O., Dennett, M. R., Mathot, S., and Caron, D. A.: The temporal dynamics of the flagellated and colonial stages of *Phaeocystis antarctica* in the Ross Sea, Deep Sea Research Part II: Topical Studies in Oceanography, 50, 605–617, https://doi.org/10.1016/S0967-0645(02)00586-6, 2003.

Smith, W. O., Dinniman, M. S., Tozzi, S., DiTullio, G. R., Mangoni, O., Modigh, M., and Saggiomo, V.: Phytoplankton photosynthetic pigments in the Ross Sea: Patterns and relationships among functional groups, Journal of Marine Systems, 82, 177–185, https://doi.org/10.1016/j.jmarsys.2010.04.014, 2010.

Smith, W. O., Shields, A. R., Dreyer, J. C., Peloquin, J. A., and A., V.: Interannual variability in vertical export in the Ross Sea: Magnitude, composition, and environmental correlates, Deep Sea Research Part I: Oceanographic Research Papers, 58, 147–159, https://doi.org/10.1016/j.dsr.2010.11.007, 2011.

Smith, W. O., Ainley, D. G., Arrigo, K. R., and Dinniman, M. S.: The Oceanography and Ecology of the Ross Sea, Annual Review of Marine Science, 6, 469–487, https://doi.org/10.1146/annurev-marine-010213-135114, 2014.

Soppa, M., Hirata, T., Silva, B., Dinter, T., Peeken, I., Wiegmann, S., and Bracher, A.: Global retrieval of diatom abundance based on phytoplankton pigments and satellite data, Remote Sensing, 6, 10 089–10 106, https://doi.org/10.3390/rs61010089, 2014.

Soppa, M., Völker, C., and Bracher, A.: Diatom phenology in the Southern Ocean: mean patterns, trends and the role of climate Oscillations, Remote Sensing, 8, 420, https://doi.org/10.3390/rs8050420, 2016.

Stange, P., Bach, L. T., Le Moigne, F. A. C., Taucher, J., Boxhammer, T., and Riebesell, U.: Quantifying the time lag between organic matter production and export in the surface ocean: Implications for estimates of export efficiency, Geophysical Research Letters, 44, 268–276, https://doi.org/10.1002/2016GL070875, 2017.

Stefels, J., Steinke, M., Turner, S., Malin, G., and Belviso, S.: Environmental constraints on the production and removal of the climatically active gas dimethylsulphide (DMS) and implications for ecosystem modelling, in: *Phaeocystis*, major link in the biogeochemical cycling of climate-relevant elements, pp. 245–275, Springer Netherlands, https://doi.org/10.1007/978-1-4020-6214-8_18, 2007.

Steinberg, D. K. and Landry, M. R.: Zooplankton and the ocean carbon cycle, Annual Review of Marine Science, 9, 413–444, https://doi.org/10.1146/annurev-marine-010814-015924, 2017.

Swan, C. M., Vogt, M., Gruber, N., and Laufkötter, C.: A global seasonal surface ocean climatology of phytoplankton types based on CHEMTAX analysis of HPLC pigments, Deep-Sea Research Part I, 109, 137–156, https://doi.org/10.1016/j.dsr.2015.12.002, 2016.

Tagliabue, A. and Arrigo, K. R.: Iron in the Ross Sea: 1. Impact on CO_2 fluxes via variation in phytoplankton functional group and non-Redfield stoichiometry, Journal of Geophysical Research: Oceans, 110, 1–15, https://doi.org/10.1029/2004JC002531, 2005.

Tang, K. W., Smith, W. O., Elliott, D. T., and Shields, A. R.: Colony size of *Phaeocystis Antarctica* (Prymnesiophyceae) as influenced by zooplankton grazers, Journal of Phycology, 44, 1372–1378, https://doi.org/10.1111/j.1529-8817.2008.00595.x, 2008.

Tang, K. W., Smith, W. O., Shields, A. R., and Elliott, D. T.: Survival and recovery of *Phaeocystis antarctica* (Prymnesiophyceae) from prolonged darkness and freezing, Proceedings of the Royal Society B: Biological Sciences, 276, 81–90, https://doi.org/10.1098/rspb.2008.0598, 2009.

Thomalla, S. J., Racault, M.-F., Swart, S., and Monteiro, P. M. S.: High-resolution view of the spring bloom initiation and net community production in the Subantarctic Southern Ocean using glider data, ICES Journal of Marine Science: Journal du Conseil, 72, 1999–2020, https://doi.org/10.1093/icesjms/fsv105, 2015.

Timmermans, K. R., van der Wagt, B., and de Baar, H. J. W.: Growth rates, half saturation constants, and silicate, nitrate, and phosphate depletion in relation to iron availability of four large open-ocean diatoms from the Southern Ocean, Limnology and Oceanography, 49, 2141–2151, https://doi.org/10.4319/lo.2004.49.6.2141, 2004.

Turner, J. T.: Zooplankton fecal pellets, marine snow, phytodetritus and the ocean's biological pump, Progress in Oceanography, 130, 205–248, https://doi.org/10.1016/j.pocean.2014.08.005, 2015.

Tyrrell, T. and Charalampopoulou, A.: Coccolithophore size, abundance and calcification across Drake Passage (Southern Ocean), 2009, https://doi.org/10.1594/PANGAEA.771715, 2009.

van Boekel, W. H. M., Hansen, F. C., Riegman, R., and Bak, R. P. M.: Lysis-induced decline of a *Phaeocystis* spring bloom and coupling with the microbial foodweb, Marine Ecology Progress Series, 81, 269–276, https://doi.org/10.3354/meps081269, 1992.

van Hilst, C. M. and Smith, W. O.: Photosynthesis/irradiance relationships in the Ross Sea, Antarctica, and their control by phytoplankton assemblage composition and environmental factors, Marine Ecology Progress Series, 226, 1–12, https://doi.org/10.3354/meps226001, 2002.

Veldhuis, M. J. W., Colijn, F., and Admiraal, W.: Phosphate Utilization in *Phaeocystis pouchetii* (*Haptophyceae*), Marine Ecology, 12, 53–62, https://doi.org/10.1111/j.1439-0485.1991.tb00083.x, 1991.

Verity, P. G.: Grazing experiments and model simulations of the role of zooplankton in *Phaeocystis* food webs, Journal of Sea Research, 43, 317–343, https://doi.org/10.1016/S1385-1101(00)00025-3, 2000.

Vogt, M., O'Brien, C., Peloquin, J., Schoemann, V., Breton, E., Estrada, M., Gibson, J., Karentz, D., Van Leeuwe, M. A., Stefels, J., Widdicombe, C., and Peperzak, L.: Global marine plankton functional type biomass distributions: *Phaeocystis* spp., Earth System Science Data, 4, 107–120, https://doi.org/10.5194/essd-4-107-2012, 2012.

Wang, S. and Moore, J. K.: Incorporating *Phaeocystis* into a Southern Ocean ecosystem model, Journal of Geophysical Research, 116, C01 019, https://doi.org/10.1029/2009JC005817, 2011.

Wang, S., Elliott, S., Maltrud, M., and Cameron-Smith, P.: Influence of explicit *Phaeocystis* parameterizations on the global distribution of marine dimethyl sulfide, Journal of Geophysical Research: Biogeosciences, 120, 2158–2177, https://doi.org/10.1002/2015JG003017, 2015.

Ward, B. A., Schartau, M., Oschlies, A., Martin, A. P., Follows, M. J., and Anderson, T. R.: When is a biogeochemical model too complex? Objective model reduction and selection for North Atlantic time-series sites, Progress in Oceanography, 116, 49–65, https://doi.org/10.1016/j.pocean.2013.06.002, 2013.

Winter, A., Henderiks, J., Beaufort, L., Rickaby, R. E. M., and Brown, C. W.: Poleward expansion of the coccolithophore *Emiliania huxleyi*, Journal of Plankton Research, 36, 316–325, https://doi.org/10.1093/plankt/fbt110, 2013.

Wright, S. W., van den Enden, R. L., Pearce, I., Davidson, A. T., Scott, F. J., and Westwood, K. J.: Phytoplankton community structure and stocks in the Southern Ocean (30-80°E) determined by CHEMTAX analysis of HPLC pigment signatures, Deep-Sea Research Part II, 57, 758–778, https://doi.org/10.1016/j.dsr2.2009.06.015, 2010.

Yang, S., Gruber, N., Long, M. C., and Vogt, M.: ENSO-driven variability of denitrification and suboxia in the Eastern Tropical Pacific Ocean, Global Biogeochemical Cycles, 31, 1470–1487, https://doi.org/10.1002/2016GB005596, 2017.

Zondervan, I.: The effects of light, macronutrients, trace metals and CO_2 on the production of calcium carbonate and organic carbon in coccolithophores—A review, Deep-Sea Research Part II, 54, 521–537, https://doi.org/10.1016/j.dsr2.2006.12.004, 2007.

Zweng, M. M., Reagan, J. R., Antonov, J. I., Mishonov, A. V., Boyer, T. P., Garcia, H. E., Baranova, O. K., Johnson, D. R., Seidov, D., and Bidlle, M. M.: World Ocean Atlas 2013, Volume 2: Salinity, NOAA Atlas NESDIS 74, 2, 39 pp, 2013.

Supplementary material

The supporting information provides additional figures with respect to the nutrient limitation of phytoplankton growth in ROMS-BEC (S1), the data coverage in a SO satellite derived chlorophyll product (S2), the model evaluation (S3-S6), the bloom timing (S7), the ecological niche analysis (~~S8~~S8-S9), and the sensitivity simulations ~~allowing for a half-saturation constant of iron of *Phaeocystis* that varies with the surrounding light levels (S9~~(S10-S11).

S1: Additional figures

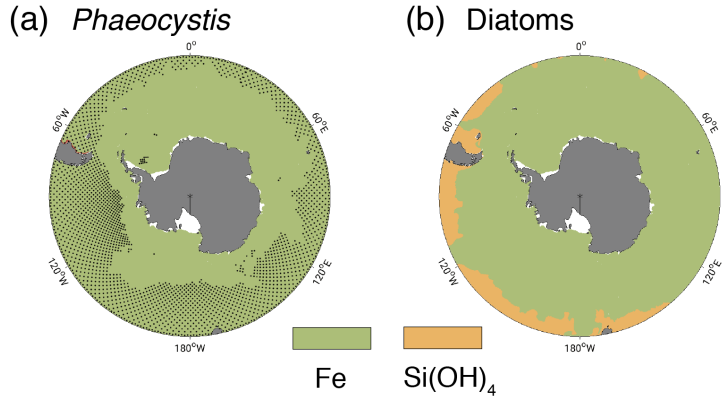

Figure S1: Annual mean most limiting nutrient at the surface south of 45° S for growth rates of a) *Phaeocystis* and b) diatoms in the *Baseline* simulation of ROMS-BEC. High-latitude phytoplankton growth in the model is most limited by either iron (green) or silicic acid (yellow, diatoms only). The stippling in panel a) denotes areas where peak monthly mean chlorophyll concentrations of Phaeocystis do not exceed 0.1 mg chl m^{-3}.

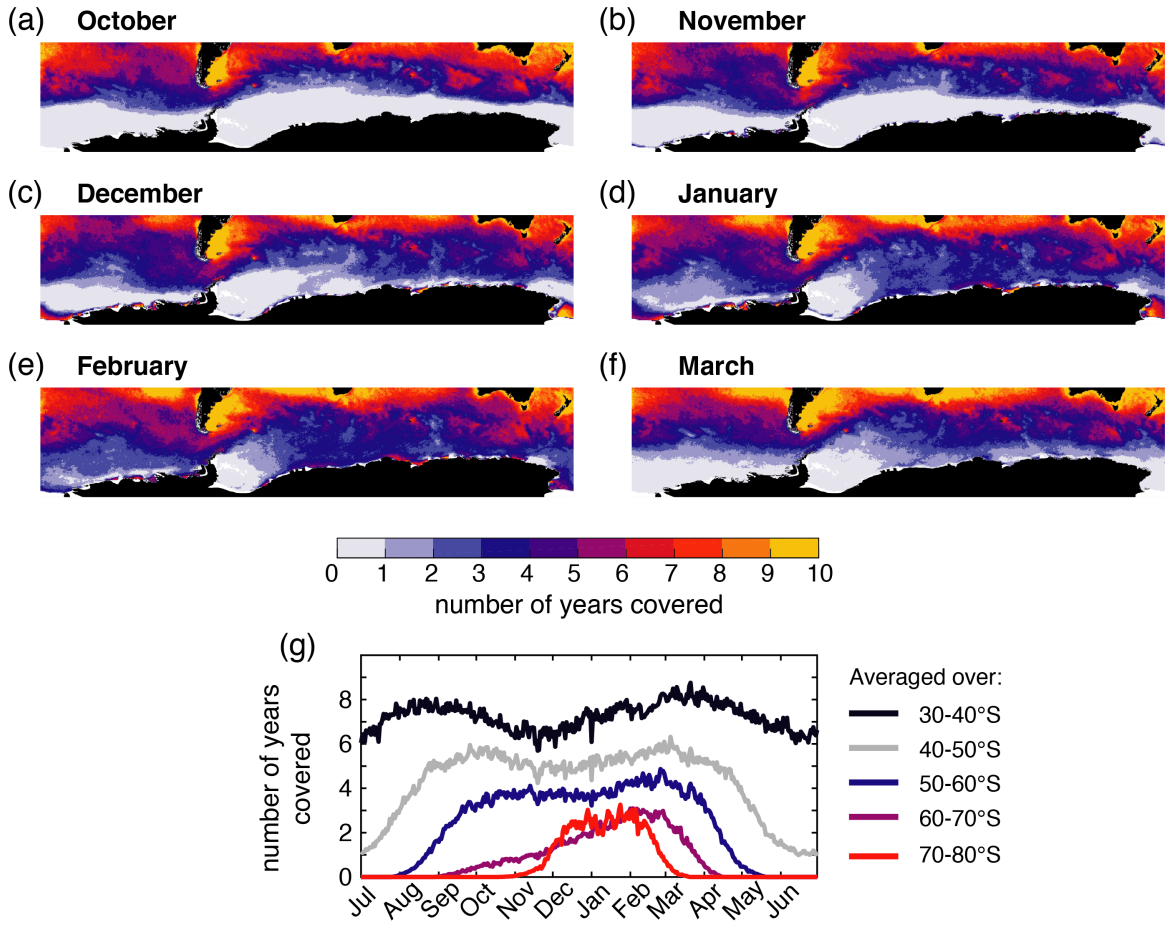

Figure S2: Assessment of the SO data coverage in the climatological (1998-2018, i.e. 21 years) daily Globcolor chlorophyll product (Fanton d'Andon et al., 2009; Maritorena et al., 2010): a)-f) Average number of years available for the calculation of the climatological chlorophyll concentration at each grid cell for each of the shown months (October-March), respectively. No minimum number of "days with data coverage" is required for a given month to be counted as "data available" (i.e. one day of data coverage in a month is enough for that month to be counted as "covered" in the respective year). g) Average number of years available for the calculation of the climatological chlorophyll concentration on each day for 10° latitudinal bands across the SO.

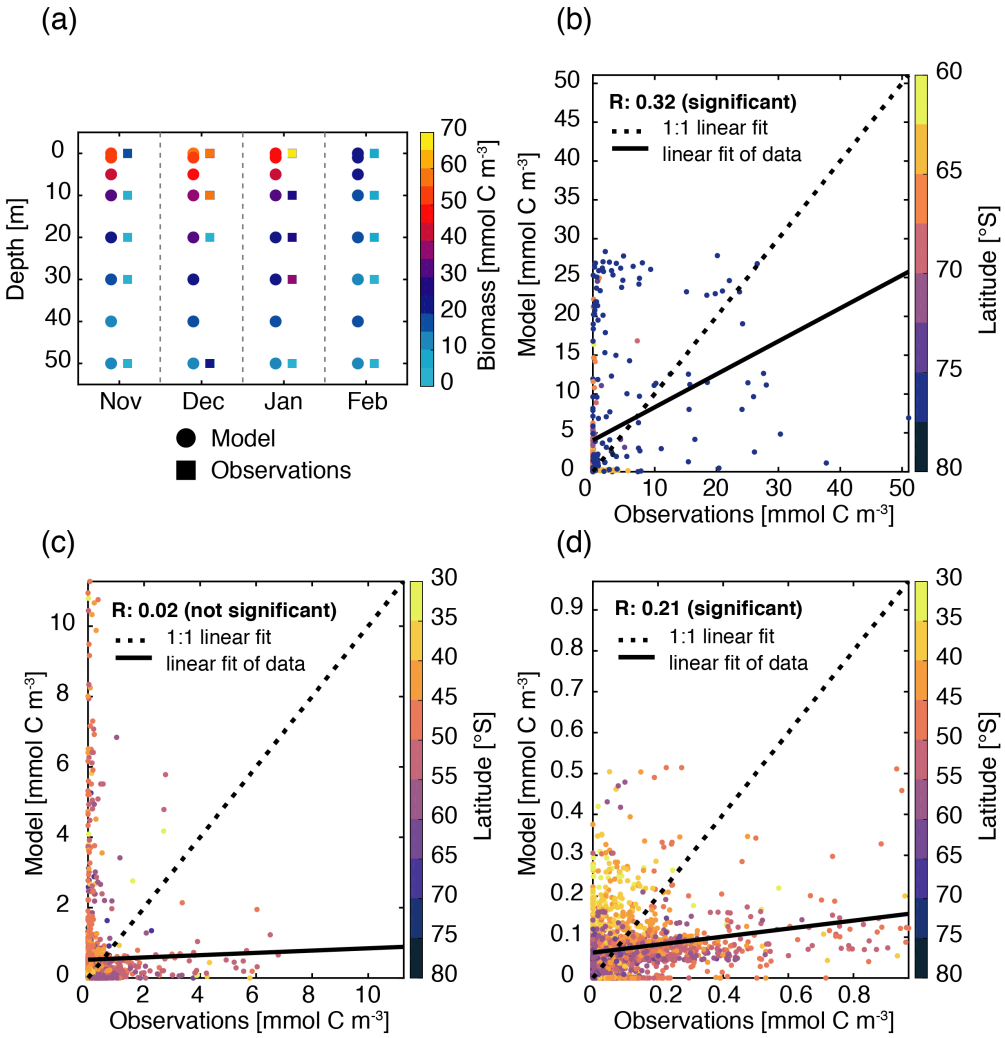

Figure S3: Validation of a) & b) *Phaeocystis*, c) diatom, and d) coccolithophore carbon biomass [mmol C m^{-3}]. Panel a) shows the maximum *Phaeocystis* carbon biomass concentrations [mmol C m^{-3}] in ROMS-BEC (circles) and in observations (squares, Vogt et al., 2012) for each month between November-February and in the the upper 50 meters of the water column. For panels b)-d), the model output is colocated with observations in space and time, and observational data from all months and from above 1000 m are considered here (Balch et al., 2016; Saavedra-Pellitero et al., 2014; O'Brien et al., 2013; Vogt et al., 2012; Leblanc et al., 2012; Tyrrell and Charalampopoulou, 2009; Gravalosa et al., 2008; Cubillos et al., 2007). For more details on the biomass evaluation, see Nissen et al. (2018). The dotted line shows the perfect linear 1:1 fit, whereas the solid line is the actual fit of the data (linear regression). Pearson correlation coefficients of these regressions are given in the top right, those for *Phaeocystis* and coccolithophores are statistically significant ($p<0.05$). Points are color-coded according to the sampling latitude.

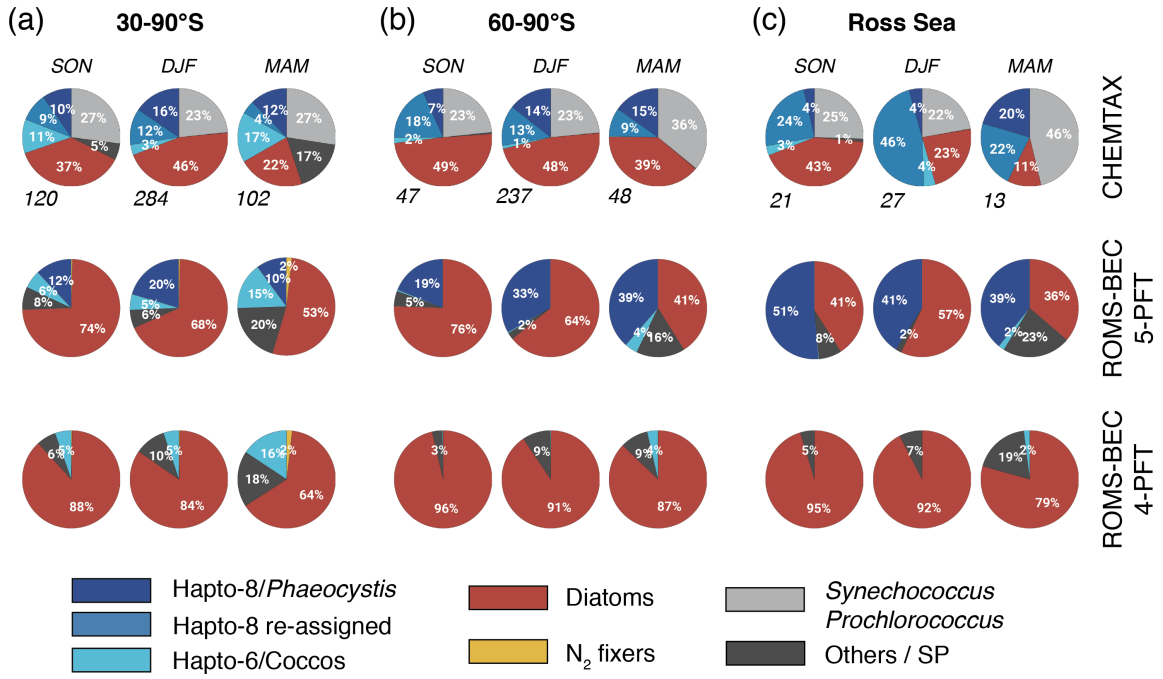

Figure S4: a)-c) Relative contribution of the five phytoplankton PFTs to total chlorophyll biomass [mg chl m^{-3}] for a) 30-90° S, b) 60-90° S, and c) the Ross Sea. The top pie charts denote the climatological mixed layer average community composition suggested by CHEMTAX analysis of HPLC pigments for spring, summer, and fall, respectively (the total number of available observations for a given region and season is given at the lower left side, Swan et al., 2016), and the lower pie charts denote the corresponding community structure in the top 50 m in ROMS-BEC in the 5-PFT setup (middle row, same as in Fig. 2 in the main text) and in the 4-PFT setup (lowest row, no *Phaeocystis*, Nissen et al., 2018), respectively. Note that the categories in the CHEMTAX analysis are not 100% equivalent to the model PFTs, and here, "Hapto-8 reassigned" corresponds to the contribution of Hapto-6 where the temperature is <2°C (see also section 2.3.1 in the main text).

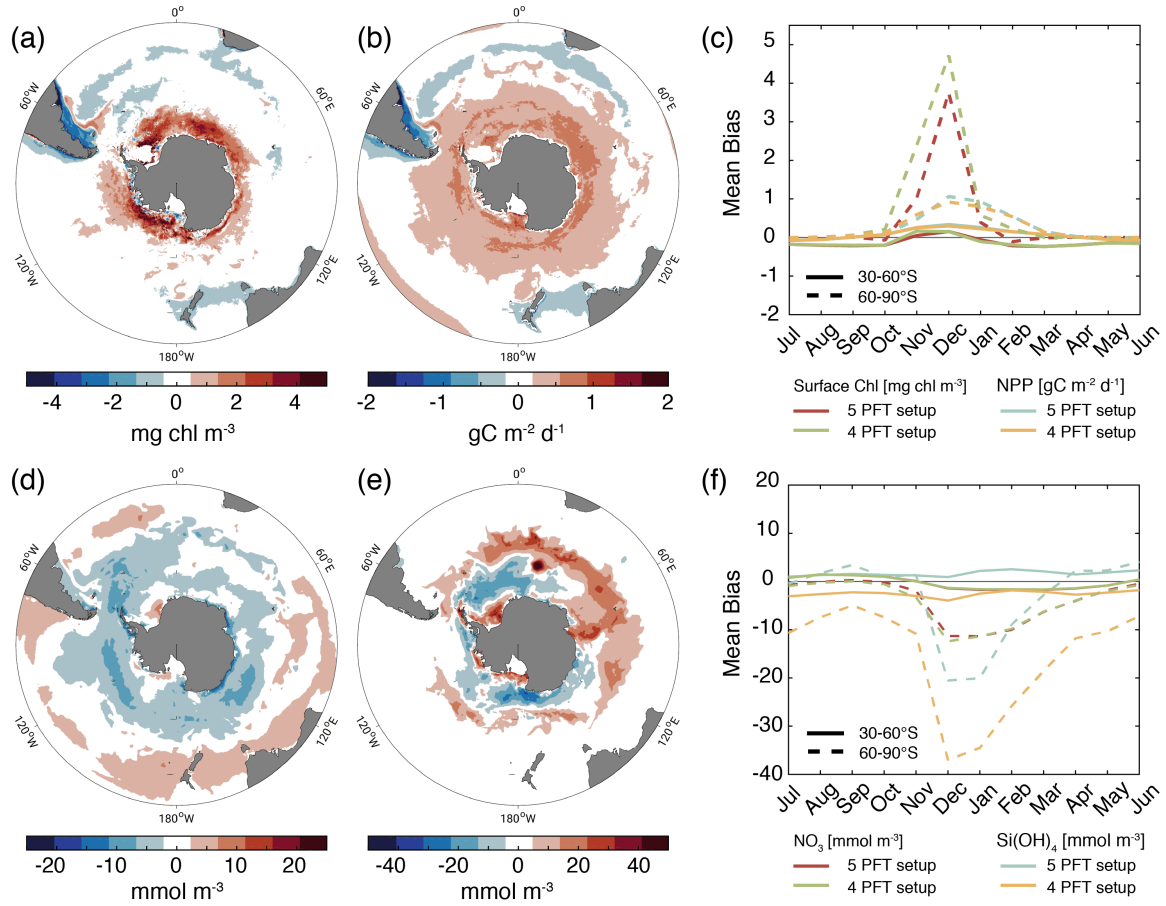

Figure S5: Annual mean bias (*Baseline* simulation minus observations) of a) total surface chlorophyll concentrations [g chl m^{-3}], b) total vertically integrated NPP [mg C m^{-2} d^{-1}], d) surface nitrate concentrations [mmol m^{-3}], and e) surface silicic acid concentrations [mmol m^{-3}]. The panels c) & f) denote the temporal evolution of the model bias of c) total surface chlorophyll concentration (red) and total NPP (blue), as well as f) surface nitrate concentrations (red), and silicic acid concentrations (blue) in the 5-PFT setup of ROMS-BEC between 30-60° S (solid) and 60-90° S (dashed), respectively. For comparison, the model bias obtained with the 4 PFT setup of ROMS-BEC is included in both panels in green (chlorophyll and nitrate) and yellow (NPP and silicic acid), respectively (see also supplement in Nissen et al., 2018).

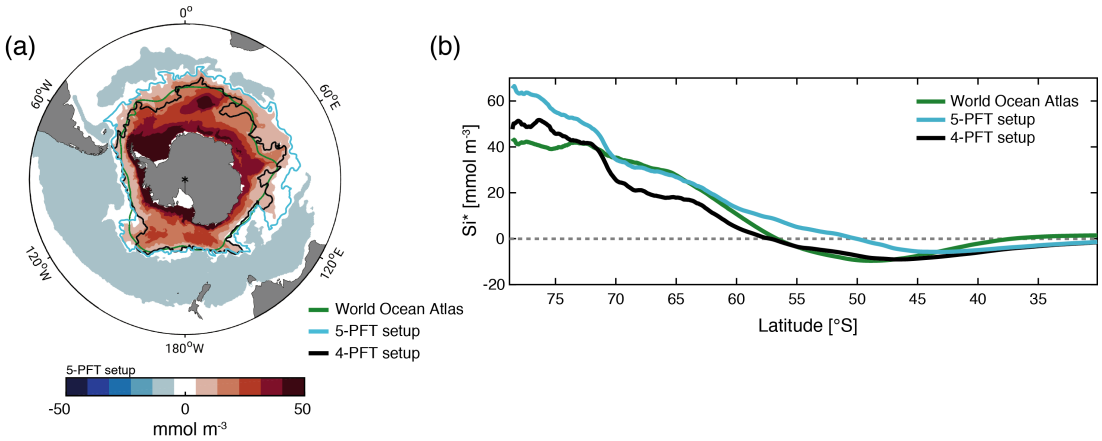

Figure S6: Annual mean top 100 m average a) Si* [mmol m^{-3}], which is defined as the difference in concentration between silicic acid and nitrate (Freeman et al., 2018), in the *Baseline* simulation of the 5-PFT setup of ROMS-BEC (colors). The contours denote the latitude of the silicate front, i.e. where Si*=0, in data from the World Ocean Atlas (green, Garcia et al., 2014) and in the *Baseline* simulation of the 5-PFT setup (light blue) and the 4-PFT setup (black, Nissen et al., 2018) of ROMS-BEC, respectively. b) zonal average Si* [mmol m^{-3}], colors are the same as the contours in panel a).

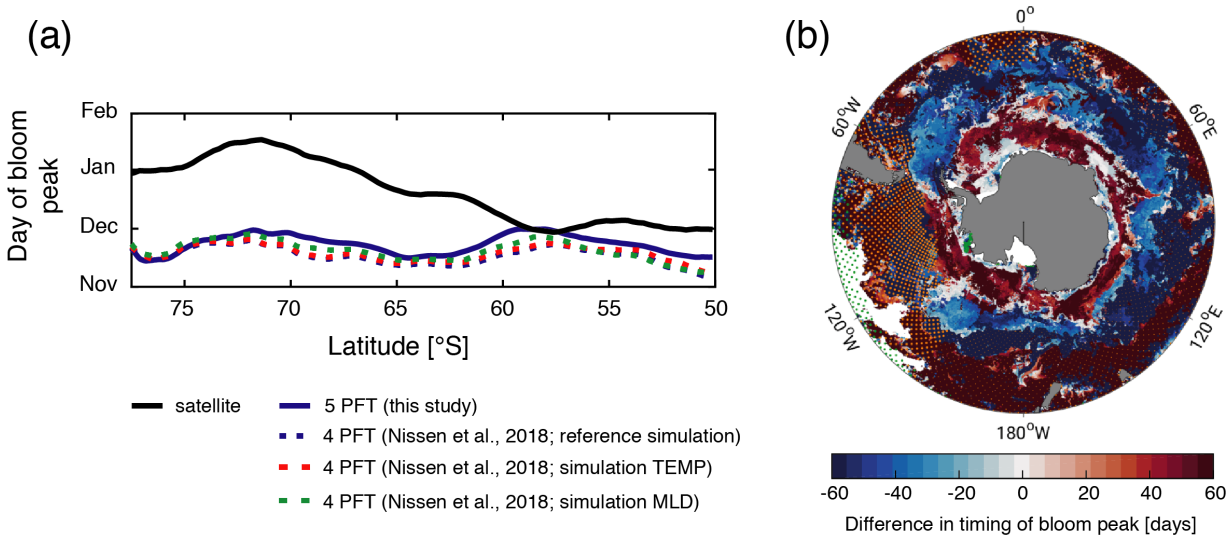

Figure S7: a) Same as Fig. 3 in the main text, Hovmoller plots south of 50° S of the day of maximum total chlorophyll concentrations in a satellite product (black line, Globcolor climatology from 1998-2018 based on the daily 25 km chlorophyll product, see Fanton d'Andon et al., 2009; Maritorena et al., 2010), the *Baseline* simulation of this study (solid blue line), the *Baseline* simulation of Nissen et al. (2018, dashed blue line; without *Phaeocystis*). Additionally, two sensitivity simulations in the 4 PFT setup from Nissen et al. (2018) are shown here to show the impact of biases in the simulated physical fields on phytoplankton phenology: The simulations TEMP (dashed red line) and MLD (dashed green line) correct for the simulated average temperature and MLD biases, respectively, within the biological subroutine of the model. b) Difference in day of bloom peak between *Phaeocystis* and diatoms, based on chlorophyll concentrations in the 5-PFT *Baseline* simulation. Stippling indicates locations where maximum chlorophyll concentrations never exceed 0.1 mg chl m^{-3} for *Phaeocystis* (orange) and diatoms (green), respectively. White areas correspond to areas where the peak total chlorophyll concentrations do not exceed 0.5 mg chl m^{-3}.

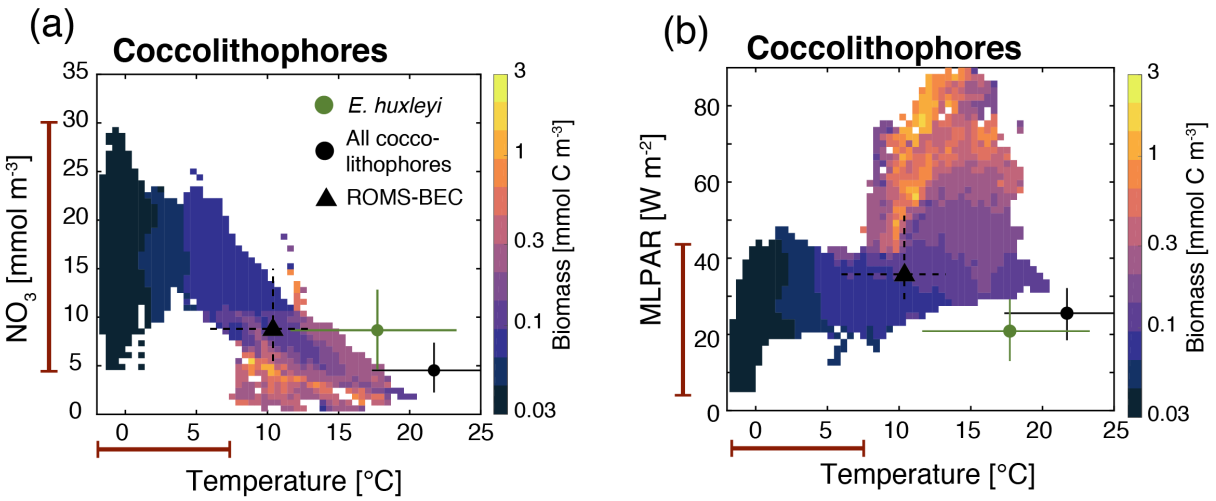

Figure S8: Simulated DJFM average top 50 m average ~~a)~~ coccolithophore carbon biomass concentrations (mmol C m^{-3}) south of 40° S as a function of the simulated temperature (° C) and a) nitrate concentrations (mmol N m^{-3}) and b) mixed layer PAR levels (W m^{-2}). Overlain are the observed ecological niche centers (median) and breadths (inter quartile ranges) for example taxa from Brun et al. (2015, circles and solid lines) and as simulated in ROMS-BEC (triangles and dashed lines; area and biomass weighted). The red bars on the axes indicate the simulated range of the respective environmental condition in ROMS-BEC between 60-90° S and averaged over DJFM and the top 50 m.

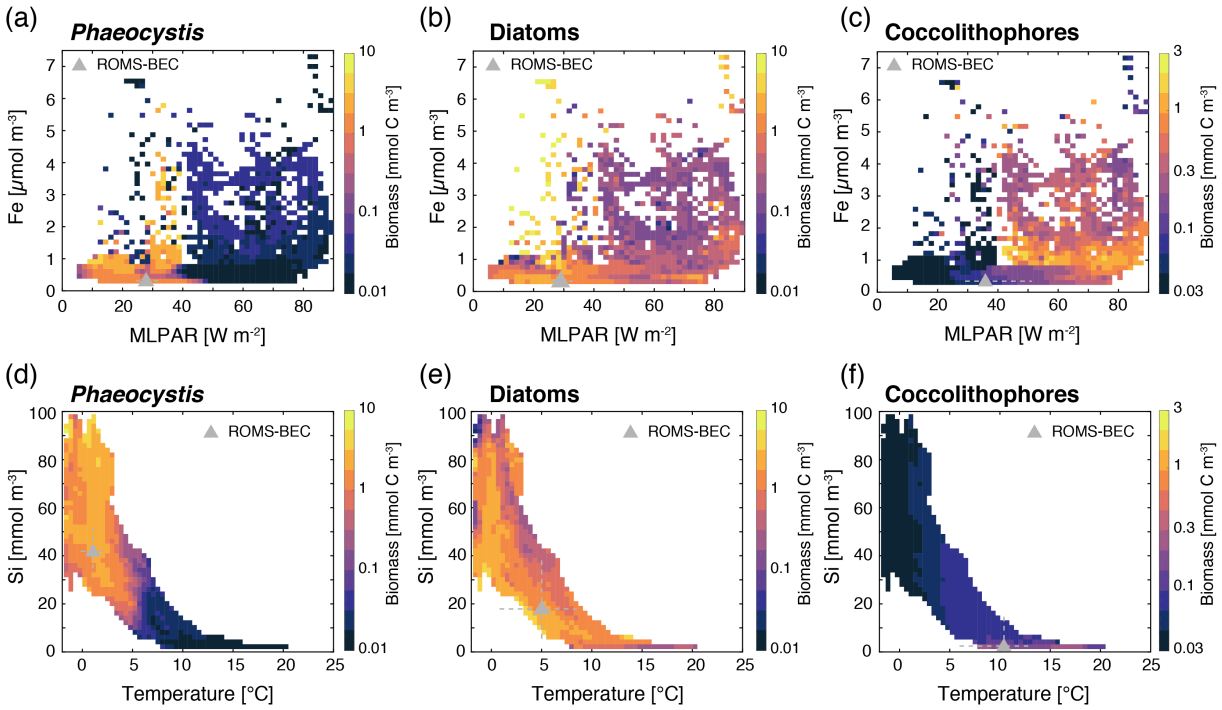

Figure S9: Simulated DJFM average top 50 m average a) *Phaeocystis*, b) diatom, and c) coccolithophore carbon biomass concentrations (mmol C m^{-3}) south of 40° S as a function of the simulated ~~concurrent~~ a)-c) dissolved iron concentrations (μmol Fe m^{-3}) and mixed layer PAR levels (W m^{-2}) and d)-f) temperature (° C) and dissolved silicic acid concentrations [mmol Si m^{-3}] in the 5-PFT *Baseline* simulation of ROMS-BEC. Overlain are the simulated area and biomass weighted ecological niche centers (median, triangle) and breadths (inter quartile ranges, dashed lines) for the three functional types.

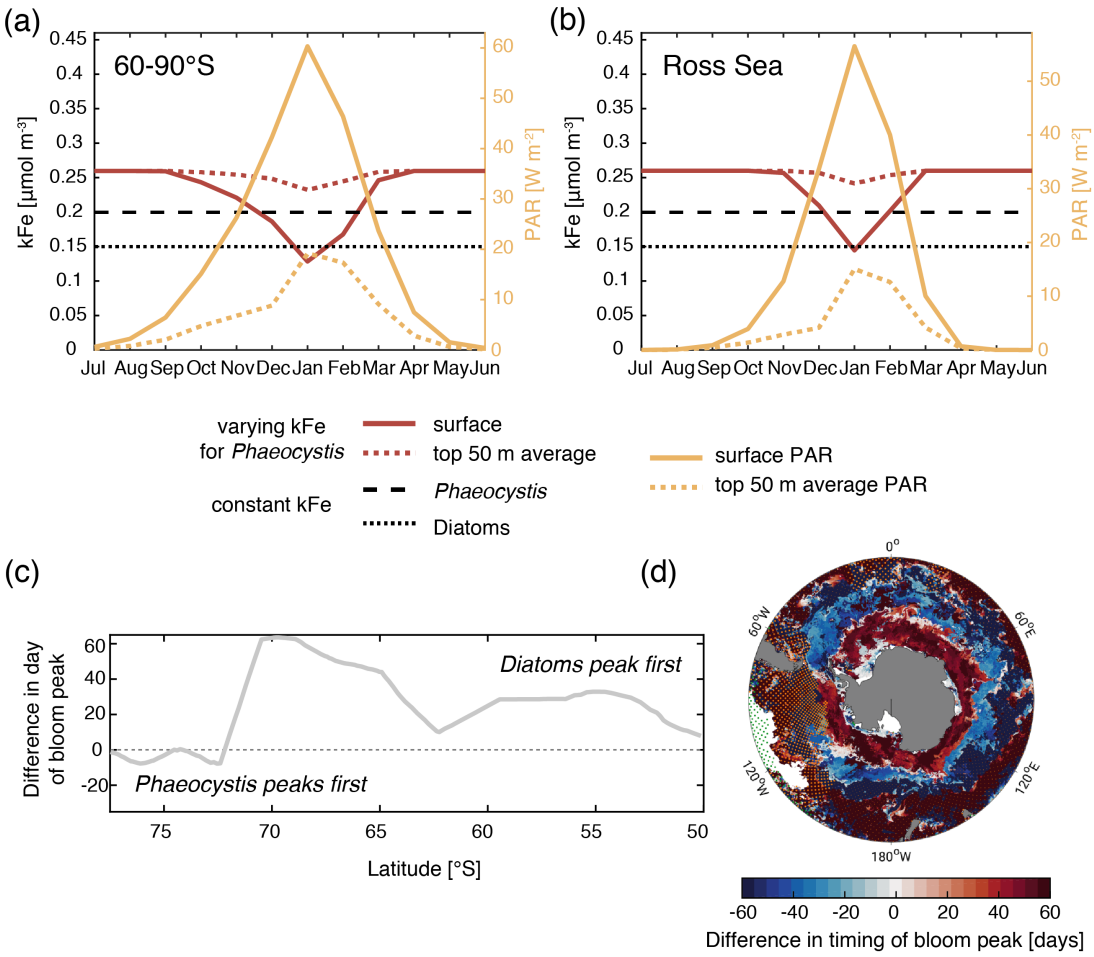

Figure S9S10: Results from the simulation VARYING_kFE (see section 2.2 in the main text): Varying half-saturation constant of iron of *Phaeocystis* (k_{Fe}, red, left y axis) and PAR (yellow, right y axis) as a function of time (x axis) for the surface (solid) and averaged over the top 50 m (dashed) for a) between 60-90° S and b) in the Ross Sea. Black lines indicate the constant k_{Fe} of *Phaeocystis* (dashed) and diatoms (dotted) used in the *Baseline* simulation of this study. c) Difference in days in the timing of the bloom peak of diatoms and *Phaeocystis* for each latitude, with negative values denoting a succession from *Phaeocystis* to diatoms throughout the season. d) Difference in day of bloom peak between *Phaeocystis* and diatoms. Stippling indicates locations where maximum chlorophyll concentrations never exceed 0.1 mg chl m^{-3} for *Phaeocystis* (orange) and diatoms (green), respectively. White areas correspond to areas where the peak total chlorophyll concentrations do not exceed 0.5 mg chl m^{-3}.

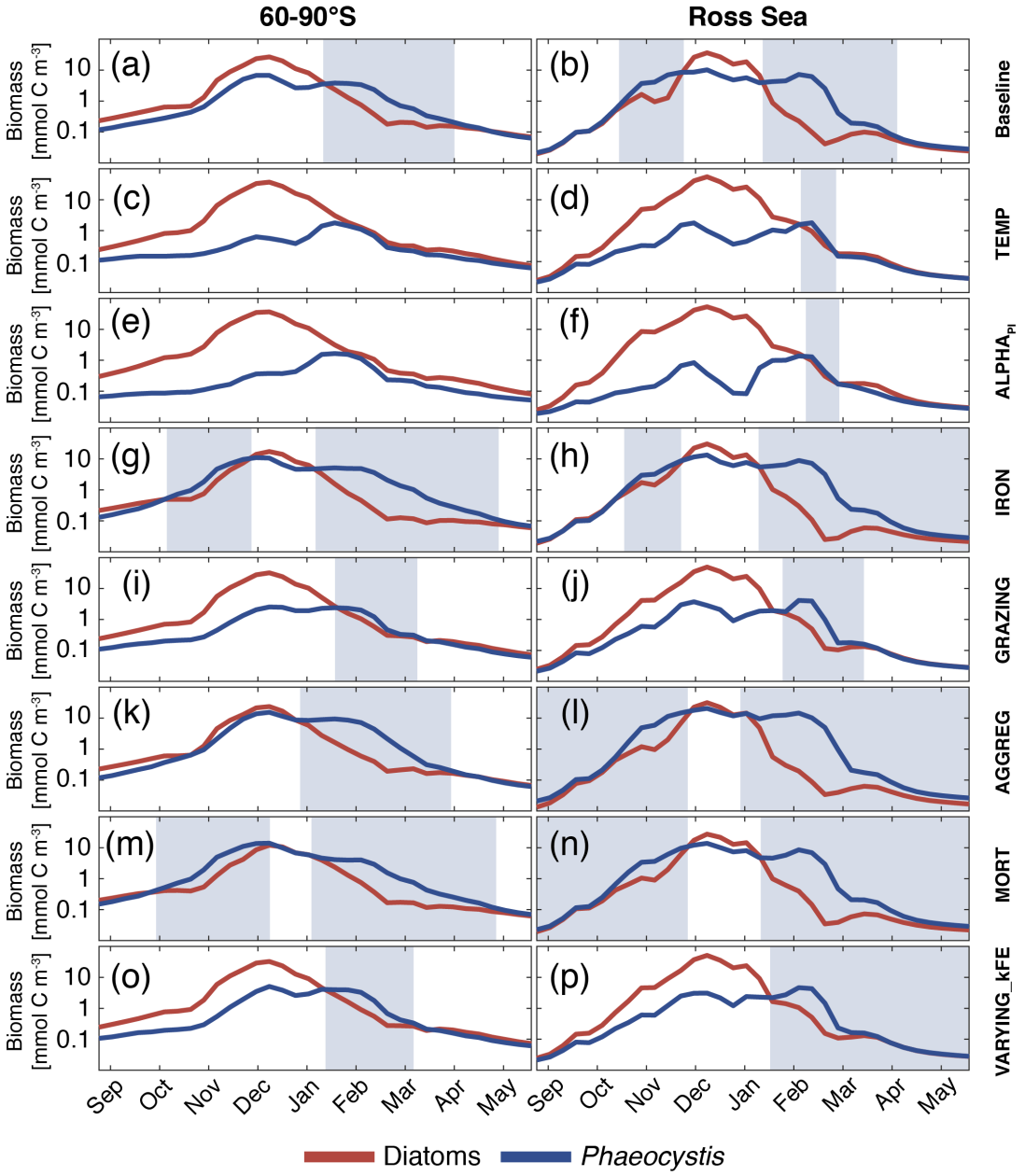

Figure S11: Diatom (red) and *Phaeocystis* (blue) surface carbon biomass concentrations [mmol C m^{-3}] in the different simulations performed in this study. See section 2.2. in the main text for details. The left panels are surface averages over 60-90° S and those on the right for the Ross Sea. Light blue area indicate times of the year when *Phaeocystis* biomass is larger than diatom biomass.

References

Balch, W. M., Bates, N. R., Lam, P. J., Twining, B. S., Rosengard, S. Z., Bowler, B. C., Drapeau, D. T., Garley, R., Lubelczyk, L. C., Mitchell, C., and Rauschenberg, S.: Factors regulating the Great Calcite Belt in the Southern Ocean and its biogeochemical significance, Global Biogeochemical Cycles, 30, 1199–1214, https://doi.org/10.1002/2016GB005414, 2016.

Brun, P., Vogt, M., Payne, M. R., Gruber, N., O'Brien, C. J., Buitenhuis, E. T., Le Quéré, C., Leblanc, K., and Luo, Y.-W.: Ecological niches of open ocean phytoplankton taxa, Limnology and Oceanography, 60, 1020–1038, https://doi.org/10.1002/lno.10074, 2015.

Cubillos, J. C., Wright, S. W., Nash, G., de Salas, M. F., Griffiths, B., Tilbrook, B., Poisson, A., and Hallegraeff, G. M.: Calcification morphotypes of the coccolithophorid *Emiliania huxleyi* in the Southern Ocean: changes in 2001 to 2006 compared to historical data, Marine Ecology Progress Series, 348, 47–54, https://doi.org/10.3354/meps07058, 2007.

Fanton d'Andon, O., Mangin, A., Lavender, S., Antoine, D., Maritorena, S., Morel, A., Barrot, G., Demaria, J., and Pinnock, S.: GlobColour - the European Service for Ocean Colour, in: Proceedings of the 2009 IEEE International Geoscience & Remote Sensing Symposium, IEEE International Geoscience & Remote Sensing Symposium (IGARSS), ISBN: 9781424433957, 2009.

Freeman, N. M., Lovenduski, N. S., Munro, D. R., Krumhardt, K. M., Lindsay, K., Long, M. C., and Maclennan, M.: The variable and changing Southern Ocean silicate front: Insights from the CESM large ensemble, Global Biogeochemical Cycles, 32, 752–768, https://doi.org/10.1029/2017GB005816, 2018.

Garcia, H. E., Locarnini, R. A., Boyer, T. P., Antonov, J. I., Baranova, O. K., Zweng, M. M., Reagan, J. R., and Johnson, D. R.: World Ocean Atlas 2013, Volume 4 : Dissolved inorganic nutrients (phosphate, nitrate, silicate), NOAA Atlas NESDIS 76, 4, 25 pp, 2014.

Gravalosa, J. M., Flores, J.-A., Sierro, F. J., and Gersonde, R.: Sea surface distribution of coccolithophores in the eastern Pacific sector of the Southern Ocean (Bellingshausen and Amundsen Seas) during the late austral summer of 2001, Marine Micropaleontology, 69, 16–25, https://doi.org/10.1016/j.marmicro.2007.11.006, 2008.

Leblanc, K., Arístegui, J., Armand, L., Assmy, P., Beker, B., Bode, A., Breton, E., Cornet, V., Gibson, J., Gosselin, M.-P., Kopczynska, E., Marshall, H., Peloquin, J., Piontkovski, S., Poulton, A. J., Quéguiner, B., Schiebel, R., Shipe, R., Stefels, J., van Leeuwe, M. A., Varela, M., Widdicombe, C., and Yallop, M.: A global diatom database - abundance, biovolume and biomass in the world ocean, Earth System Science Data, 4, 149–165, https://doi.org/10.5194/essd-4-149-2012, 2012.

Maritorena, S., Fanton D'Andon, O., Mangin, A., and Siegel, D. A.: Merged satellite ocean color data products using a bio-optical model: Characteristics, benefits and issues, Remote Sensing of Environment, 114, 1791–1804, https://doi.org/10.1016/j.rse.2010.04.002, 2010.

Nissen, C., Vogt, M., Münnich, M., Gruber, N., and Haumann, F. A.: Factors controlling coccolithophore biogeography in the Southern Ocean, Biogeosciences, 15, 6997–7024, https://doi.org/10.5194/bg-15-6997-2018, 2018.

O'Brien, C. J., Peloquin, J. A., Vogt, M., Heinle, M., Gruber, N., Ajani, P., Andruleit, H., Arístegui, J., Beaufort, L., Estrada, M., Karentz, D., Kopczyńska, E., Lee, R., Poulton, A. J., Pritchard, T., and Widdicombe, C.: Global marine plankton functional type biomass distributions: coccolithophores, Earth System Science Data, 5, 259–276, https://doi.org/10.5194/essd-5-259-2013, 2013.

Saavedra-Pellitero, M., Baumann, K.-H., Flores, J.-A., and Gersonde, R.: Biogeographic distribution of living coccolithophores in the Pacific sector of the Southern Ocean, Marine Micropaleontology, 109, 1–20, https://doi.org/10.1016/j.marmicro.2014.03.003, 2014.

Swan, C. M., Vogt, M., Gruber, N., and Laufkötter, C.: A global seasonal surface ocean climatology of phytoplankton types based on CHEMTAX analysis of HPLC pigments, Deep-Sea Research Part I, 109, 137–156, https://doi.org/10.1016/j.dsr.2015.12.002, 2016.

Tyrrell, T. and Charalampopoulou, A.: Coccolithophore size, abundance and calcification across Drake Passage (Southern Ocean), 2009, https://doi.org/10.1594/PANGAEA.771715, 2009.

Vogt, M., O'Brien, C., Peloquin, J., Schoemann, V., Breton, E., Estrada, M., Gibson, J., Karentz, D., Van Leeuwe, M. A., Stefels, J., Widdicombe, C., and Peperzak, L.: Global marine plankton functional type biomass distributions: *Phaeocystis* spp., Earth System Science Data, 4, 107–120, https://doi.org/10.5194/essd-4-107-2012, 2012.